UNIVERSIDAD DE MURCIA

ESCUELA INTERNACIONAL DE DOCTORADO

Two-dimensional Speckle Tracking Echocardiography in Dogs: a Focus on Unexplored Aspects of the Technique

Ecocardiografía Bidimensional con Rastreo de Marcas (*speckle tracking*) en Perros: un Enfoque sobre Aspectos Inexplorados de la Técnica

Dña. Giorgia Santarelli

2018

UNIVERSIDAD DE MURCIA

ESCUELA INTERNACIONAL DE DOCTORADO

Two-dimensional speckle tracking echocardiography in dogs: a focus on unexplored aspects of the technique

Ecocardiografía bidimensional con rastreo de marcas (*speckle tracking*) en perros: un enfoque sobre aspectos inexplorados de la técnica

Doctoranda: Giorgia Santarelli

Programa de Doctorado: Ciencias Veterinarias

Director de Tesis: Dra. Mª Josefa Fernández del Palacio

Murcia, 2018

A mi padre

UNIVERSIDAD DE
MURCIA

Dª. Mª Josefa Fernández del Palacio, Profesora Titular de Universidad del Área de Medicina y Cirugía en el Departamento de Medicina y Cirugía Animal, AUTORIZA:

La presentación de la Tesis Doctoral titulada "Two-dimensional speckle tracking echocardiography in dogs: a focus on unexplored aspects of the technique"/ "Ecocardiografía bidimensional con rastreo de marcas (speckle tracking) en perros: un enfoque sobre aspectos inexplorados de la técnica", realizada por D. Giorgia Santarelli, bajo mi inmediata dirección y supervisión, y que presenta para la obtención del grado de Doctor por la Universidad de Murcia.

En Murcia, a 03 de septiembre de 2018

TABLE OF CONTENTS

ABBREVIATIONS

2-D STE	Two-dimensional speckle tracking echocardiography
Ao	Aorta
ACP	Acepromazine
Ant	Anterior segment
AntSept	Antero-septal segment
Apex	Apical segment
ApL	Apical lateral segment
ApS	Apical septal segment
ASE	American Society of Echocardiography
AVC	Aortic valve closure
A wave	Peak velocity of late transmitral diastolic flow
A' sep	Late diastolic velocity of the septal side of the mitral annulus
A' tri	Late diastolic velocity of the lateral side of the tricuspid annulus
BL	Basal lateral segment
bpm	Beats per minute
BS	Basal septal segment
BUT	Butorphanol
CV	Coefficients of variation
DAP	Diastolic arterial pressure
DCM	Dilated cardiomyopathy
DICOM	Digital Images and Communications in Medicine
E/A	E wave to A wave ratio
EACVI	European Association of Cardiovascular Imaging and
ECG	Electrocardiography
EDV	End-diastolic volume
EDVI	Left ventricular end-diastolic volume index
EF	Left ventricular ejection fraction
ESV	End-systolic volume
ESVI	Left ventricular end-systolic volume index
E wave	Peak velocity of early transmitral diastolic flow
FR	Frame rate
FS	Fractional shortening
GCS	Global circumferential strain
GE	General Electric
GLS	Global longitudinal strain

HR	Heart rate
ICC	Intra-class correlation coefficients
IM	Intramuscular
Inf	Inferior segment
LA	Left atrium
LA/Ao	Left atrium to aorta ratio
LAp4Ch	Left apical four-chamber view
Lat	Lateral segment
LOA	Limits of agreement
LV	Left ventricle
LVAd	Left ventricular end-diastolic luminal area
LVAs	Left ventricular end-systolic luminal area
LVIDd	Left ventricular diastolic internal diameter
LVIDs	Left ventricular systolic internal diameter
LVET	Left ventricular ejection time
LVPEP	Left ventricular pre-ejection period
LVPEP/LVET	Left ventricular pre-ejection period to ejection time ratio
MAP	Mean arterial pressure
MMVD	Myxomatous mitral valve disease
MRI	Magnetic resonance imaging
ML	Mid-lateral segment
MS	Mid-septal segment
Post	Posterior segment
PDA	Patent ductus arteriosus
RP4Ch	Right parasternal four-chamber view
SAP	Systolic arterial pressure
SD	Standard deviation
Sept	Septal segment
SR	Strain rate
STI	Synchrony time index
ROI	Region of interest
RV	Right ventricle
TDI	Tissue Doppler Imaging
VTI	Left ventricular velocity time integral

INTRODUCTION

1. INTRODUCTION

1.1 Echocardiography in veterinary cardiology

Veterinary cardiology is the clinical specialty dedicated to the diagnosis and treatment of animal cardiovascular diseases. Estimates indicate that slightly more than 10% of all domestic animals examined by a veterinarian have some form of cardiovascular disease (Cunningham & Roderick, 2016).

Echocardiography is the main noninvasive technique for the diagnosis and management of cardiovascular disease, both in human and veterinary patients (Chetboul, 2010). The technique allows noninvasive assessment of the dimension of the cardiac chambers and walls (Boon, 2011). It also provides information about cardiac function and blood flow, permitting the diagnosis of structural cardiac disease, and assisting in the assessment of hemodynamic status and disease progression (Boon, 2011).

The feasibility, relatively low cost and potential for morphological and hemodynamic assessment of the heart has also increased the use of echocardiography in the research field (Abduch et al., 2014). Validation of new echocardiographic technologies in an experimental setting, before their clinical application, is common (Abduch et al., 2014).

Echocardiography has developed enormously since the 1950s, when Edler and Herz recorded movements of cardiac structures using M-mode (Abduch, Assad, Mathias, & Aiello, 2014; Bélanger, 2017). Since its introduction in veterinary medicine, veterinary cardiologists have adapted the different echocardiographic modalities employed in humans for use in animals (Thomas et al., 1993).

In animals, pharmacological tranquilization can sometimes become necessary to aid the echocardiographic examination and to obtain good quality ultrasound scans (Kellihan, Stepien, Hassen, & Smith, 2015). Sedation is used for cardiovascular diagnostic procedures to provide adequate immobilization and to reduce anxiety, and should preserve the hemodynamic condition to the utmost (Saponaro, Crovace, De Marzo, Centonze, & Staffieri, 2013; Stepien, 1995).

1.2 Echocardiography: techniques and imaging modalities

Echocardiography uses the basic principle of reflection of ultrasound to impart information about the presence and position of a reflective boundary or the direction and velocity of a moving target such as red blood cells or tissue (Armstrong & Ryan, 2010). Furthermore, it involves processing of the returned signals, and display of the data in some recognizable visual or auditory format (Armstrong & Ryan, 2010).

Two-dimensional and M-mode echocardiography create dynamic images of the contracting heart and provide data regarding its anatomy and size, as well as information about wall motion (Armstrong & Ryan, 2010; Boon, 2011). Spectral and color flow Doppler imaging allow visualization and measurement of blood flow through the heart, yielding information about systolic and diastolic function, intracardiac pressures, stroke volumes, regurgitant fractions and shunt ratios (Armstrong & Ryan, 2010; Boon, 2011). Spectral Doppler is acquired through two different methods, continuous and pulsed wave (Armstrong & Ryan, 2010). Color flow Doppler is a variation of pulsed wave Doppler imaging (Armstrong & Ryan, 2010).

Advanced ultrasound techniques provide additional measures of myocardial performance, including regional myocardial velocities and deformation, ventricular twist and mechanical synchrony (Chetboul, 2010). Tissue Doppler imaging (TDI) targets tissue rather than red blood cells to investigate the myocardium or the fibrous skeleton of the heart, applying filters opposite to those that would be needed to detect red blood cells motion (Armstrong & Ryan, 2010). However, the technique is highly angle dependent and does not discriminate between actively contracting myocardium and passive motion due to translational movement of the heart (Chetboul, 2010). Two-dimensional (2-D) speckle tracking echocardiography (STE) is a more recently developed approach to assess myocardial deformations and relies on tracking of unique myocardial ultrasound signals. It overcomes some of the limitations associated with TDI (Armstrong & Ryan, 2010; Chetboul, Serres, Gouni, Tissier & Pouchelon, 2007).

1.3 Two-dimensional speckle tracking echocardiography

Two-dimensional STE employs a post-processing software algorithm that tracks over time the motion of fixed patterns of speckles (**Fig. 1**; Blessberger & Binder, 2010).

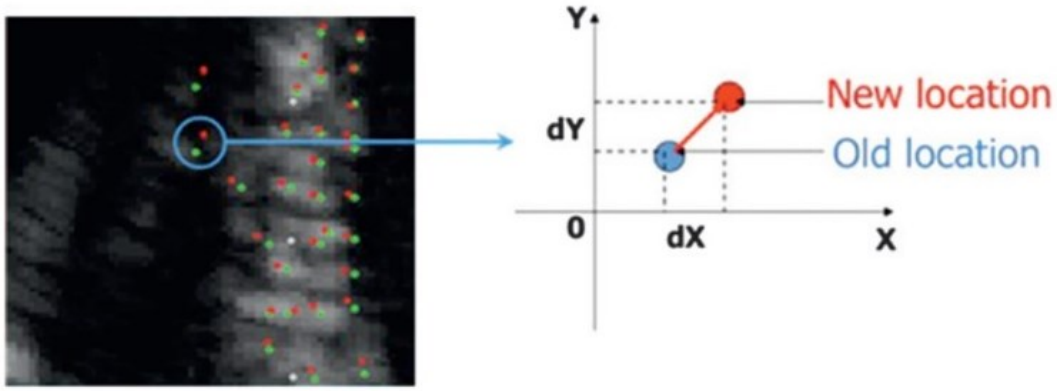

Figure 1. Representation of the frame-to-frame motion of the acoustic markers, where the green dot corresponds to the intial location and the red dot to the final location of the speckle. *Source:* Blessberger, H., & Binder, T. (2010). Non-invasive imaging: two-dimensional speckle tracking echocardiography: basic principles. *Heart,* 96(9), 716-722. Used by permission of the journal.

The speckles represent a series of artifacts that are generated by reflection, refraction and scattering of ultrasound beams, and are present in grayscale 2-D echocardiographic images (Armstrong & Ryan, 2010; Blessberger & Binder, 2010; Chetboul, 2010; Chetboul et al., 2007; Gorcsan & Tanaka, 2011; Voigt et al., 2015). A specific region of interrogation contains a unique or nearly unique pattern of speckles that acts as an acoustic fingerprint, and through tracking of the speckles of that myocardial region of interest over time, the algorithm can calculate the direction and velocity of movement of a myocardial segment. Via comparison of two regions of the myocardium, strain and strain rate (SR) can be calculated (Armstrong & Ryan, 2010).

In contrast to Doppler-based techniques, 2-D STE is less dependent on insonation angle and only reflects active contraction, as it is not influenced by passive traction of scar tissue or adjacent vital myocardium, or cardiac translation (Blessberger & Binder, 2010; Chetboul, 2010). However, the technique is not free of limitations, which include dependence on frame rate (FR) and image resolution. Furthermore, out-of-sector movements of myocardial regions containing speckles can decrease the reliability of the tracking process (Chetboul, 2010).

1.4 Basics of myocardial mechanics

In healthy subjects, due to the presence of helically oriented myofibers (**Fig. 2**), the left ventricle (LV) undergoes a twisting motion leading to a decrease in the radial and

longitudinal length of the LV cavity (Armstrong & Ryan 2010; Blessberger & Binder 2010; Zois et al., 2013).

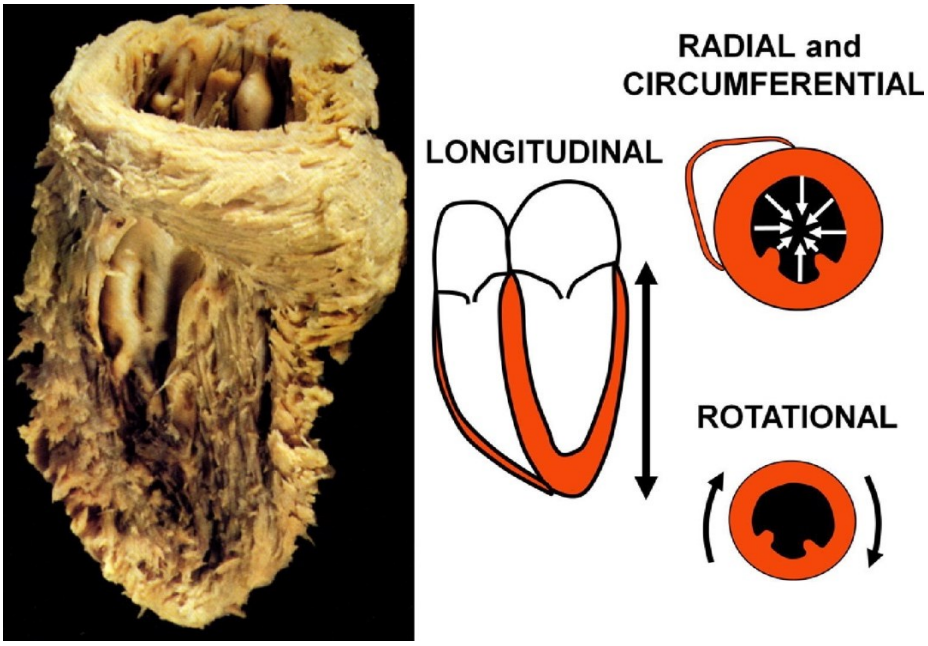

Figure 2. Left ventricular myocardial fiber orientation, and different directions of contraction. *Source:* Gorcsan, J., 3rd, & Tanaka, H. (2011). Echocardiographic assessment of myocardial strain. *Journal of the American College of Cardiology*, 58(14), 1401-1413. Used by permission of the journal.

The LV rotates clockwise in early systole, and subsequently the base continues with clockwise rotation while the apex develops counterclockwise rotation. A recoiling and untwisting motion occurs primarily during early diastole, contributing to active suction (Armstrong & Ryan 2010; Blessberger & Binder 2010; Zois et al., 2013). The torsion motion has complementary effects to that of systolic ejection forces, with three different components of contraction identified: radial, circumferential, and longitudinal (**Fig. 2**; Blessberger & Binder 2010; Decloedt, Verheyen, Sys, De Clercq, & van Loon, 2011).

1.5 Myocardial deformation variables – strain, strain rate, synchrony parameters, rotation and torsion

Myocardial deformation can be evaluated by means of strain, SR and torsional movement measurements, each of which define a different parameter of shape change with contraction (Armstrong & Ryan, 2010). Intraventricular segmental mechanical synchrony of the LV can also be assessed through analysis of segmental myocardial motion (Chetboul

et al., 2007; Griffiths, Fransioli, & Chigerwe, 2011; Suffoletto, Dohi, Cannesson, Saba, & Gorcsan, 2006; Takano, Fujii, Ishikawa, Aoki, & Wakao, 2010).

Myocardial strain represents the deformation of a myocardial segment over time, expressed as the % change from its original dimension; it is a dimensionless quantity expressed as a proportion of initial segment length (**Fig. 3**; Chetboul, 2010; Chetboul et al., 2007). A common approach to define this change in length is to use the so-called Lagrangian strain, defined as the length of a myocardial segment at a given point in time, usually end-systole, compared to a reference length, usually the relaxed length at end-diastole (Voigt et al., 2015).

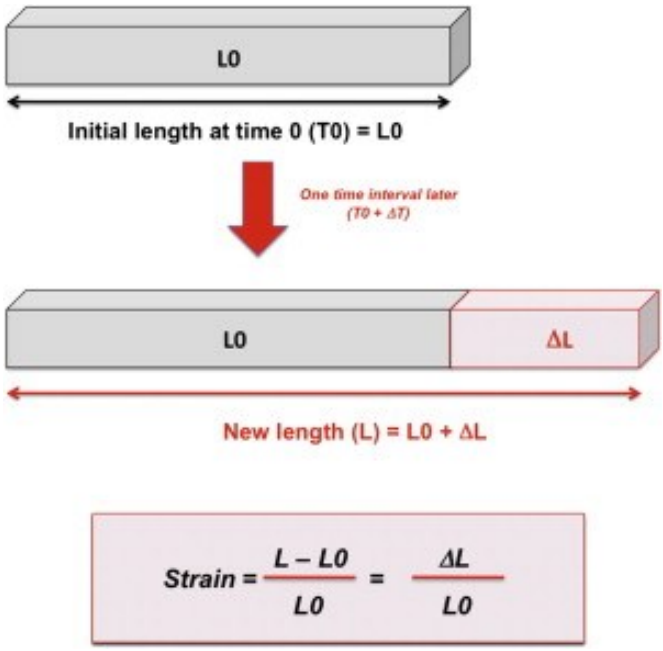

Figure 3. Calculation of strain. The myocardial length at time 0 (T0) is L0 (gray bar). One time interval later (T0 + ΔT), the myocardial length increased from L0 to L0 + ΔL (red bar added to gray bar). The strain undergone by the myocardial segment, expressed in %, is ΔL/L0. *Source:* Chetboul, V. (2010). Advanced techniques in echocardiography in small animals. *Veterinary Clinics of North America: Small Animal Practice*, 40(4), 529-543. Used by permission of the journal.

Myocardial SR represents the temporal derivative of strain and describes the rate of myocardial deformation (Chetboul & Tissier, 2010; Chetboul et al., 2007). It is calculated as the change in velocity between two points divided by their distance, and it is expressed in s^{-1} (Armstrong & Ryan, 2010).

Strain and SR calculation allows assessment of a myocardial region with reference to an adjacent segment rather than to the transducer position and, as such, provides theoretically accurate data about ventricular deformation during the cardiac cycle, being less affected by rotation, translational motion and tethering compared to other more conventional parameters of LV function (Armstrong & Ryan, 2010). Strain and SR can each be calculated either from TDI or from speckle tracking techniques (Armstrong & Ryan, 2010). Echocardiographic strain was first obtained with TDI, from which SR is derived using the velocity data, and is then integrated over time to determine strain (Gorcsan & Takana, 2011). Conversely, the primary calculation with speckle tracking is of tissue displacement and the primary parameter derived is strain (Armstrong & Ryan, 2010).

Strain and SR may be calculated in any of three orthogonal planes, representing longitudinal, circumferential, and radial contraction (Armstrong & Ryan, 2010; Blessberger & Binder, 2010; Chetboul & Tissier, 2012; Chetboul et al., 2007; Gorcsan & Tanaka, 2011; Voigt et al., 2015).

Negative strain indicates fiber shortening or myocardial thinning, whereas a positive value describes lengthening or thickening (Blessberger & Binder, 2010). Normal contraction is defined by negative longitudinal (**Fig. 4**) and circumferential (**Fig. 5**) systolic strain, followed by positive biphasic diastolic strain related to early and late diastolic filling, respectively. On the other hand, radial strain is positive in systole and reflects wall thickening (Armstrong & Ryan, 2010).

Strain analysis may be performed over several segmental regions of interest or throughout the entire perimeter of the ventricle, the latter resulting in calculation of global ventricular strain, which correlates to LV ejection fraction (EF), and SR (Armstrong & Ryan, 2010). Moreover, strain and SR can be measured over the full myocardial thickness, at the endocardial or epicardial borders, or at the myocardial midline (Voigt et al., 2015). The segmental strain or SR represents the average value in the segment of interest (Voigt et al., 2015). The global strain or SR can be calculated by using the entire myocardial line length, by averaging the values obtained from a number of points along the myocardial line, or by averaging the segmental values; other methods exist, but are not mathematically equivalent to the previous, and make comparison between different software more difficult (Voigt et al., 2015).

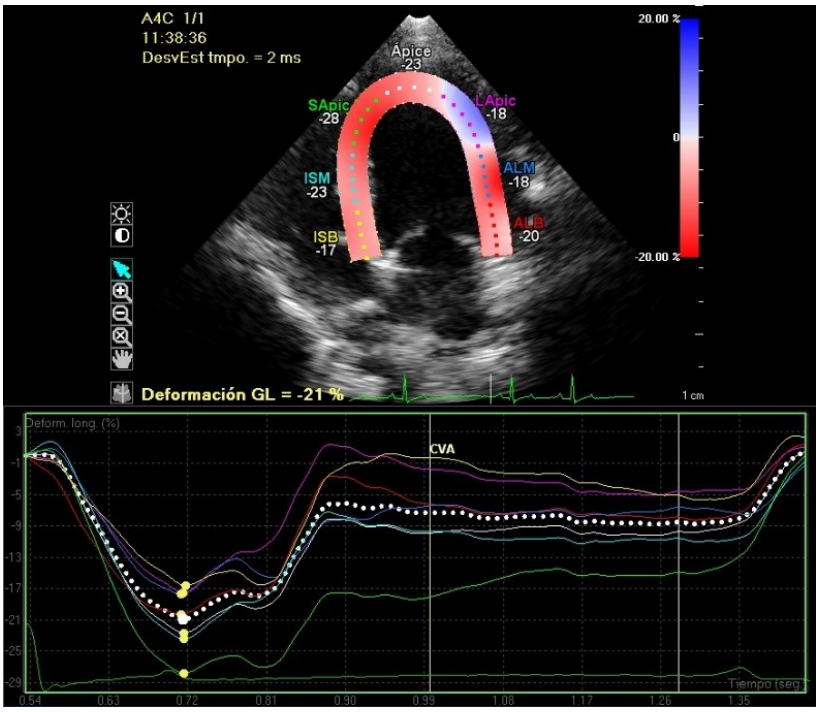

Figure 4. Example of segmental and global longitudinal strain of the left ventricle obtained with speckle tracking in a healthy dog. Note the homogeneous timing of peak systolic strain and the characteristic negative values observed in systole. In addition, notice the heterogeneity of segmental strain values which range from -17% to -28%. Used by permission of the Veterinary Teaching Hospital of the University of Murcia.

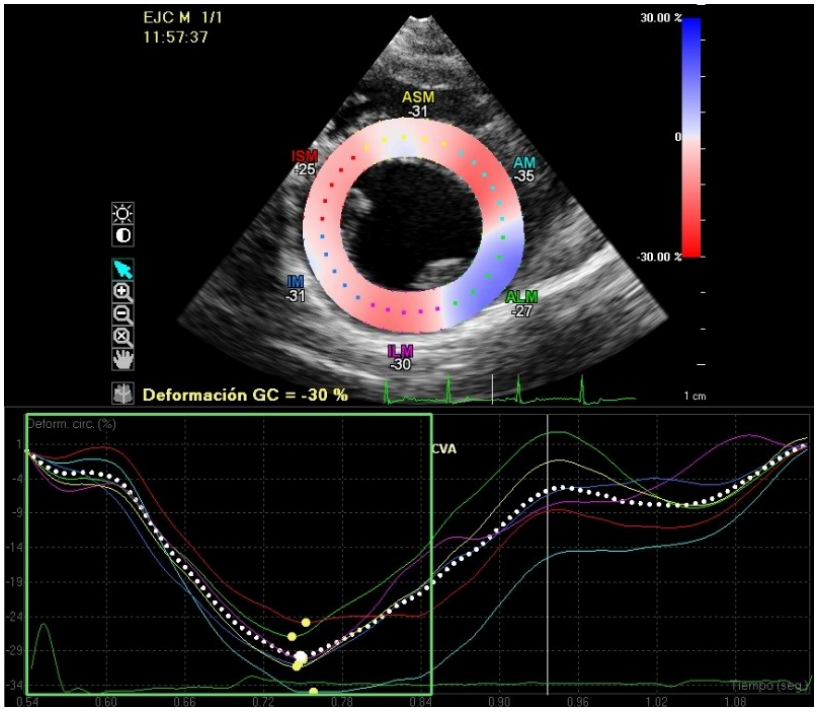

Figure 5. Example of segmental and global circumferential strain of the left ventricle obtained with speckle tracking in a healthy dog. Note the relatively homogeneous timing of peak systolic strain and the characteristic negative values observed in systole. In addition, notice the heterogeneity of segmental strain values which range from -25% to -35%. Used by permission of the Veterinary Teaching Hospital of the University of Murcia.

Various strain values can be of clinical interest during the cardiac cycle (Voigt et al., 2015). These include, among others: end-systolic strain, representing the strain value obtained at end-systole; peak systolic strain, representing the peak strain value during systole; peak strain, representing the peak value during the entire heart cycle that may or may not coincide with the systolic or end-systolic peak (Voigt et al., 2015).

Strain is not uniform among all myocardial segments (**Fig. 4** and **Fig. 5**). In humans, while velocities and displacement show higher basal parameters than apical ones, longitudinal strain has less variability from apex to base. However, variability in strain between segments is substantial around the circumference. Also, there is high patient-to-patient variability resulting in a wide range of normal values (Armstrong & Ryan, 2010).

Intraventricular segmental mechanical synchrony of the LV can also be assessed through 2-D STE analysis of segmental myocardial motion (Chetboul et al., 2007; Griffiths et al., 2011; Suffoletto et al., 2006; Takano et al., 2010). Time from the onset of ventricular electrical activity (identified as the beginning of the Q wave on simultaneous ECG recording) to peak systolic strain and peak early diastolic strain, and time from onset of atrial electrical activity (identified as the beginning of the P wave on simultaneous ECG recording) to peak atrial diastolic strain can be measured for each LV myocardial segment (Griffiths et al., 2011). Myocardial synchrony can subsequently be assessed by calculating the synchrony time index (STI), defined as the difference in timing of peak strain from the earliest to latest segment (Chetboul et al., 2007; Takano et al., 2010), or the dispersion of systolic LV synchrony, defined as the average maximal systolic time difference and standard deviation (SD) of timing between peak segmental strains (Griffiths et al., 2011). Dispersion of diastolic LV synchrony can also be calculated as the average maximal diastolic time difference and standard deviation of timing between segmental strains for early and atrial diastolic motion (Griffiths et al., 2011).

Ventricular torsion measurements analyze the twisting motion of the heart. The rotation of the heart is described in degrees, and the difference between the positive rotation at the base and the negative rotation at the apex represents the total rotation. Calculation of torsion is achieved by dividing the total rotation by the distance between the two analyzed segments. It is defined as the twist in degrees divided by the distance (Armstrong & Ryan, 2010; Zois et al., 2013).

1.6 Validation, feasibility and reproducibility of two-dimensional speckle tracking echocardiography for left ventricular function assessment in healthy dogs

Speckle tracking echocardiography has been shown to provide accurate measurements of LV dimensions and strains when validated in healthy anesthetized dogs against sonomicrometry, which is the gold standard method for evaluation of systolic myocardial deformation (Amundsen et al., 2006). In the same and in another study (Amundsen et al., 2009), the technique was validated against tagged magnetic resonance imaging (MRI) in human subjects. Tagged MRI is widely used in human research and clinical practice for the qualitative and quantitative assessment of myocardial contraction, but is rarely employed in small animal medicine due to the small cardiac size relative to standard human grid sizes used in tagging (Gilbert, McConnell, Holden, Sivananthan, & Dukes-McEwan, 2010).

Quantification of LV systolic twist by the use of 2-D STE has also been validated against sonomicrometry in healthy anesthetized dogs (Helle-Valle et al., 2005). Furthermore, various deformation parameters have shown good correlation with invasive indices of LV function in the canine species. Specifically, it has been shown that there is a strong correlation of longitudinal SR values with invasively measured maximum rate of rise of LV systolic pressure, a parameter commonly used for validation of noninvasive indices of ventricular contractility or global systolic function (Culwell, Bonagura, & Schober, 2011).

Two-dimensional STE has also been compared with other advanced echocardiographic techniques in nonanesthetized healthy dogs, where a good correlation between LV longitudinal and radial strain and SR values derived from color TDI and 2-D STE was demonstrated (Chetboul et al., 2007; Chetboul, Serres, Gouni, Tissier, & Pouchelon, 2008; Culwell et al., 2011).

Various studies have focused on feasibility, reproducibility, and repeatability of STE-derived LV deformation parameters in dogs (Chetboul et al., 2007, 2008; Culwell et al., 2011; Wess, Keller, Klausnitzer, Killich, & Hartmann, 2011).

Chetboul and colleagues were the first to demonstrate adequate repeatability and reproducibility for clinical and research use of 2-D STE-derived radial strain and SR indices, and STI in healthy dogs (Chetboul et al., 2007). Global values of LV radial function obtained

by the aforementioned authors in 37 healthy dogs were as follows: peak systolic strain 46.7 ± 12.2%; peak systolic SR 2.69 ± 0.76 s^{-1}; STI 15 ± 15 msec (Chetboul et al., 2007).

Good reproducibility was also found by Wess and colleagues for longitudinal strain measurement in both myocardial walls, while this was lower for longitudinal SR values, especially when considering the average of segments constituting the LV free wall (Wess et al., 2011).

In healthy, awake dogs, repeatability and reproducibility of 2-D STE indices of systolic LV torsional deformation were assessed too, showing within-day and between-day coefficients of variation of less than 20%, considered acceptable for clinical use (Chetboul et al., 2008). Parameters of LV torsion obtained by the aforementioned authors in 35 healthy dogs were as follows: peak apical rotation -1.6 ± 0.8° and 5.4 ± 3.2° (early and late motion, respectively); peak basal rotation 3.9 ± 2.8° and -3.1 ± 1.3° (early and late motion, respectively); torsion at end systole 8.4 ± 3.8° (Chetboul et al., 2008).

As adult dogs can display a wide range of weights, any definition of normal heart size has to take into account the variation caused by differences in body size (Cornell et al., 2004). The impact of body size on LV 2-D STE-derived measurements was investigated by Takano and colleagues (Takano et al., 2010), who demonstrated that peak systolic circumferential strain and SR are decreased, together with fractional shortening (FS), in large healthy dogs (weighting more than 20 Kg) compared with small (body weight less than 7 Kg) and medium (body weight 7 to 20 Kg) dogs. In their study, 2-D STE-derived variables were matched on the basis of R–R interval to eliminate its influence. The differences encountered were therefore considered to be most likely related to the size of the dog, and so should not be misinterpreted as a sign of decreased systolic function (Takano et al., 2010). Increased STI was also identified in large dogs, which may contribute to decreased FS; on the other hand, peak systolic radial strain and SR were not affected by body weight, and were therefore suggested as better indices of LV systolic function (Takano et al., 2010).

While normal reference values for several canine breeds are available to aid in the interpretation of conventional echocardiographic parameters (Boon, 2011), only a few reports of breed-specific reference intervals for 2-D STE-derived measures of LV function have been published. Investigated breeds include the English Springer Spaniel (Dickson, Shave, Rishniw, & Patteson, 2017), Great Dane (Pedro, Stephenson, Linney, Cripps, & Dukes-McEwan, 2017), Irish Wolfhound (Westrup & McEvoy, 2013) and Labrador Retriever

(Carnabuci et al., 2013). In the English Springer Spaniel breed, conventional measures of LV size and function, such as FS, EF or end-systolic volume index, often fall outside of published canine reference intervals. However, global longitudinal strain (GLS) and other longitudinal parameters, such as TDI-derived myocardial velocities, appear similar to data published for other breeds, suggesting that these measurements could be more helpful in the assessment of myocardial performance and could prevent the inaccurate diagnosis of systolic dysfunction, which can occur with conventional techniques (Dickson et al., 2017). In Great Danes, as previously shown in humans, a statistically significant progressive increase from base to apex was noted for circumferential and radial strain and SR parameters (Armstrong & Ryan, 2010; Pedro et al., 2017). In the Irish Wolfhound breed, a wide range of normal values were found, confirming the high patient-to-patient variability described in humans (Armstrong & Ryan, 2010; Westrup & McEvoy, 2013).

The effect of age on 2-D STE-derived variables of LV systolic and diastolic function has been investigated by Suzuki and colleagues (Suzuki, Matsumoto, Teshima, & Koyama, 2013b) in a group of healthy beagle dogs. While in humans, a significant reduction in LV systolic function measured by 2-D STE with age has been repeatedly observed (Alcidi et al., 2017; Dalen et al., 2010), Suzuki and colleagues found similar systolic myocardial performance in young and old healthy beagle dogs. However, diastolic deformations varied, highlighting the need for using age-matched control subjects when investigating diastolic function (Suzuki et al., 2013b). More specifically, the early diastolic circumferential SR, basal rotation rate, and torsion rate were significantly lower, and late diastolic longitudinal and radial SR were significantly higher in old dogs compared with young dogs (Suzuki et al., 2013b). On the other hand, Pedro and colleagues could not identify an influence of age on the STE variables measured in healthy Great Danes, either in systole or in diastole (Pedro et al., 2017).

Heart rate (HR) can also affect accuracy of 2-D STE-derived measurements, and high HR at conventional FR might result in underestimation of GLS (D'hooge et al., 2016). The effect of HR on LV myocardial function was investigated by Suzuki and colleagues (Suzuki, Matsumoto, Teshima, & Koyama, 2013c) using 2-D STE in healthy anesthetized dogs. In their study, HR was controlled through right atrial pacing, and myocardial deformation indices were assessed at pacing rates of 120, 140, 160, and 180 bpm. Their results showed that, while torsion rate in early diastole was elevated at 180 bpm, longitudinal, circumferential, and radial strain and SR were not affected by increases in HR, providing FR was also progressively increased.

1.7 Two-dimensional speckle tracking echocardiography for clinical use in other species

Quantification of LV function by 2-D STE in cats (**Fig. 6**) has been proposed. Left ventricular longitudinal strain and SR values were first calculated by means of 2-D STE in the feline species by Silva and colleagues (Silva et al., 2013). This study, investigating 30 nonsedated healthy cats, demonstrated that 2-D STE was feasible for measuring the research variables, and preliminary reference values for global and segmental longitudinal strain and SR were established (-15.65 ± 5.46% and -1.80 ± 0.59 s^{-1}, respectively). Sugimoto and colleagues (Sugimoto, Fujii, Sunahara, & Aoki, 2015) later confirmed the low variability and clinical applicability of longitudinal 2-D STE analysis in cats, and provided normal GLS, systolic and early and late diastolic SR values obtained from a group of 13 healthy cats (-24.6 ± 2.6%, -3.50 ± 0.46 s^{-1}, 5.07 ± 0.96 s^{-1} and 3.08 ± 0.25 s^{-1}, respectively), which seem to differ from those previously published by Silva and colleagues. However, different post-processing software packages were used in the above studies, which may explain, at least partially, the difference observed.

Additionally, Takano and colleagues (Takano, Isogai, Aoki, Wakao, & Fujii, 2015) reported the feasibility of circumferential and radial 2-D STE strain analysis in 16 healthy cats. In this study, intra- and inter-observer variability were investigated, and most variables showed measurement errors less than 15%, considered adequate for clinical use.

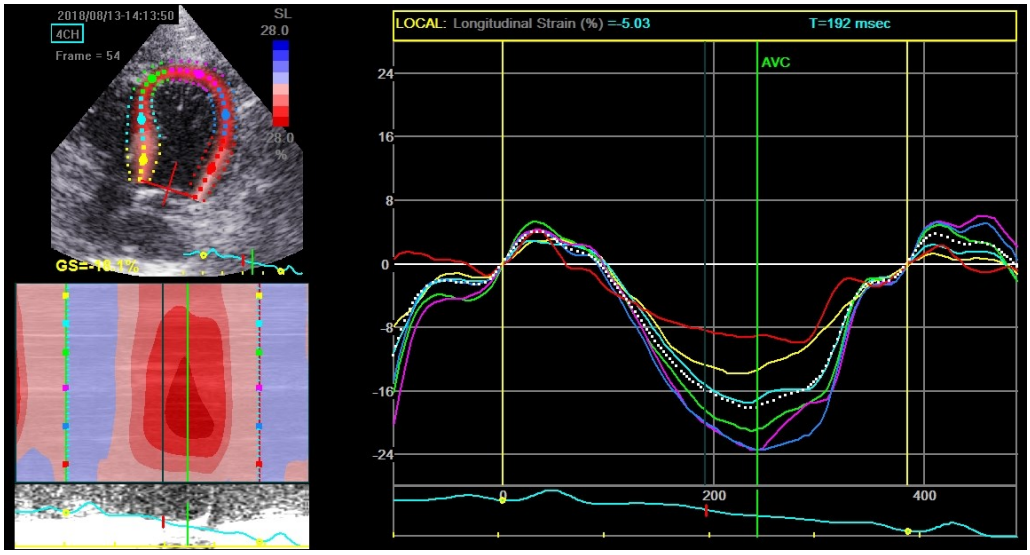

Figure 6. Example of segmental and global longitudinal strain analysis of the left ventricle performed through two-dimensional speckle tracking echocardiography in a healthy cat. Note the heterogeneity of segmental strain values. The global strain (GS) value reported on the left below the two-dimensional gray image represents global longitudinal peak strain (-18.1%). Used by permission of the Hospital for Small Animals of the University of Edinburgh.

Left ventricular myocardial torsional deformations were also assessed using 2-D STE by Suzuki and colleagues (Suzuki et al., 2016) in 14 healthy cats, and the repeatability of the measurements was reported as acceptable, with CV less than 15%.

Several studies on 2-D STE have been conducted in healthy horses at rest, and the feasibility of the technique for the quantification of equine radial, circumferential and longitudinal LV function has been demonstrated (Decloedt et al., 2011; Decloedt, Verheyen, Sys, De Clercq, & van Loon, 2013; Schwarzwald, Schober, Berli, & Bonagura, 2009). Furthermore, longitudinal and radial strain and SR by 2-D STE proved to be feasible for quantitative assessment of stress echocardiograms in athletic horses after high-speed treadmill exercise, while TDI was deemed technically difficult and inaccurate (Schefer, Bitschnau, Weishaupt, & Schwarzwald, 2010).

Schwarzwald and colleagues (Schwarzwald et al., 2009) reported good reliability of 2-D STE for characterization of LV radial systolic wall motion in healthy horses, when segmental and averaged indices including strain, SR, displacement, and rotation were examined. However, in this study, circumferential measurements were less reliable, and diastolic measurements were invalid because of inaccurate tracking. Reported averaged values of LV radial function measured at the level of the chordae tendinae in 6 healthy adult horses at rest were as follows: peak strain 48.61 ± 10.71%; peak systolic SR 1.38 ± 0.17 s^{-1}; peak early diastolic SR -1.21 ± 0.32; peak late diastolic SR -1.23 ± 0.43 (Schwarzwald et al., 2009).

In another study by Decloedt and colleagues (Decloedt et al., 2013), measurements of radial displacement and global and averaged systolic circumferential and radial strain and SR could be obtained with low to moderate variability; however, early and late diastolic SR and systolic rotation showed moderate variability. In this study, segmental peak timing and radial strain were the most reliable parameters for evaluation of regional LV function. Reported global values of LV circumferential function measured at the level of the chordae tendinae and papillary muscles in 10 healthy adult trotter horses at rest were, respectively, as follows: peak strain -19.3 ± 1.79% and -19.7 ± 1.88%; peak systolic SR -0.63 ± 0.08 s^{-1} and -0.69 ± 0.09 s^{-1}; peak early diastolic SR 1.22 ± 0.14 s^{-1} and 1.10 ± 0.17 s^{-1}; peak late diastolic SR 0.38 ± 0.08 s^{-1} and 0.40 ± 0.09 s^{-1} (Decloedt et al., 2013).

Decloedt and colleagues (Decloedt et al., 2011) also found 2-D STE to be a reliable technique for the measurement of global and regional longitudinal myocardial strain, SR, velocity, and displacement in healthy horses, with strain and SR exhibiting lower variability than velocity and displacement. In this study, measurements in systole showed higher reliability than in diastole, as previously found by Schwarzwald and colleagues (Schwarzwald et al., 2009) for circumferential and radial parameters. Decloedt and colleagues also established preliminary reference values for 2-D STE-derived longitudinal indices based on measurements obtained in 10 healthy adult trotter horses at rest. Global values of LV longitudinal function reported were as follows: peak strain -24.3 ± 1.72%; peak systolic SR -0.88 ± 0.05 s^{-1}; peak early diastolic SR 0.98 ± 0.09 s^{-1}; peak late diastolic SR 0.63 ± 0.12 s^{-1} (Decloedt et al., 2011).

The effects of HR on 2-D STE indices were explored by Schefer and colleagues (Schefer et al, 2010) during stress echocardiography in horses. The authors demonstrated that radial and longitudinal strain decreased while systolic SR increased at HR higher than 100 bpm, indicating HR dependence of the values, and the need for instantaneous HR assessment together with LV function quantification.

An effect of aging on cardiac function has also been shown in healthy horses, with age exerting a significant influence on LV free wall systolic SR and early diastolic relaxation, as well as interventricular septum systolic and late diastolic contraction velocities (Gehlen & Bildheim, 2018).

Furthermore, the effects of endurance riding on healthy horses were examined by Flethøy and colleagues (Flethøy et al., 2016), who demonstrated transient diastolic dysfunction after prolonged exercise, characterized by a small but significant decrease in early diastolic SR, both in longitudinal and circumferential directions, only partially explained by the altered loading conditions.

At present, 2-D STE remains to be validated in cats and horses against a gold standard technique for LV function assessment, such as sonomicrometry or tagged MRI.

Short-axis 2-D STE for the evaluation and quantification of LV function has also been investigated in calves, where good intra- and inter-observer agreements were found for most global and systolic measurements, and radial strain and SR showed less variability than circumferential values (Lecoq, Moula, Amory, Rollin, & Leroux, 2018).

1.8 The effects of sedation on two-dimensional speckle tracking echocardiography-derived parameters of left ventricular function in dogs

Since sedatives are sometimes needed in veterinary medicine to facilitate the echocardiographic examination when a patient is anxious or not cooperative, the influence of sedation on echocardiographic variables has been a subject of interest for clinicians and researchers. While numerous studies investigating the effects of different sedatives on conventional echocardiographic variables have been published (Kellihan et al., 2015; Page, Edmunds & Atwell, 1993; Saponaro et al., 2013; Ward, Schober, Luis Fuentes, & Bonagura, 2012), data regarding the influence of sedation on 2-D STE-derived indices are scarce.

The effects of a combination of acepromazine (ACP) and buprenorphine on 2-D STE-derived global radial and circumferential strain and systolic and early diastolic SR have been assessed in six healthy beagles by Takano and colleagues (Takano, Fujii, Yugeta, Takeda, & Wakao, 2011). In this study, parameters were obtained at baseline and 15 minutes after sedation with ACP (0.01 mg/kg, IV) and buprenorphine (0.0075 mg/kg, IV), and then compared. While a few conventional echocardiographic variables showed a significant difference between pre- and post-sedation values, no significant effect on 2-D STE-derived variables was noted (Takano et al., 2011).

1.9 Assessment of left ventricular function by two-dimensional speckle tracking echocardiography in cardiac disease: veterinary clinical studies

The main areas of application of 2-D STE in human medicine have been assessment of myocardial mechanics, ischemic heart disease, cardiomyopathies, LV diastolic dysfunction and subclinical myocardial dysfunction in patients affected by valvular disease or undergoing chemotherapy (Voigt et al., 2015).

The 2-D STE technique has also been used in animals with spontaneously occurring cardiovascular diseases. Several 2-D STE-derived indices have been assessed in canine patients with myxomatous mitral valve disease (MMVD) of different severities (Smith, Bonagura, Culwell, & Schober, 2012; Suzuki, Matsumoto, Teshima, & Koyama, 2013a, 2013d; Zois et al., 2012; Zois et al., 2013), dilated cardiomyopathy (DCM; Chetboul et al., 2007, 2008; Pedro et al., 2017), patent ductus arteriosus (PDA; Chetboul et al., 2007, 2008; Hamabe et al., 2015; Spalla, Locatelli, Zanaboni, Brambilla, & Bussadori, 2016a, 2016b), and LV hypertrophy secondary to hyperadrenocorticism (Chen, Lien & Huang, 2014).

Furthermore, the applicability of 2-D STE in feline hypertrophic cardiomyopathy (HCM) has interested various clinical researchers (Sugimoto et al., 2015; Suzuki et al., 2016; Takano et al., 2015), and its contribution to the detection of LV systolic dysfunction has been investigated in horses accidentally exposed to lasalocid (Decloedt, Verheyen, Sys, De Clercq, & van Loon, 2012).

In dogs with naturally occurring MMVD, 2-D STE has been shown to be feasible in a majority of patients, and the repeatability and within-day and between-day reproducibility of the measurements acceptable (Smith et al., 2012; Suzuki et al., 2013a; Zois et al., 2012; Zois et al., 2013).

Mitral regurgitation caused by MMVD is the most common cause of LV remodeling and heart failure in dogs, and echocardiographic studies using conventional parameters of LV function have demonstrated a hyperdynamic global state of the LV in advanced stages of the disease in small-breed dogs (Smith et al., 2012). In a group of 20 dogs with MMVD and LV remodeling (ACVIM Stage B2; Atkins et al., 2009), Smith and colleagues (Smith et al., 2012) measured significantly higher segmental radial strain and SR and global circumferential strain values than in a control group of healthy dogs of similar weight and age, demonstrating that, similar to conventional indices, 2-D STE-derived parameters indicate hyperdynamic deformation of the LV in the short-axis plane. Therefore, there is no obvious advantage in using strain analysis in small-breed dogs at this stage of the disease, because either systolic function is preserved, or strain parameters are influenced by the same loading conditions that confound conventional indices (Smith et al., 2012).

Similarly, in another study by Zois and colleagues (Zois et al., 2012), asymptomatic dogs with LV remodeling showed higher radial SR parameters compared with dogs with no or minimal mitral regurgitation. In the same study, increased longitudinal and radial strain and SR values were also demonstrated in dogs with congestive heart failure, compared with dogs with no or minimal mitral regurgitation. In addition, the above-mentioned variables exhibited significant curvilinear associations with the left atrium to aorta ratio (LA/Ao), an echocardiographic parameter used as an index of disease severity. The findings of increased strain parameters in dogs with congestive heart failure seemed therefore to extend the abovementioned findings by Smith and colleagues to symptomatic stages of the disease.

However, Suzuki and colleagues (Suzuki et al., 2013a) did not find a significant difference in longitudinal strain and SR or radial SR between different severity categories, while circumferential strain and SR and radial strain did increase with disease progression, being higher in dogs with moderate to severe clinical signs compared with those with only mild signs. It seems therefore that, in the clinical progression of the disease, the behavior of myocardial deformation may differ according to the contractile direction of the myofibers (Suzuki et al., 2013a), but the results of different investigators are not in complete agreement. However, their use of different severity classifications makes an accurate comparison between studies difficult.

Left ventricular function has also been assessed using 2-D STE in dogs with LV systolic dysfunction (**Fig. 7**; Chetboul et al., 2007, 2008; Pedro et al., 2017).

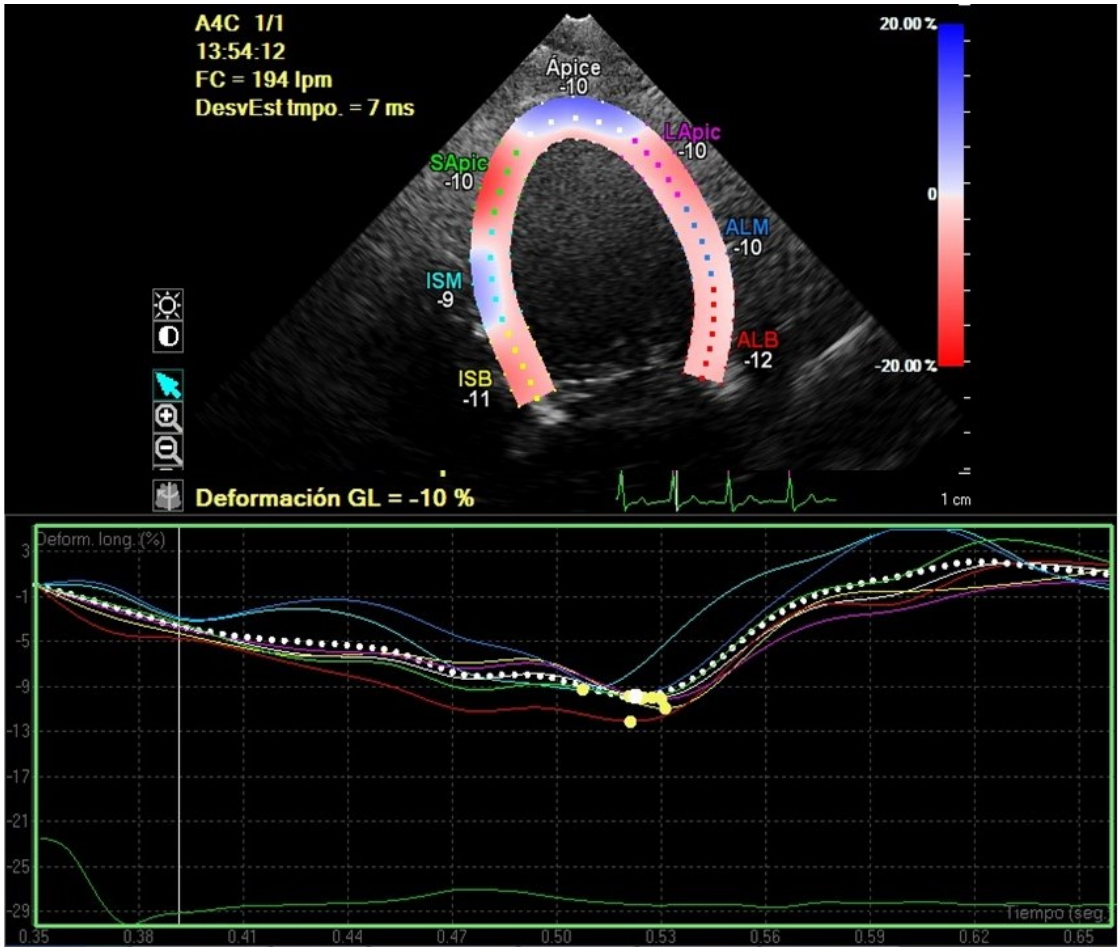

Figure 7. Example of segmental (colored curves) and global (white dotted curve) longitudinal strain of the left ventricle, obtained with two-dimensional speckle tarcking echocardiography in a dog with idiopathic dilated cardiomyopathy. Note the inhomogeneous timings of segmental peak strains, and the characteristic low values observed. Used by permission of the Veterinary Teaching Hospital of the University of Murcia.

Chetboul and colleagues (Chetboul et al., 2007, 2008) compared 2-D STE-derived values obtained in healthy dogs with those from a small group of diseased dogs with reduced LV myocardial function, including dogs with DCM and PDA. Peak systolic radial LV strain and SR were found to be significantly decreased and the STI significantly increased in dogs with reduced LV systolic function compared with healthy dogs; furthermore, some dyskinetic segments showing negative systolic strain were identified in a few diseased dogs (Chetboul et al., 2007). Moreover, peak end-systolic basal and apical rotations, and LV torsion were significantly decreased in dogs with hypokinesia compared with healthy dogs (Chetboul et al., 2008).

In Great Danes, an overall decrease in 2-D STE-derived strain and SR values was noted in dogs with DCM when compared to healthy ones, with both systolic and diastolic function affected (Pedro et al., 2017). In the same study, SR variables showed more significant differences than strain, potentially representing more reliable indicators of early myocardial dysfunction; however, the high inter- and intra-observer measurement variability found for most 2-D STE-derived indices was suggested to preclude their use for screening purposes (Pedro et al., 2017).

In a group of 34 dogs with a left-to-right shunting PDA, 2-D STE-derived global longitudinal, radial and circumferential strain and SR were found to be increased compared to healthy sex- and weight-matched controls, together with conventional parameters such as LV dimensions and volumes (Spalla et al., 2016a). As EF and FS were not different between groups, 2-D STE was suggested by the authors as a more appropriate tool to assess LV systolic function, which appeared enhanced, in dogs with PDA (Spalla et al., 2016a). The same authors (Spalla et al., 2016b) investigated the effects of percutaneous ductal closure on conventional and 2-D STE-derived echocardiographic parameters, and found that a statistically significant decrease in the absolute values of radial and circumferential strain and SR was produced 24 hours after the procedure, associated with a reduction in systolic and diastolic dimensions, volumes, and other indices of systolic function such as EF and FS. The above changes were therefore interpreted as a result of the marked modification of loading conditions, however no evidence of systolic dysfunction was apparent as none of the 2-D STE-derived parameters were below reference ranges (Spalla et al., 2016b). Integrating the results of the two studies, it was therefore suggested that in the short-term after PDA closure, longitudinal function might be enhanced while, in the short-axis, normality is re-established (Spalla et al., 2016a, 2016b). Hamabe and

colleagues (Hamabe et al., 2015), who investigated 17 dogs with left-to-right shunting PDA before and after surgical closure, also observed significant decreased in FS and radial and circumferential strain values three days after the procedure. However, in the latter study, LV dyssynchrony was also observed, and the decrease in strain values was considered an indication of systolic dysfunction. While the interpretation of the results obtained by the different authors seem conflicting, a comparison is difficult due to the lack of healthy controls in the study by Hamabe and colleagues.

In dogs with hyperadrenocorticism and LV hypertrophy, 2-D STE-derived global circumferential strain, longitudinal strain and longitudinal systolic and early diastolic SR decreased linearly with increased diastolic dimension of the interventricular septum, revealing a significant reduction in systolic function not detected by conventional echocardiography (Chen et al., 2014).

In cats with HCM, longitudinal strain analysis was first performed via color TDI, and showed significantly decreased myocardial strain in diseased cats despite apparently normal LV systolic function as assessed by conventional echocardiography (Wess, Sarkar, & Hartmann, 2010). The presence of abnormal systolic function in cats with HCM and a normal or supernormal contractile state based on conventional echocardiography was also demonstrated through the use of 2-D STE by Suzuki and colleagues (Suzuki et al., 2017).

On the other hand, 2-D STE appeared to be more sensitive than TDI to detect myocardial diastolic dysfunction in asymptomatic cats with HCM. In fact, in a study by Sugimoto and colleagues, longitudinal early diastolic SR was significantly decreased in cats with HCM and normal TDI measurements, even in segments without echocardiographic evidence of hypertrophy (Sugimoto et al., 2015). Radial and circumferential early diastolic SR values were also significantly lower in asymptomatic cats with HCM than in healthy controls (Takano et al., 2015), confirming the presence of diastolic dysfunction in early stages of the disease, detectable in the three directions of deformation. However, segmental analysis in cats with HCM revealed that radial strain and early diastolic SR were lower in hypertrophied segments compared to non-hypertrophied segments (Takano et al., 2015), in contrast to what was observed by Sugimoto and colleagues with longitudinal strain parameters (Sugimoto et al., 2015), suggesting different and contrasting utility of the technique depending on the direction interrogated. Additionally, higher peak systolic torsion and peak systolic apical rotation were found in a group of 26 cats with HCM compared with healthy controls (Suzuki et al., 2016).

In horses accidentally exposed to lasalocid, 2-D STE allowed accurate detection and quantification of long-term LV dysfunction secondary to myocardial damage caused by the toxic effects of the drug, revealing significantly decreased radial, circumferential and longitudinal strain values, correlating well with changes in FS, TDI, and cardiac troponin levels (Decloedt et al., 2012).

1.10 Two-dimensional speckle tracking echocardiography for evaluation of chambers other than the left ventricle

Although the most common use of 2-D STE is to aid the analysis of LV function, its utility in the functional assessment of the left atrium and right ventricle (RV) has also been demonstrated (Cameli et al., 2009; Carluccio et al., 2018).

In human medicine, speckle tracking imaging has been shown to be a feasible and reproducible technique to assess left atrial longitudinal strain in healthy subjects (Cameli et al., 2009). Quantification of left atrial phasic function by 2-D STE has also been recently proposed in veterinary medicine, and investigated in healthy dogs by means of time-left atrial area curve analysis (Osuga et al., 2013; Osuga et al., 2015) and longitudinal strain and SR (Caivano et al, 2016). With the former method, the area of the left atrium is calculated by the software throughout the cardiac cycle, and used to derive time-area curves and different variables that reflect the three phases (reservoir, conduit and contractile) of left atrial function (Osuga et al., 2013). The time-left atrial area curve analysis has been demonstrated to be feasible and reproducible in healthy dogs (Osuga et al., 2013). On the other hand, left atrial longitudinal strain and SR analysis, while feasible in most of the healthy dogs included in the study by Caivano and colleagues (Caivano et al., 2016), showed nonuniform reproducibility, varying according to the phase investigated and being low in some cases.

Two-dimensional STE has also been used to evaluate the left atrium in dogs with MMVD (**Fig. 8**), proving to be helpful in detecting a decline of left atrial function as the disease progresses (Baron Toaldo et al., 2017; Caivano et al., 2018; Nakamura et al., 2017). Moreover, the maximal left atrial strain seems to predict cardiac death in dogs with MMVD (Baron Toaldo et al., 2018).

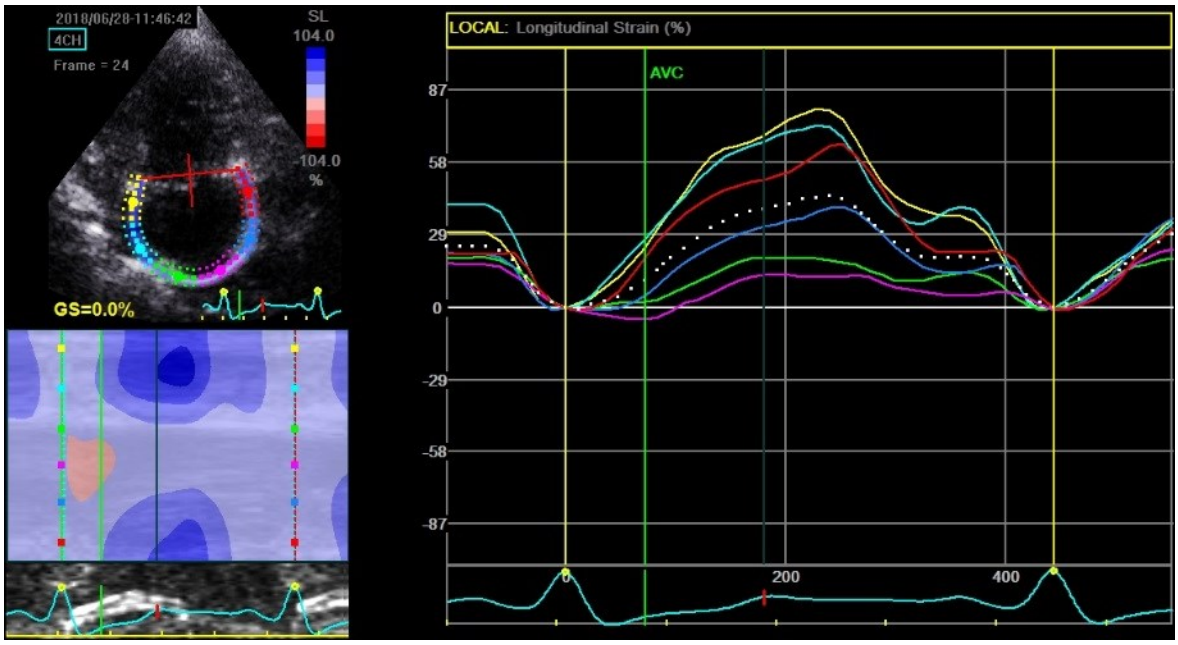

Figure 8. Representative image of a left atrial longitudinal strain profile, obtained with 2-D STE in a dog with advanced compensated MMVD. Segmental (colored curves) and global (white dotted curve) longitudinal time-strain curves are displayed. An erroneous GLS value of 0% is displayed as the algorithm used is designed for LV assessment and is created to exhibit negative values. However, correct strain values could be visualized if the cursor was positioned over the time-strain curve at the desired time point. Used by permission of the Hospital for Small Animals of the University of Edinburgh.

Concerning the RV, its function is more difficult to quantify compared to the LV. However, its quantitative assessment also seems to play an important role, even in diseases previously considered as left heart specific (Carluccio et al., 2018; Visser, 2017). Longitudinal strain and SR are considered useful parameters for the assessment of RV regional and global systolic function in humans (Lang et al., 2015).

In veterinary medicine, where the echocardiographic investigation of the RV has recently gained more attention, longitudinal strain analysis has also been evaluated, among other methods of myocardial functional evaluation (Morita et al., 2017; Visser, 2017; Visser, Scansen, Brown, Schober, & Bonagura; Visser, Scansen, Schober, & Bonagura, 2015). Visser and colleagues (Visser, Scansen, Schober, et al., 2015) demonstrated that 2-D STE-derived global longitudinal RV free wall strain and SR were feasible to obtain, and their repeatability and intra- and inter-observer variability were clinically acceptable (CV less than 10%) in a group of healthy dogs. Furthermore, another research project by Visser and colleagues (Visser, Scansen, Brown, et al., 2015), enrolling the same population of healthy dogs, showed how these values could accurately track expected changes in RV systolic function following pimobendan and atenolol administration.

In healthy horses, RV functional measurements obtained by 2-D STE showed low variability, except for segmental SR (Decloedt, De Clercq, et al., 2017).

In dogs with MMVD, 2-D STE-derived parameters of RV systolic function, including RV free wall and global longitudinal strain and SR, varied significantly between different severity categories, with a tendency to increase in advanced compensated disease, and to decrease with decompensation (Chapel, Scansen, Schober, & Bonagura, 2018). However, in the same study by Chapel and colleagues, while global RV longitudinal strain demonstrated clinically acceptable measurement variability, free wall RV longitudinal strain and SR showed high variability. The latter was in contrast with the acceptable variability found in healthy subjects, therefore revealing a potentially limited use in dogs with cardiac disease and remodelled hearts (Chapel et al., 2018).

In asthmatic horses, altered RV function could be detected by 2-D STE; more specifically, acute pulmonary obstruction induced a significant decrease in GLS, and the comparison of severely asthmatic horses in remission and healthy controls demonstrated significant differences in several 2-D STE-derived measurements of longitudinal RV function (Decloedt, Borowicz, et al., 2017).

1.11 A focus on the echocardiographic planes used for left ventricular deformation analysis

In humans, longitudinal deformation of the LV is evaluated by integrating values obtained from the apical two-chamber, four-chamber and five-chamber views (Blessberger & Binder, 2010). In dogs, the standard left apical four-chamber (LAp4Ch) view is typically used for this purpose (**Fig. 9**), and 2-D STE performed from this view has been validated in healthy anesthetized subjects against sonomicrometry, providing accurate measurements of LV dimensions and strains (Amundsen et al., 2006). However, in some dogs, especially if deep-chested, a good quality four-chamber image can be difficult to obtain from the left parasternal apical location (Dukes-McEwan, 2002), and the LAp4Ch view has been associated with tracking errors that can invalidate strain data obtained from the LV free wall, mainly due to side lobe artifacts (Griffiths et al., 2011; Wess et al., 2011).

Different echocardiographic planes might be recommended in other species based on their peculiar anatomic characteristics (Abduch et al., 2014). In cats, the LAp4Ch view is typically chosen (Silva et al., 2013; Sugimoto et al., 2015; Suzuki et al., 2017), as it is in

dogs. In horses, a modified four-chamber view obtained by adjusting the standard right parasternal four-chamber (RP4Ch) view is employed (Decloedt et al., 2011, 2012; Schefer et al., 2010; Schwarzwald et al., 2009). Similarly, the RP4Ch view has been adopted for this purpose in goats, in which the right parasternal approach is considered to be the only reliable one for transthoracic echocardiography, as in other ruminants (Abduch et al., 2014; Berli, Jud Schefer, Steininger, & Schwarzwald, 2015). A subxiphoid approach providing an apical four-chamber view has been chosen in pigs (Ishikawa et al., 2015), while left parasternal long-axis planes in mice, rats and rabbits (Kusunose et al., 2012), and sagittal long-axis planes in zebrafish are used (Hein et al., 2015).

For the evaluation of LV radial and circumferential strain and SR, parasternal short-axis views of the LV are employed (**Fig. 10**), and in most species, a right parasternal approach is achievable (Abduch et al., 2014). The use of the right parasternal short–axis view for this purpose has been described in dogs, cats, and horses (Chetboul et al., 2007; Decloedt et al., 2012; Schefer et al., 2010; Suzuki et al., 2017; Takano et al., 2010; Takano et al., 2011; Takano et al., 2015; Zois et al., 2013). The planes analyzed are the ones obtained either at the level of the papillary muscles (Chetboul et al., 2007; Decloedt et al., 2012; Suzuki et al., 2017; Zois et al., 2012), or at the level of the chordae tendinae (Decloedt et al., 2012; Schefer et al., 2010; Schwarzwald et al., 2009; Takano et al., 2010; Takano et al., 2011; Takano et al., 2015).

A right parasternal short-axis view of the LV, with recordings made at the basal and apical imaging planes, is used for torsional deformation analysis, as described in dogs and cats (Chetboul et al., 2008; Suzuki et al., 2013, 2016). Basal views are typically obtained at the mitral valve level, while apical views are obtained at the apex with no visible papillary muscles (Chetboul et al., 2008; Suzuki et al., 2013; Suzuki et al., 2016). From these views, rotation values are obtained, and included in calculations that allow derivation of torsion parameters.

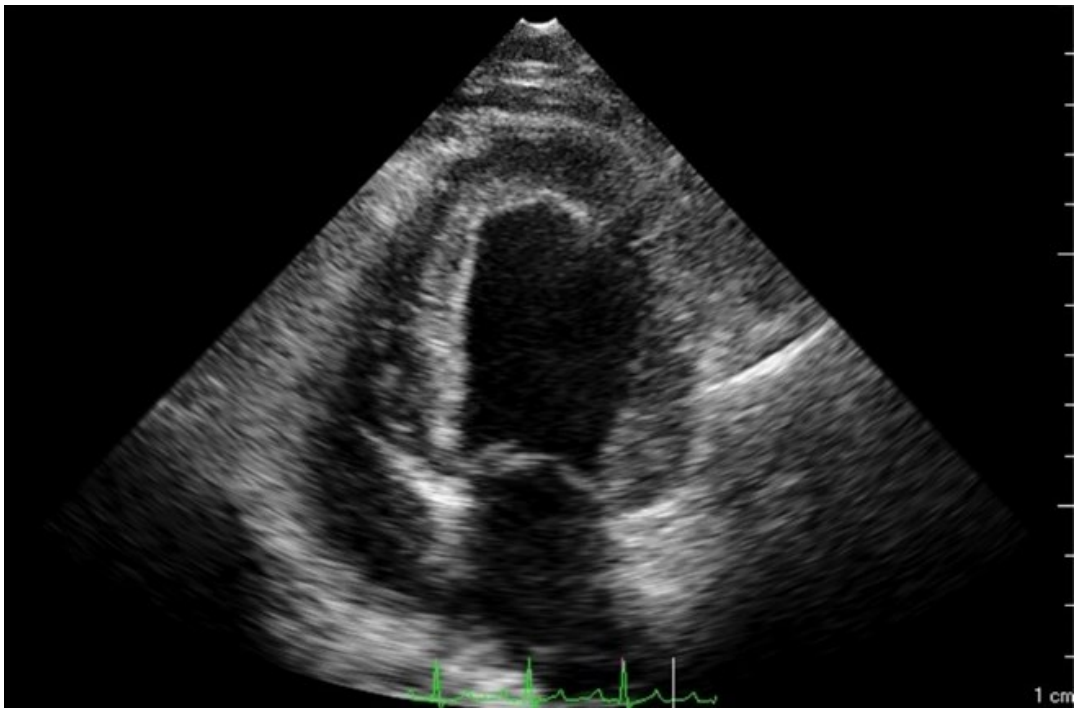

Figure 9. Representative two-dimensional echocardiographic image obtained from a healthy dog providing a left apical 4-chamber view of the left ventricle. Used by permission of the Veterinary Teaching Hospital of the University of Murcia.

Figure 10. Representative two-dimensional echocardiographic image obtained from a healthy dog providing a right parasternal short-axis view at the level of the papillary muscles. Used by permission of the Veterinary Teaching Hospital of the University of Murcia.

1.12 Inter-software variability of two-dimensional speckle tracking echocardiography-derived parameters

Several vendor dependent and independent software platforms have been developed in the past few years to perform strain analysis by 2-D STE (van Everdingen et al., 2017). Discrepancies between platforms potentially leading to significantly different results are recognized in human medicine, and post-processing has been addressed as an important determinant of this intervendor variability (Farsalinos et al., 2015). Various researchers have focused their attention on the intervendor variability of LV deformation analysis (Biaggi et al., 2011; Costa et al., 2014; D'hooge et al., 2016; Nagata et al., 2015; Nagata, Wu, Otsuji, & Takeuchi, 2017; Risum et al., 2012; Shiino et al., 2017; van Everdingen et al., 2017). Furthermore, a taskforce of the European Association of Cardiovascular Imaging and American Society of Echocardiography (EACVI/ASE) was appointed to standardize deformation imaging (Farsalinos et al., 2015; Voigt et al., 2015). The taskforce identified a moderate but statistically significant variation in GLS values among vendors, with an absolute difference between platforms reaching up to 3.7% strain units in the same patient, which could become especially meaningful when performing serial studies (Farsalinos et al., 2015).

Publications on 2-D STE parameters in veterinary medicine mainly use vendor dependent software, including different versions of General Electric (GE) EchoPac (Chicago, Illinois; Chetboul et al., 2007, 2008; Culwell et al., 2011; Dickson et al., 2017; Pedro et al., 2017; Smith et al., 2012; Sugimoto et al., 2015; Suzuki et al., 2013a, 2013b, 2013c, 2013d; Suzuki et al., 2016; Suzuki et al., 2017; Takano et al., 2011; Takano et al., 2015; Wess et al., 2011; Zois et al., 2012; Zois et al., 2013), Esaote XStrain (Firenze, Italy; Silva et al., 2013; Spalla et al., 2016a, 2016b), Philips Qlab (Andover, Massachusetts; Baron Toaldo et al., 2017, 2018), and Hitachi DAS-RS1 (Tokyo, Japan; Hamabe et al., 2015).

The algorithms used to perform deformation analysis in dogs are therefore mainly proprietary, and are not open-source. Furthermore, they have been designed for use in people, and it might thus be speculated that similar variability as in human medicine exist. However, while the limitations related to the poor algorithm standardization across manufacturers have been mentioned (Smith et al., 2012), systematic studies that could provide a better insight into the matter are lacking.

OBJECTIVES

2. OBJETIVES

The objectives of the Ph. D. project reported here were:

- to determine the effects of a commonly used sedative protocol, combining acepromazine and butorphanol, on strain values obtained using two-dimensional (2-D) speckle tracking echocardiography (STE) in healthy dogs (**Study 1**).
- to determine the feasibility and reliability of the right parasternal four-chamber (RP4Ch) view for longitudinal strain and strain rate (SR) assessment in dogs, and to compare the values obtained from this view and the left apical four-chamber (LAp4Ch) view to establish whether the two projections can be used interchangeably (**Study 2**).
- to determine the agreement of vendor-specific and vendor-independent software on 2-D STE-derived longitudinal global strain and SR parameters in dogs (**Study 3**).

MATERIALS & METHODS

3. MATERIALS & METHODS

3.1 Study 1: Effects of a sedation protocol combining acepromazine and butorphanol on two-dimensional speckle tracking echocardiography-derived myocardial strain in healthy dogs

3.1.1 Study population

Adult dogs with no history of cardiac or respiratory disease, otherwise healthy and free of medication, were prospectively recruited between April 2013 and December 2014. The dogs were staff and student owned at the University of Murcia. Owner consent was obtained before enrolment in the study. Further, the study protocol received the approval of the Ethics Committee of the University of Murcia.

The subjects included in the study were medium to large-sized dogs (weighing between 15 and 50 Kg), and were older than 12 months of age. The animals were confirmed to be healthy based on the results of physical examination, complete blood count, serum biochemistry, noninvasive blood pressure measurement, electrocardiography (ECG) and conventional echocardiography.

3.1.2 Experimental procedures

The experiment consisted of two parts: the baseline examination and the sedation study, with the latter always carried out straight after the former, and both involving a noninvasive systemic arterial blood pressure determination and an echocardiographic examination. Before the baseline examination, fur was clipped from the chest of the dogs bilaterally over the area of projection of the heart, and from the cranial portion of their abdomen just caudal to the sternum. The dogs were given time to acclimatize to the examination room for a minimum of 15 minutes. Owners were allowed to remain in the room, upon their request, if this was considered helpful to minimize the stress of their pets.

The sedation protocol consisted of a combination of acepromazine (ACP; 0.02 mg/Kg) and butorphanol (BUT; 0.2 mg/Kg), given intramuscularly (IM). The above drug dosages were chosen after consulting published recommendations to obtain an ambulatory mild to moderate sedation in dogs (Armitage-Chan E, 2008). Following treatment administration, dogs were allowed to ambulate in the examination room or lay voluntarily,

and the echocardiographic examination was performed 30 to 40 minutes after the injection. The degree of sedation shown during the echocardiography was assessed. More specifically, this was deemed adequate if the operator could comfortably perform a quality diagnostic examination, and if the dogs maintained the lateral recumbence voluntarily with only minimal restraint, breathing calmly with negligible respiration artifacts. Attention was paid to any possible adverse effects of the treatment, which were recorded if observed.

3.1.3. Noninvasive systemic blood pressure measurement

Just prior to each echocardiographic examination, noninvasive systemic arterial blood pressure estimates were obtained by the Ph. D. student using a high-definition oscillometric device VET HDO MD PRO (S+B MedVet GmBH, Germany), designed for veterinary use. The dogs were positioned in sternal or lateral recumbence according to individual preference, and the cuff was fixed at the base of the tail.

Blood pressure was assessed after at least five minutes of gentle restraint, when the stress was reduced at the minimum possible. Three to five indirect estimates were attained, and the values of systolic (SAP), mean (MAP) and diastolic (DAP) arterial pressure recorded. Reliability of the recordings was assessed inspecting the blood pressure waveforms displayed on a computer monitor, using the dedicated MDSWIN analyse Software (S+B MedVet GmBH, Germany), designed for Windows. At least three reliable readings for each subject were averaged and employed for statistical analysis.

3.1.4. Echocardiographic examination

All the echocardiographic studies were performed with an iE33 ultrasound system (**Fig. 11**; Philips Medical Systems, Andover, MA, USA) with simultaneous ECG recording. The machine was equipped with a multifrequency 1-5 MHz phased-array sectorial transducer. The scans were obtained with the dogs gently restrained, first in right and then in left lateral recumbence. The images were obtained from beneath a scanning table with a cutout, designed for the purpose (**Fig. 11**).

Figure 11. Photograph of the echocardiographic unit employed in the study, located in the examination room where all the experimental procedures where realized. Part of the scanning table with cutout is also visualised on the right side of the picture. Used by permission of the Veterinary Teaching Hospital of the University of Murcia.

All echocardiographic examinations were carried out and measured by the Ph. D. supervisor using standard methods described elsewhere (Hansson, Häggström, Kvart, & Lord, 2002; Lang et al., 2005; Lang et al., 2015; Quiñones et al., 2002; Thomas et al., 1993). Each echocardiogram was stored digitally for offline analysis. The investigator was blinded to the sedation status when realizing the offline measurements. The data used for statistical analysis, detailed in the following sections, were averaged from at least three consecutive cardiac cycles displaying stable sinus rhythm.

3.1.4.1 M-mode measurements

M-mode measurements were obtained from two-dimesional (2-D) echocardiography-guided M-mode images of the left ventricle (LV) in short-axis, and the leading edge to leading edge method was used for this purpose. The variables measured at the level of the papillary muscles included: systolic and diastolic internal diameters (LVIDs and LVIDd), systolic and diastolic interventricular septum and posterior wall thicknesses, and percentage of fractional shortening (FS), the latter calculated using the formula [LVIDd-LVIDs]/LVIDd x 100%. At the level of the mitral valve, the E-point to septal separation was measured.

3.1.4.2 Two-dimensional measurements

From the right parasternal four-chamber (RP4Ch) view, measurements obtained included: LV end-systolic and end-diastolic volumes (ESV and EDV, respectively), obtained by the modified single plane Simpson's method, and LV ejection fraction, determined using the formula [EDV-ESV]/EDV x 100%. Left ventricular end-systolic and end-diastolic volume indices (ESVI and EDVI) were derived from the previously measured ESV and EDV, respectively, divided by body surface area.

From the right parasternal long-axis outflow view, the aortic annulus diameter was measured using the inner edge to inner edge method. The cross-sectional area of the annulus was then calculated as πr^2, where π is equal to 3.14 and r represents the radius of the annulus, corresponding to half of the diameter.

From the right parasternal short-axis view acquired at the level of the papillary muscles, LV luminal areas at end-systole and end-diastole (LVAs and LVAd) were obtained, and LV shortening area calculated using the formula [LVAd-LVAs]/LVAd x 100%.

From the right parasternal short-axis view acquired at the level of the left atrium and aortic valve, measurements of the left atrium (LA) and aorta (Ao) dimensions were made at the first frame after aortic valve closure in early ventricular diastole. The LA/Ao was subsequently calculated.

3.1.4.3 Spectral Doppler measurements

From the right parasternal short-axis view, acquired at the level of the pulmonary artery, pulmonary artery flow was interrogated with pulsed wave Doppler. Pulmonary artery peak velocity and transvalvular pressure gradient were obtained.

From the subcostal three- or five-chamber view, aortic flow was interrogated with continuous wave Doppler (**Fig. 12**). Aortic peak velocity, transvalvular pressure gradient, LV pre-ejection period (LVPEP), ejection time (LVET), and velocity time integral (VTI) were obtained. The PEP/LVET ratio was also calculated as an index of systolic function. The cardiac output was determined using the formula HR x cross-sectional area of the aortic annulus x VTI.

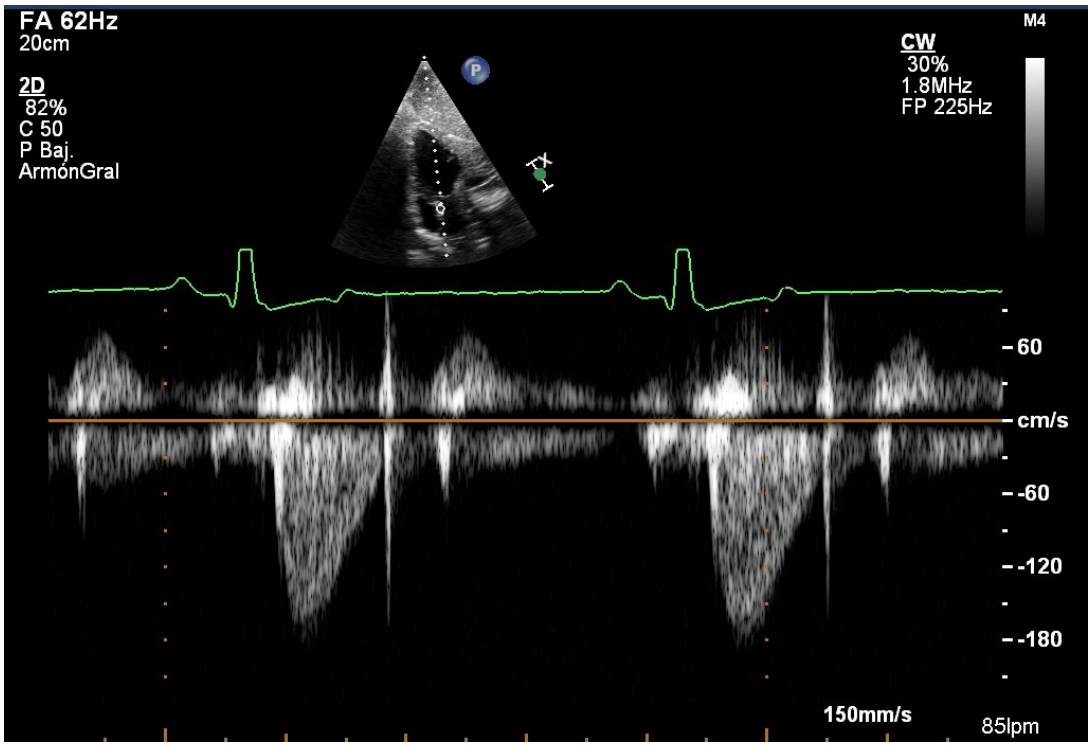

Figure 12. Representative image of aortic flow interrogation with continuous wave Doppler from a subcostal three-chamber view of the left ventricle, obtained in a healthy dog. Used by permission of the Veterinary Teaching Hospital of the University of Murcia.

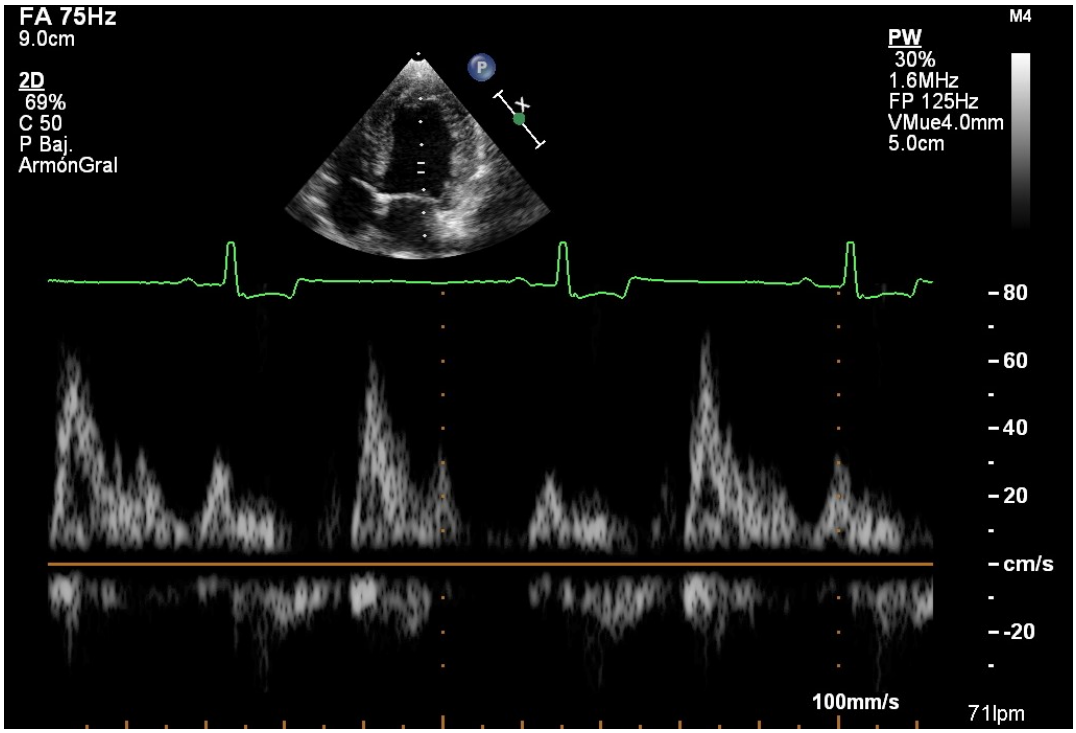

Figure 13. Representative image of transmitral flow interrogation with pulsed wave Doppler from a left apical four-chamber view of the left ventricle, obtained in a healthy dog. Used by permission of the Veterinary Teaching Hospital of the University of Murcia.

From the left apical four-chamber (LAp4Ch) view, transmitral flow was interrogated with pulsed-wave Doppler (**Fig. 13**). Variables measured included: peak velocity of early diastolic flow (E wave), E wave deceleration time, peak velocity of late diastolic flow (A wave), and A wave duration. Subsequently, the ratio between E wave and A wave (E/A) was calculated.

3.1.4.4 Spectral pulsed tissue Doppler measurements

From the LAp4Ch view, myocardial velocities (peak systolic, early diastolic, and late diastolic) were obtained using TDI, with the pulsed Doppler sample volume positioned first on the lateral side and then on the septal side of the mitral annulus. The ratio of E wave to tissue Doppler early diastolic lateral mitral annulus velocity was subsequently calculated. The LV myocardial performance index was also derived via TDI, and calculated as the sum of the isovolumic contraction time and isovolumic relaxation time divided by LVET. Tricuspid lateral annular velocities (peak systolic, early diastolic and late diastolic) were also determined.

3.1.4.5 Two-dimensional speckle tracking echocardiography

Strain analysis was conducted offline on a separate personal computer workstation using Qlab 2D Strain software, version 9.0 (Philips Medical Systems, Andover, MA, USA). Recordings of good quality 2-D cine loops of the LV, acquired at FR of 60 to 90 Hz for a minimum of four consecutive cardiac cycles were used**.**

Event timing for aortic valve closure was first recorded from the LV outflow tract flow profile obtained by Pulsed-wave Doppler. More specifically, the software allowed the operator to tag the first frame where the valve was observed closed at the end of systole, and later displayed its timing, on the same graphic where the time-strain curves were provided.

Longitudinal strain was calculated from the LA4Ch view as explained hereafter. Three reference points were manually placed, one on each side of the mitral valve annulus and the third at the apical endocardial border (**Fig. 14**).

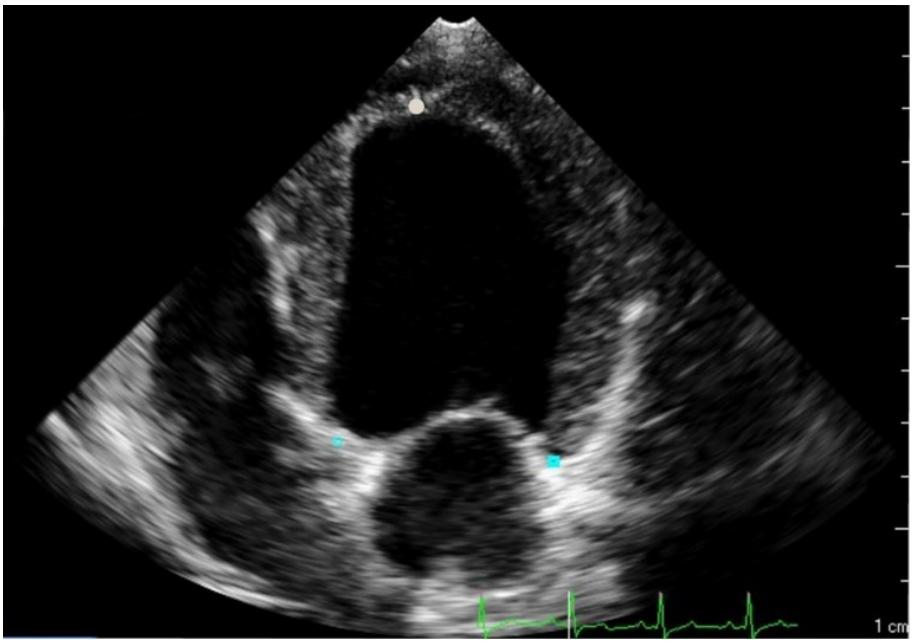

Figure 14. Left apical four-chamber view obtained in a healthy dog and analyzed with 2-D STE dedicated software. The image illustrates the first step of the process: the operator has manually placed three reference points, one on each side of the mitral valve annulus (light blue squares) and the third at the apical endocardial border (white dot). Used by permission of the Veterinary Teaching Hospital of the University of Murcia.

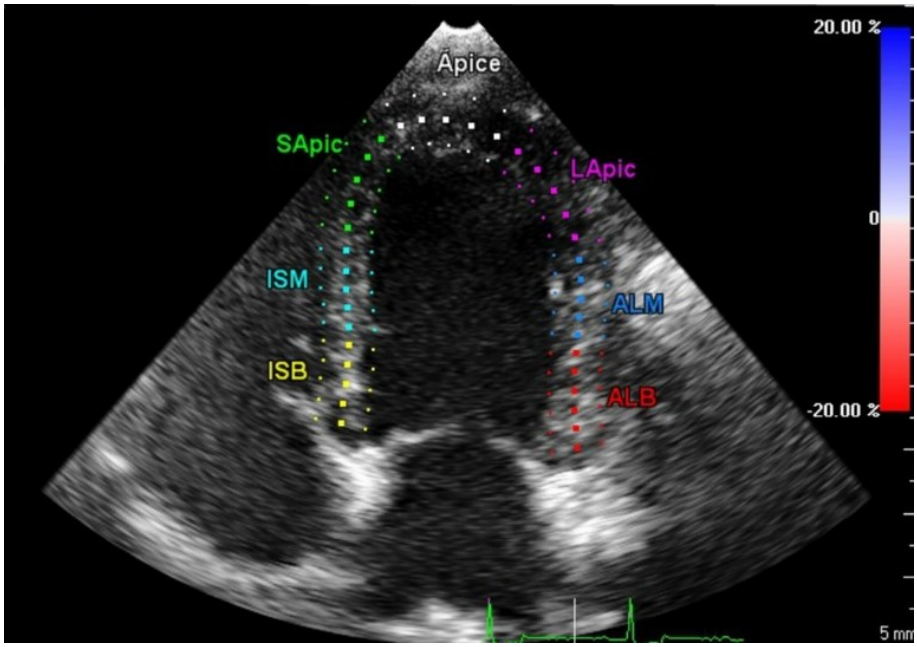

Figure 15. Left apical four-chamber view obtained in a healthy dog and analyzed with 2-D STE dedicated software. The image illustrates the ROI created by the software, to be adjusted by the operator to incorporate the entire myocardial thickness (note how the septal segments of the ROI exclude the portion closest to the right ventricle). The ROI is divided by the software in 7 segments according to standard segmentation models used in humans. The abbreviations in the pictures are different from the text as derived from the spanish designation of the segments. Used by permission of the Veterinary Teaching Hospital of the University of Murcia.

The software created a region of interest (ROI) with the automatic delineation of endocardial and epicardial borders, and divided the LV in seven segments (**Fig. 15**), according to standard segmentation models used in humans: basal septal (BS), midseptal (MS), apical septal (ApS), apical (Apex), apical lateral (ApL), midlateral (ML), basal lateral (BL).

The operator adjusted the ROI to incorporate the entire myocardial thickness and inspected the adequacy of segmentation. Subsequently, visual inspection of the loop in motion mode was performed to verify that the ROI correctly followed the movements of each segment throughout the cardiac cycle.

Figure 16. Left apical four-chamber view obtained in a healthy dog and analyzed with 2-D STE dedicated software. At the top of the image, the ROI created by the software and subsequently adjusted by the operator can be observed. Further, numeric values for segmental strain are displayed next to each segment. A numeric value for GLS is also provided (-25%), and can be observed on the left of the ECG tracing. At the bottom of the image, longitudinal segmental (couloured lines) and global (white dotted line) time-strain curves, calculated by the software, are provided. Used by permission of the Veterinary Teaching Hospital of the University of Murcia.

The software algorithm then tracked the speckles across the myocardium, deriving segmental and global strain values from a weighted average of the myocardial deformation with the weighting greatest at the endocardium. Global longitudinal strain (GLS) was calculated from the entire ROI considered as a single segment, and corresponded to a weighted average of the segmental strains. Segmental and global time-strain curves were then displayed by the software, and numeric values for segmental strains and GLS were provided on the screen (**Fig. 16**). These numeric values, representing the negative peak of the strain curves (peak strain), were recorded for analysis.

Circumferential strain was calculated from the right parasternal short axis view, acquired at the level of the papillary muscle, as explained hereafter. In each short-axis view, a circular ROI was automatically drawn by the software (**Fig. 17A**). The operator then adjusted the ROI manually to better incorporate the entire myocardial thickness (**Fig. 17B**). The software algorithm automatically segmented the LV short-axis in six segments (**Fig. 17**), according to standard segmentation models used in humans: antero-septal (AntSept), anterior (Ant), lateral (Lat), posterior (Post), inferior (Inf), septal (Sept). The adequacy of segmentation was inspected by the operator, and adjustment were made if necessary, rotating the ROI clockwise or counterclockwise.

Subsequently, visual inspection of the loop in motion mode was performed to verify that the ROI followed adequately followed the movements of each segment throughout the cardiac cycle. The software algorithm then tracked the speckles across the myocardium, deriving segmental and global strain values from a weighted average of the myocardial deformation with the weighting greatest at the endocardium. Global circumferential strain (GCS) was automatically calculated from the entire ROI, considered as a single segment, and corresponded to a weighted average of the segmental strains. Segmental and global time-strain curves were eventually displayed by the software, and numeric values for segmental strains and GCS were provided on the screen (**Fig. 18**). These numeric values, representing the negative peak of the strain curves (peak strain), were recorded for analysis.

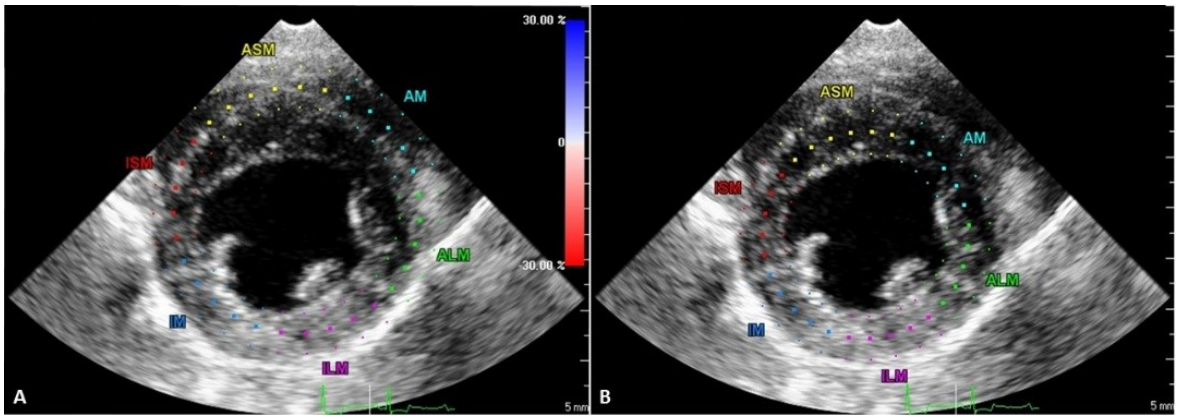

Figure 17. Short-axis view of the LV acquired at the level of the papillary muscles in a healthy dog and analyzed with 2-D STE dedicated software. Caption A shows a circular ROI automatically drawn by the software as a first step of the analysis (note how the ROI is not properly adjusted to the image of the LV). Caption B shows the ROI resulting from manual adjustment by the operator. In both captions, the ROI has been divided by the software in 6 segments according to standard segmentation models used in humans. The abbreviations in the pictures are different from the text as derived from the spanish designation of the segments. Used by permission of the Veterinary Teaching Hospital of the University of Murcia.

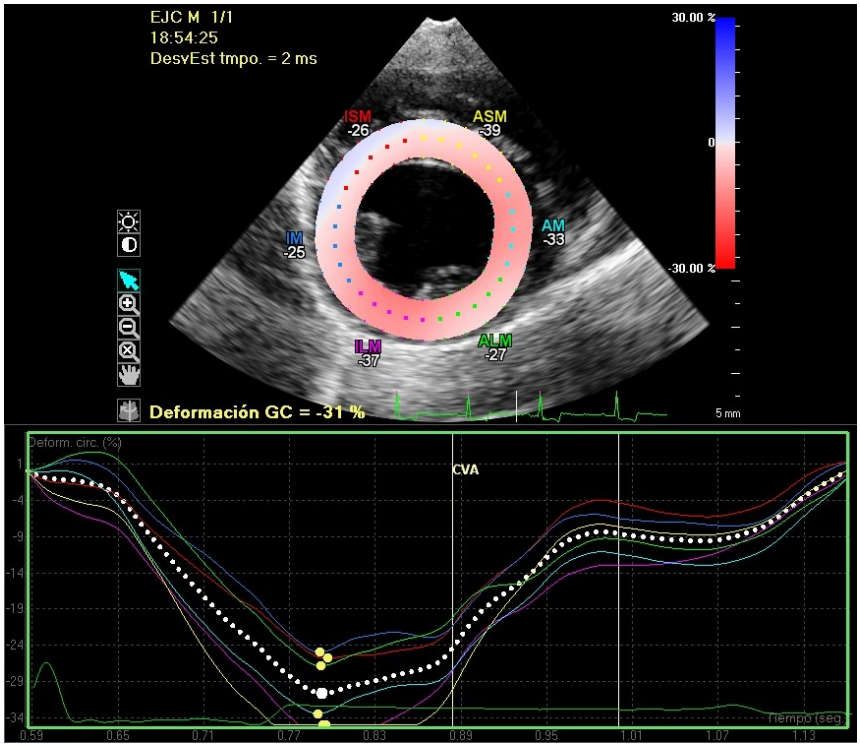

Figure 18. Right parasternal short-axis view, acquired in a healthy dog at the level of the papillary muscles and analyzed with 2-D STE dedicated software. At the top of the image, the ROI created by the software and adjusted by the operator can be observed. Further, numeric values for segmental strain are displayed next to each segment. A numeric value for GCS is also provided (-30%), and can be observed on the left of the ECG tracing. At the bottom of the image, circumferential segmental (couloured lines) and global (white dotted line) time-strain curves, calculated by the software, are provided. Used by permission of the Veterinary Teaching Hospital of the University of Murcia.

3.1.5 Measurement reliability

The between-day intra-observer repeatability of 2-D speckle tracking echocardiography (STE)-derived variables was determined using loops obtained from six unsedated dogs. For the purpose, strain analysis was performed using the same loop on two different days over a two-week period. Each 2-D STE-derived variable was measured three times on the same three consecutive cardiac cycles, and the mean value was recorded to calculate the between-day repeatability.

3.1.6 Statistical analysis

Statistical analysis was performed with R, version 3.1.2 (2014-10-31; Copyright (C) 2014 The R Foundation for Statistical Computing, ISBN 3-900051-07-0; R Core Team, 2014) and SPSS 19 (IBM Corp. Released 2010. IBM SPSS Statistics for Windows, Version 19.0. Armonk, NY: IBM Corp).

An *a priori* power analysis was performed and suggested that a total sample of 14 dogs would be needed to detect large effects (d = 0.8) using a *t*-test between means, with power and alpha set at 0.8 and 0.05, respectively, while 33 subjects would be needed to detect medium effects (d = 0.5).

Distribution of variables was tested for normality using the Shapiro-Wilk test at the α = 0.05 level. As data were normally distributed, variables were expressed by the mean and the standard deviation (SD).

A paired Student *t*-test was used to compare the variables obtained before and after sedation. The Benjamini–Hochberg procedure was chosen to adjust for multiple comparisons, controlling the false discovery rate (FDR; Benjamini & Hochberg, 1995; Glickman, Rao, & Schultz, 2014). Accordingly, sedation was considered to significantly affect a variable when the corresponding p-value was less than 0.01 (FDR < 5%).

The Pearson correlation analysis was used to investigate possible correlations between HR and echocardiographic variables showing a significant treatment effect. P values lower than 0.05 were deemed statistically significant.

Between-day intra-observer variability for segmental and global strain values was quantified by means of coefficients of variation (CV), using the formula CV = mean difference between measurements/average of measurements x 100%. Values were considered adequate for clinical use when less than 15% (Chetboul et al., 2008).

3.2. Study 2: Use of the right parasternal four-chamber view for left ventricular longitudinal strain analysis by two-dimensional speckle tracking echocardiography in dogs

3.2.1 Study population

Cardiovascularly healthy and diseased dogs were prospectively recruited between January 2015 and May 2017. The dogs were client-owned pets attending the Veterinary Teaching Hospital of the University of Murcia, and were enrolled during routine consultations upon consent of their owners. Further, the study protocol received the approval of the Ethics Committee of the University of Murcia.

The subjects included in the study could be of any age and weight. The only inclusion criterion to fulfil was the availability of a complete ECG-gated echocardiography, with excellent-quality images of the LV acquired from the LAp4Ch view and the RP4Ch view using an adequate FR (at least 60 Hz).

The animals were confirmed to be healthy, or affected by a cardiac disease, based on their medical history and the results of a physical examination, complete blood count, serum biochemistry, noninvasive blood pressure measurement, ECG and conventional echocardiography. When congestive heart failure was suspected, thoracic radiographs were also taken. Dogs with any concurrent extra-cardiac disease were excluded.

3.2.2 Echocardiographic examination

All the echocardiographic studies were performed with an iE33 ultrasound system (**Fig. 11**; Philips Medical Systems, Andover, MA, USA) and simultaneous ECG recording. The machine was equipped with a multifrequency 1-5 MHz phased-array sectorial transducer. The scans were obtained with the dogs gently restrained, first in right (**Fig. 19**) and then in left lateral recumbency. The images were obtained from beneath a scanning table with a cutout, designed for the purpose (**Fig. 19**).

Before the examination, fur was clipped from the chest of the dogs bilaterally over the area of projection of the heart, and from the cranial portion of their abdomen just caudal to the sternum. Owners were allowed to remain in the room, upon their request, if this was considered helpful to minimize the stress of their pets.

Figure 19. Photograph of a dog gently restrained in right lateral recumbency, and scanned from beneath a table with a cutout, designed for the purpose. Used by permission of the Hospital for Small Animals of the University of Edinburgh.

If the patients showed signs of anxiety or were uncooperative, and unless clearly contraindicated, mild sedation with a combination of ACP (0.02 mg/Kg) and BUT (0.2 mg/Kg) given IM was administered, and the scans were performed 30 to 40 minutes after treatment.

All echocardiographic examinations were carried out by one of two experienced operators (Ph. D. student or supervisor) and measured by the Ph. D. supervisor, using standard methods described elsewhere (Hansson et al., 2002; Lang et al., 2005; Lang et al., 2015; Quiñones et al., 2002; Thomas et al., 1993). Each echocardiogram was stored digitally for offline analysis. The data used for statistical analysis, detailed in the following section, were averaged from at least three consecutive cardiac cycles displaying stable sinus rhythm.

3.2.2.1 Two-dimensional speckle tracking echocardiography

Strain analysis was conducted offline on a separate personal computer workstation using Qlab 2D Strain software, version 9.0 (Philips Medical Systems, Andover, MA, USA). Recordings of good quality 2-D cine loops of the LV, acquired at FR of 60 to 90 Hz for a minimum of four consecutive cardiac cycles were used.

Event timing for AVC was first recorded from the LV outflow tract flow profile obtained by Pulsed-wave Doppler. More specifically, the software allowed the operator to tag the first frame where the valve was observed closed at the end of systole, and later displayed its timing, on the same graphic where the time-strain curves were provided.

Longitudinal strain and SR were then calculated from the LAp4Ch view first, and the RP4Ch view next, as explained hereafter. When using the LAp4Ch view, the same methodology described in Section 2.1.4.5 was used. When using the RP4Ch view, the option “AP4” offered by the software, and previously selected to analyze the standard view, was chosen. Three reference points were manually placed, one on each side of the mitral valve annulus and the third at the apical endocardial border.

In both cases, soon after the manual placement of the three reference points, the software created an ROI with the automatic delineation of endocardial and epicardial borders, and divided the LV in seven segments according to standard segmentation models used in humans: basal septal (BS), midseptal (MS), apical septal (ApS), apical (Apex), apical lateral (ApL), midlateral (ML), basal lateral (BL).

The operator adjusted the ROI to incorporate the entire myocardial thickness (**Fig. 20**), and inspected adequacy of segmentation. Subsequently, visual inspection of the loop in motion was performed to verify that the ROI followed properly the movements of each segment throughout the cardiac cycle.

The software algorithm then tracked the speckles across the myocardium, deriving segmental and global strain values from a weighted average of the myocardial deformation with the weighting greatest at the endocardium. Global longitudinal strain (GLS) was calculated from the entire ROI considered as a single segment, and corresponded to a weighted average of the segmental strains. Segmental and global time-strain and SR curves were eventually displayed by the software (**Fig. 21** and **22**, respectively). Numeric values for segmental strains and GLS, representing the maximal negative peak of the strain curves (peak strain), were provided on the screen and recorded for analysis. Peak systolic and diastolic SR values, displayed after placing the cursor at the appropriate time point along the global SR curves, were also recorded.

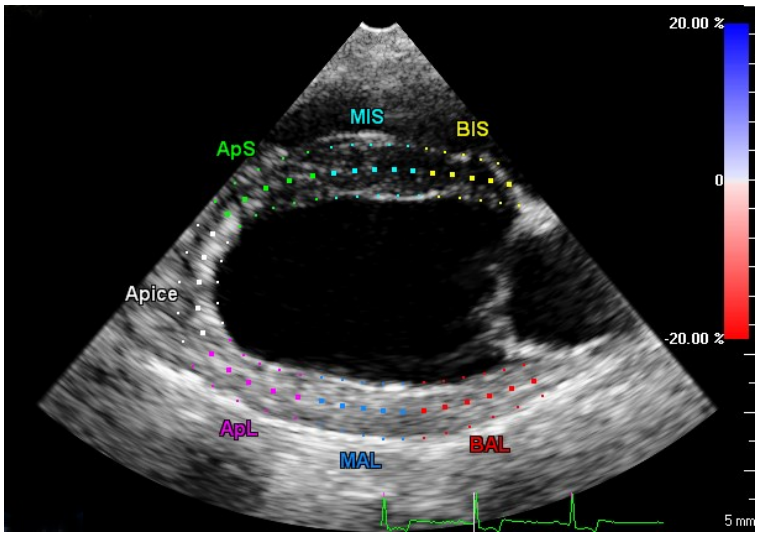

Figure 20. Right parasternal four-chamber view obtained in a healthy dog and analyzed with dedicated automated software for two-dimensional speckle tracking echocardiography. The image illustrates the region of interest (ROI), already adjusted by the operator to incorporate the entire myocardial thickness. The ROI is divided by the software in seven segments according to standard segmentation models used in humans. The abbreviations in the pictures are different from the text as derived from the spanish designation of the segments. *Source:* Santarelli, Talavera López, & Fernández del Palacio (2018). Evaluation of the right parasternal four-chamber view for the assessment of left ventricular longitudinal strain and strain rate by two-dimensional speckle tracking echocardiography in dogs. *Research in Veterinary Science,* In Press. Used by permission of the journal.

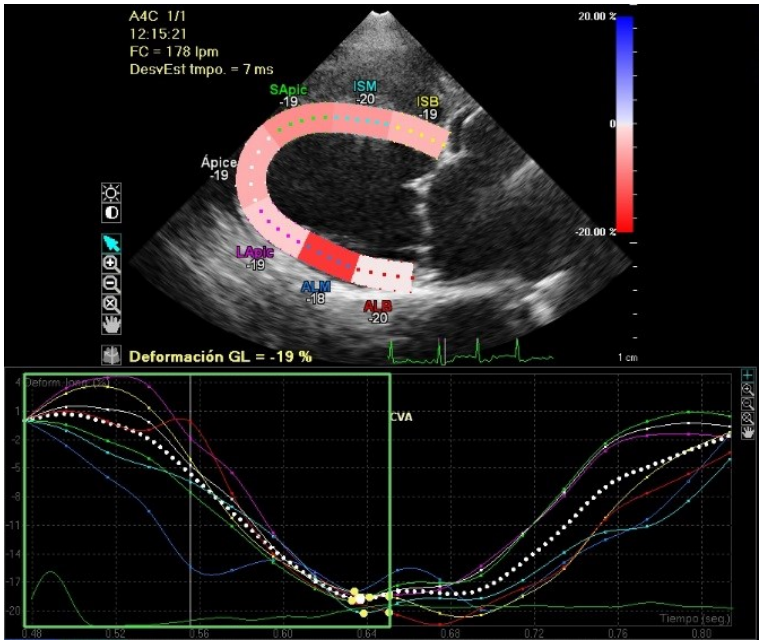

Figure 21. Right parasternal four-chamber view obtained in a dog with myxomatous mitral valve disease and analyzed with dedicated automated software for two-dimensional speckle tracking echocardiography. At the top of the image, the region of interest adjusted by the operator can be observed, and numeric values for segmental strains are displayed next to each segment. A numeric value for global longitudinal strain (GS) is also provided (-19%) on the left of the ECG tracing. At the bottom of the image, longitudinal segmental (couloured lines) and global (white dotted line) time-strain curves, calculated by the software, are provided. Aortic valve closure (CVA in the picture) timing is observed. Used by permission of the Veterinary Teaching Hospital of the University of Murcia.

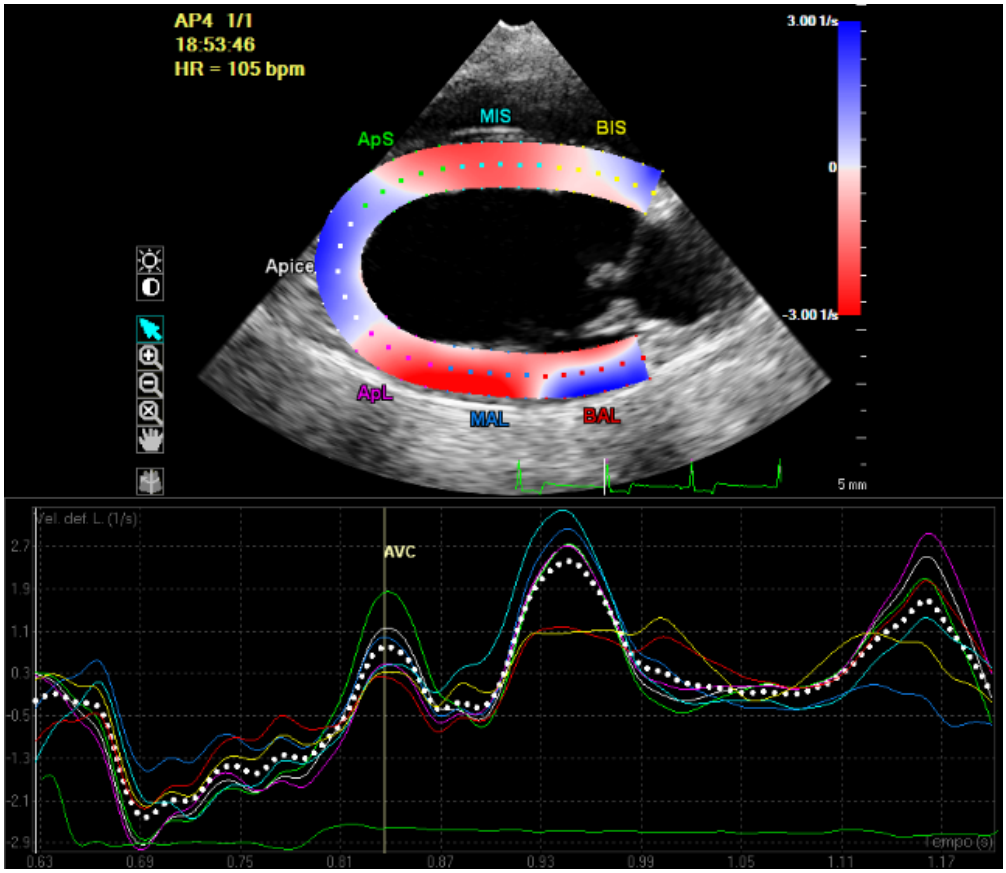

Figure 22. Right parasternal four-chamber view obtained in a dog with myxomatous mitral valve disease and analyzed with dedicated automated software for two-dimensional speckle tracking echocardiography. At the top of the image, the region of interest adjusted by the operator can be observed. Seven segments are designated. At the bottom of the image, longitudinal segmental (couloured lines) and global (white dotted line) time-strain rate curves, calculated by the software, are provided. Timing for aortic valve closure (AVC), defining the end of systole, is indicated. Used by permission of the Veterinary Teaching Hospital of the University of Murcia.

3.2.3 Measurement reliability

The intra-observer within-day and between-day measurement variabilities were determined using loops obtained from six randomly selected dogs. The loops were subjected to repeated analyses by the same investigator (the Ph. D. supervisor) at two different time points on a given day and on two different days, respectively. Inter-observer measurement variability was also determined as a second investigator (the Ph. D. student) performed independent repeated analyses on the same six echocardiograms. Each 2-D STE variable was measured three times on the same three consecutive cardiac cycles, and the mean values were recorded and used for statistical analysis.

3.2.4 Statistical analysis

Statistical analysis was performed with SPSS 19 (IBM Corp. Released 2010. IBM SPSS Statistics for Windows, Version 19.0. Armonk, NY: IBM Corp).

Study population characteristics were analyzed using descriptive statistics and expressed as medians with range. Distribution of the rest of variables was tested for normality using the Shapiro-Wilk test at the $\alpha = 0.05$ level. As data were normally distributed, variables were expressed by the mean and the SD.

According to the initial examination of each patient, dogs were assigned to one of the two following groups: (1) healthy, or (2) diseased. To compare the distribution of sex in the healthy versus the diseased group, the chi-squared test was used, while the differences in age or weight were assessed with an unpaired student *t*-test.

A paired Student *t*-test was used to compare the variables obtained from the LAp4Ch view and the RP4Ch view in the entire population, and the same comparison was then made within the separated groups of healthy and diseased dogs.

Limits of agreement (LOA) were analyzed by Bland-Altman analysis, and intra-class correlation coefficients (ICC) were calculated for GLS values, first considering the entire group of dogs and then the separated groups of healthy and diseased.

Intra- and inter-observer variability for segmental and global values resulting from strain and SR analysis of the 6 repeated examinations was quantified by means of coefficients of variation (CV), using the formula CV = mean difference between measurements/average of measurements x 100%. Values were considered adequate for clinical use when less than 15% (Chetboul et al., 2008). Further, ICC for GLS values were calculated.

Values of *P* less than 0.05 were considered significant.

3.3 Study 3: Inter-software variability of two-dimensional speckle tracking-derived parameters in dogs

3.3.1 Study population

Cardiovascularly healthy and diseased dogs were prospectively recruited between January 2015 and June 2017. The dogs were client-owned patients attending the Veterinary Teaching Hospital of the University of Murcia, and were enrolled during routine consultations upon consent of their owners. Furthermore, the study protocol received the approval of the Ethics Committee of the University of Murcia. Most of the dogs included in this population had been previously included in Study 2.

Additionally, cardiovascularly healthy and diseased canine patients attended at the cardiopulmonary service of the Hospital for Small Animals of the University of Edinburgh between October 2017 and January 2018 were recruited. Owner consent was obtained for each dog before enrollment, and the study protocol was approved by the Ethics Committees of the University of Edinburgh.

The subjects included in the study could be of any age and weight. The only inclusion criterion to fulfil was the availability of a complete ECG-gated echocardiography, with excellent-quality images of the LV acquired from the LAp4Ch view using an adequate FR (between 60 and 100 Hz).

The animals were considered cardiovascularly healthy, or affected by a cardiac disease based on the medical history and results of at least a physical examination, complete blood count, blood serum biochemical analysis, noninvasive blood pressure measurement, ECG, and conventional echocardiography. When congestive heart failure was suspected, thoracic radiographs were also taken. Dogs with any concurrent extra-cardiac disease were excluded.

3.3.2 Echocardiographic examination

At the University of Murcia, all the echocardiographic studies were performed with an iE33 ultrasound system (**Fig. 11**; Philips Medical Systems, Andover, MA, USA) equipped with a multifrequency 1-5 MHz phased-array sectorial transducer, and simultaneous ECG

recording. The echocardiograms were obtained by one of two experienced operators (the Ph. D. student or the supervisor).

At the University of Edinburgh, transthoracic echocardiograms were attained by one of two experienced operators (the Ph. D. student or a supervised veterinary cardiology resident) using a Vivid E9 ultrasound unit [**Fig. 23**; General Electric (GE) Medical Systems, Waukesha, Wisconsin] equipped with multifrequency 1.5- to 4.6-MHz and 2.4 to 8.0 MHz phased-array sector transducers, and simultaneous ECG recording.

Figure 23. Photograph of the echocardiographic unit employed for the part of the study realized at the University of Edinburgh, located in the examination room where the echogradiographic studies where performed. Part of the scanning table with cutout is also visualised on the right side of the picture. Used by permission of the Hospital for Small Animals of the University of Edinburgh.

At both institutions, the scans were realized with the dogs gently restrained, first in right and then in left lateral recumbence, and the images were obtained from beneath a scanning table with a cutout, designed for the purpose. Before the examination, fur was clipped from the chest of the dogs bilaterally over the area of projection of the heart, and from the cranial portion of their abdomen just caudal to the sternum.

The echocardiograms were performed in accordance with published veterinary recommendations (Hansson et al., 2002; Lang et al., 2005; Lang et al., 2015; Quiñones et al., 2002; Thomas et al., 1993). Images recorded at FR between 60 and 100 Hz for at least 4 consecutive cardiac cycles were used for 2-D STE analysis.

Echocardiographic examinations were stored digitally for offline analysis in standard formats and as Digital Images and Communications in Medicine (DICOM)-files on an external hard disk drive.

3.3.2.1 Two-dimensional speckle tracking echocardiography-derived analysis of images obtained with Philips ultrasound system

Echocardiographic examinations acquired with Philips ultrasound system were first analyzed on a separate personal computer workstation with Qlab 2D Strain software, version 9.0 (Philips Medical Systems, Andover, MA, USA). Subsequently, DICOM-files were analyzed through the vendor independent software TomTec 2D Cardiac Performance Analysis (2D CPA; Image-Arena version 4.6, TomTec Imaging Systems, Unterschleissheim, Germany), installed on a different computer workstation.

Longitudinal strain and SR analysis was performed by a single observer (the Ph. D. student) with Philips specific software and TomTec vendor independent software, using the same good quality 2-D cine loop recorded from the LAp4Ch view. The two software were used on different days, and during measurements, the observer was blinded to the results obtained with the software not in use.

When using Philips dedicated software, the same methodology described in Section 2.1.4.5 was used. The only difference was that the timing for AVC was not tagged, and GLS values recorded, automatically provided by the software, corresponded to the maximum strain or peak strain of the GLS waveform over the entire cardiac cycle. Further, peak systolic and diastolic SR values, displayed after placing the cursor at the appropriate time point along the global SR curves, were recorded.

When using TomTec vendor independent software, the endocardial border of the myocardium was manually traced from an end-diastolic frame starting with the septal side of the mitral annulus (**Fig. 24**). Soon after, the software marked automatically the epicardial

border. The operator could adjust the myocardial wall borders manually if deemed necessary.

The software algorithm subsequently performed speckle tracking on six segments (BS, MS, ApS, ApL, ML, and BL), and provided two separate datasets for the endocardial and epicardial borders. However, strain values obtained from the epicardial border were excluded from the analysis as this sometimes fell outside the echocardiographic window. Time-domain LV strain curves for each segment and for GLS were displayed (**Fig. 25**).

The operator recorded endocardial GLS (**Fig. 25**) and longitudinal systolic SR values, automatically provided by the software and corresponding to the maximum strain or peak strain of the endocardial GLS and global SR waveforms over the entire cardiac cycle. Global longitudinal diastolic SR values were also recorded, as displayed after placing the cursor at the appropriate time point along the global endocardial SR curves (**Fig. 26**).

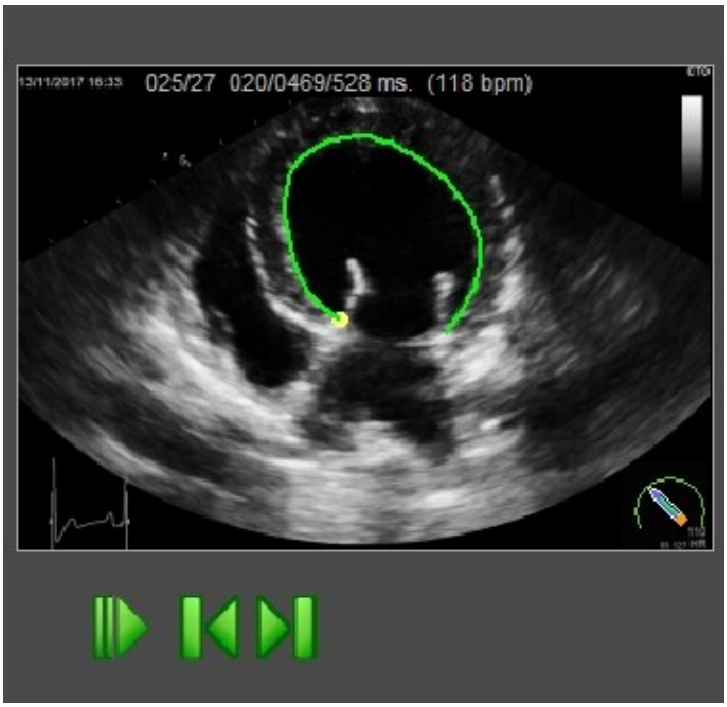

Figure 24. Left apical four-chamber view acquired in a dog with advanced compensated myxomatous mitral valve disease, and analyzed with dedicated automated software for two-dimensional speckle tracking echocardiography. The endocardial region of interest has been traced by the operator. The software allows to observe the cine loop in motion mode to ascertain that the tracing (green line) follows the movement of the endomyocardium throughout the cardiac cycle, and adjust it if deemed necessary to avoid inappropriate tracking. Used by permission of the Veterinary Teaching Hospital of the University of Zurich.

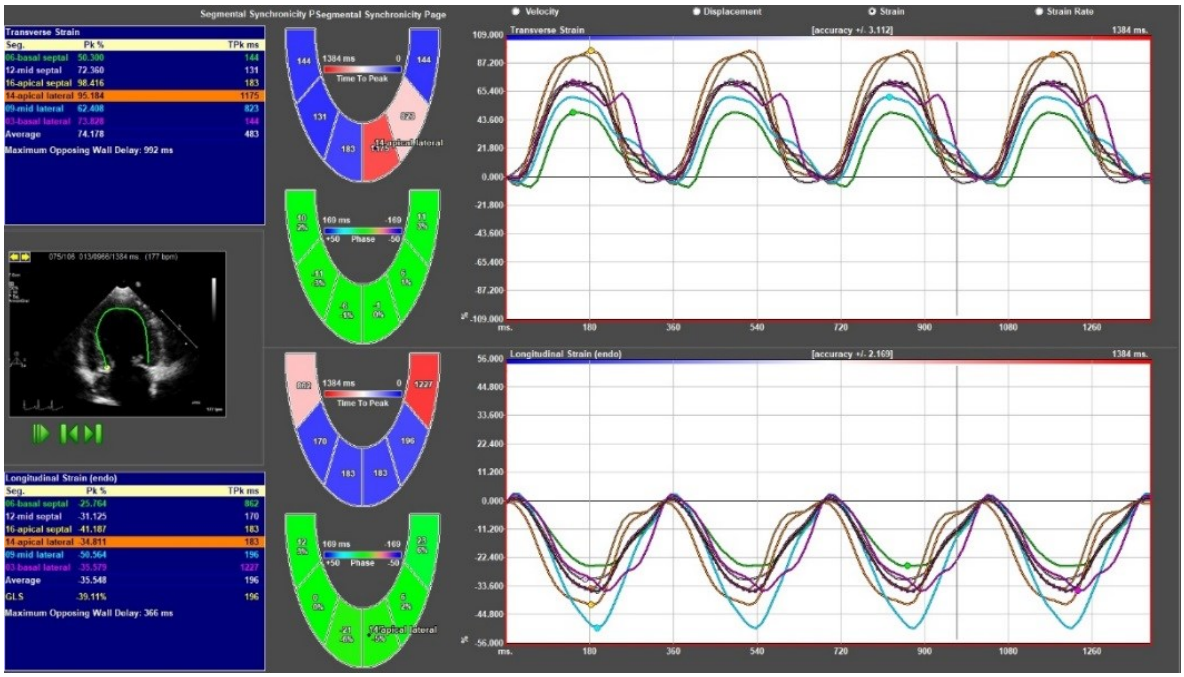

Figure 25. Screenshot of the display of longitudinal strain analysis results, obtained by vendor independent automated software for two-dimensional speckle tracking echocardiography, in a dog with advanced compensated myxomatous mitral valve disease MMVD. At the bottom right of the screen, the curves generated by the software corresponding to segmental (straight lines) and global (dotted lines) longitudinal endocardial strain curves can be observed. At the bottom left of the screen, the endocardial global longotudinal strain (GLS) value is displayed in a table together with segmental strain values, and corresponds to -39.11%. Used by permission of the Veterinary Teaching Hospital of the University of Zurich.

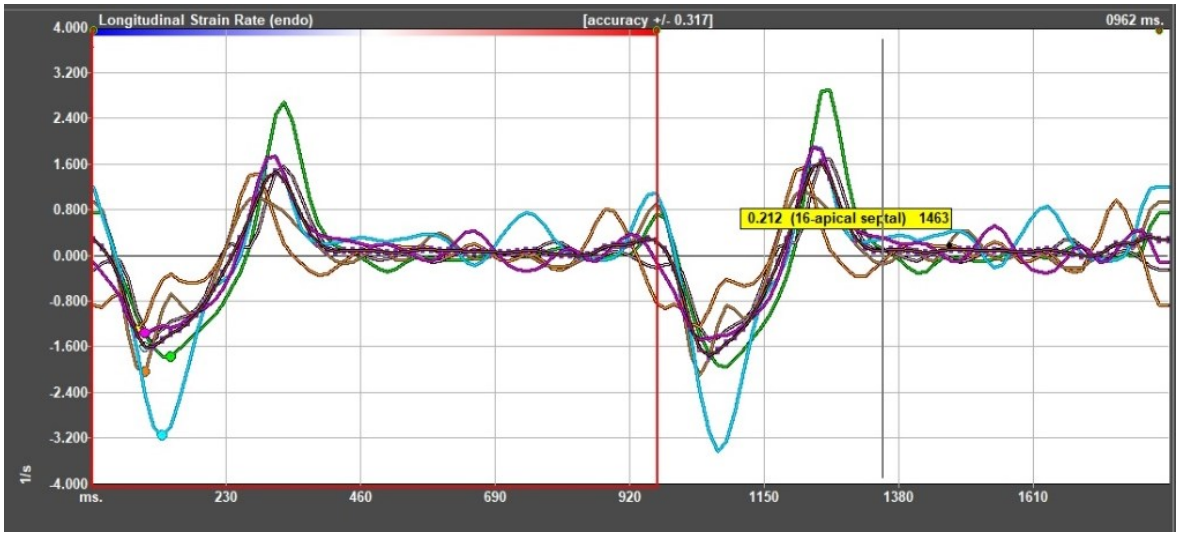

Figure 26. Time-strain rate (SR) curves obtained by vendor independent automated software for two-dimensional speckle tracking echocardiography in a healthy dog. Segmental (coloured smooth curves) and global (dotted curve) longitudinal endocardial SR are displayed. Any numeric SR value can be obtained placing the cursor at the appropriate time point along the curves, as in this example where a determinate apical segmental SR value is displayed. Used by permission of the Veterinary Teaching Hospital of the University of Zurich.

3.3.2.2 Two-dimensional speckle tracking echocardiography-derived analysis of images obtained with General Electric ultrasound system

Echocardiographic examinations acquired with GE ultrasound system were first analyzed on a separate personal computer workstation with EchoPac software, PC version 113 (GE Vingmed Ultrasound AS, Horten, Norway). Subsequently, DICOM-files containing the same images were analyzed through the vendor independent software TomTec 2D Cardiac Performance Analysis (2D CPA; Image-Arena version 4.6, TomTec Imaging Systems, Unterschleissheim, Germany), installed on a different computer workstation.

Longitudinal strain and SR analysis was performed again by the same observer (the Ph. D. student) with GE specific software and TomTec vendor independent software, using the same good quality 2-D cine loop recorded from the LAp4Ch view. Again, the two software were used on different days, and during measurements, the observer was blinded to the results obtained with the software not in use.

When using GE dedicated software, the endocardial border of the myocardium was manually traced from an end-systolic frame starting with the septal side of the mitral annulus. Subsequently, the software created an ROI with the automatic delineation of endocardial and epicardial borders, and divided the LV in six segments (BS, MS, ApS, ApL, ML, BL) according to standard segmentation models used in humans (**Fig. 27A**). The operator adjusted the ROI to incorporate the entire myocardial thickness and inspected the adequacy of segmentation (**Fig. 27B**). The software algorithm then performed speckle tracking, and assessed tracking quality for each segment (**Fig. 28**). Segments marked as of inadequate tracking quality were retraced. If unreliable segments persisted after retracing, the dog was excluded from the study.

After eventual approval, segmental and global longitudinal strain and SR were quantified by the software, and time-strain and SR curves were displayed (**Fig. 29** and **Fig. 30**). The global waveform was created using an average of the segmental strains. Global longitudinal strain, automatically calculated by the algorithm and corresponding to the peak longitudinal strain value, was recorded. The value displayed as Endo was also recorded, corresponding to the peak longitudinal strain obtained from the sub-endocardial layers of the LV myocardium.

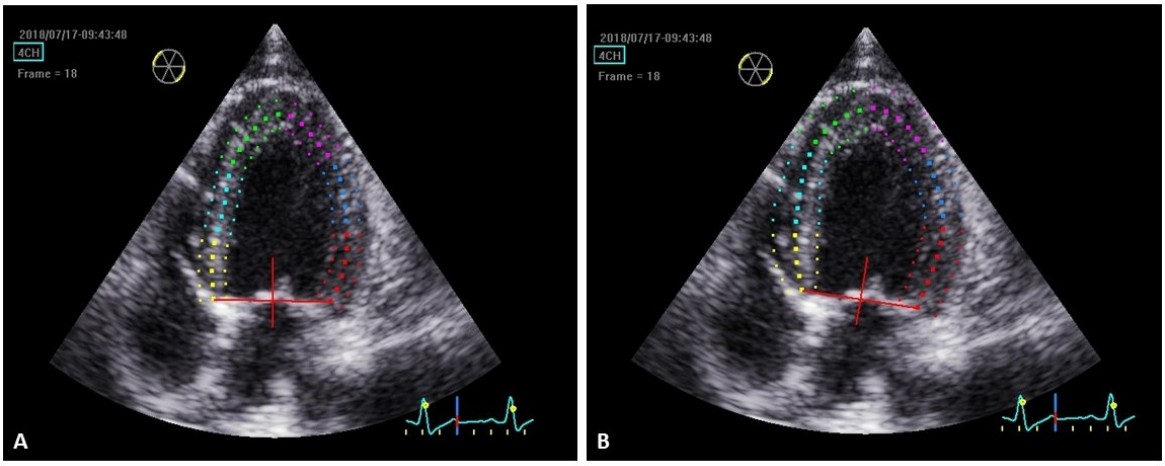

Figure 27. Left apical four-chamber view acquired in a healthy dog, analyzed with dedicated automated software for two-dimensional speckle tracking echocardiography. Caption A shows a region of interest (ROI) automatically drawn by the software as a first step of the analysis (note how the ROI is not properly adjusted to the image of the LV). Caption B shows the ROI after manual adjustment by the operator. In both captions, the ROI has been divided by the software into six segments according to standard segmentation models used in humans. Used by permission of the Hospital for Small Animals of the University of Edinburgh.

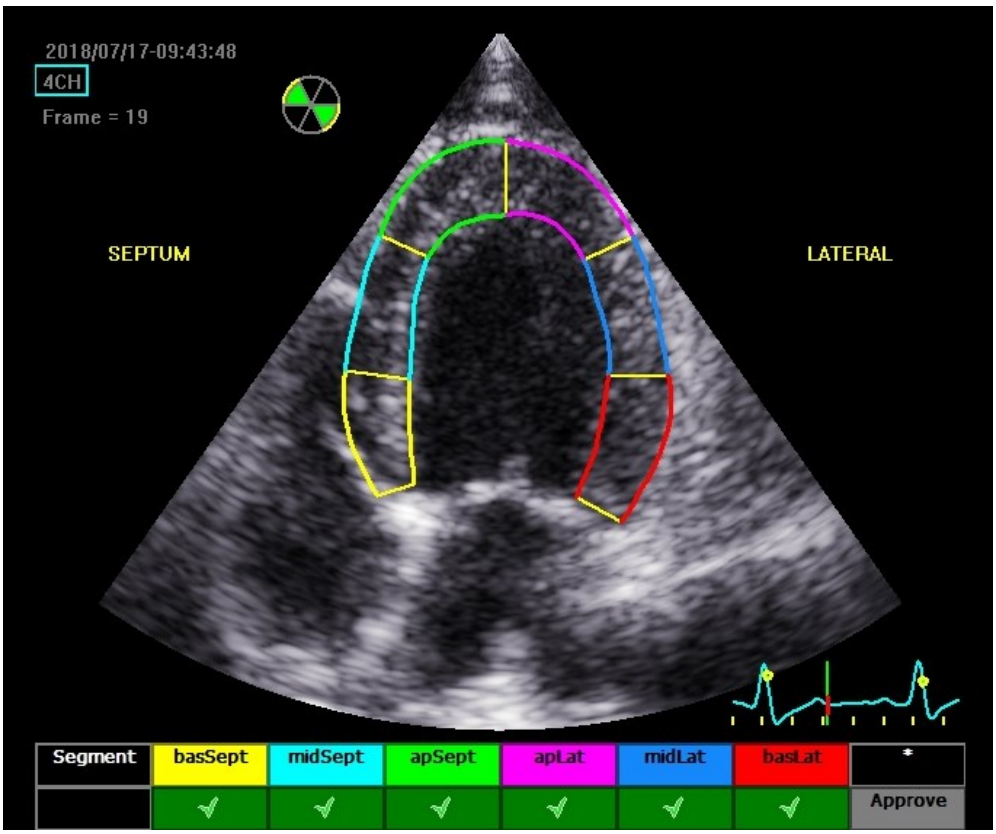

Figure 28. Left apical four-chamber view acquired in a healthy dog, analyzed with dedicated automated software for two-dimensional speckle tracking echocardiography. The picture shows the region of interest divided by the software into six segments according to standard segmentation models used in humans. Tracking quality for each segment has been assessed by the software. In this image, all the segments are marked as of adequate tracking quality. Used by permission of the Hospital for Small Animals of the University of Edinburgh.

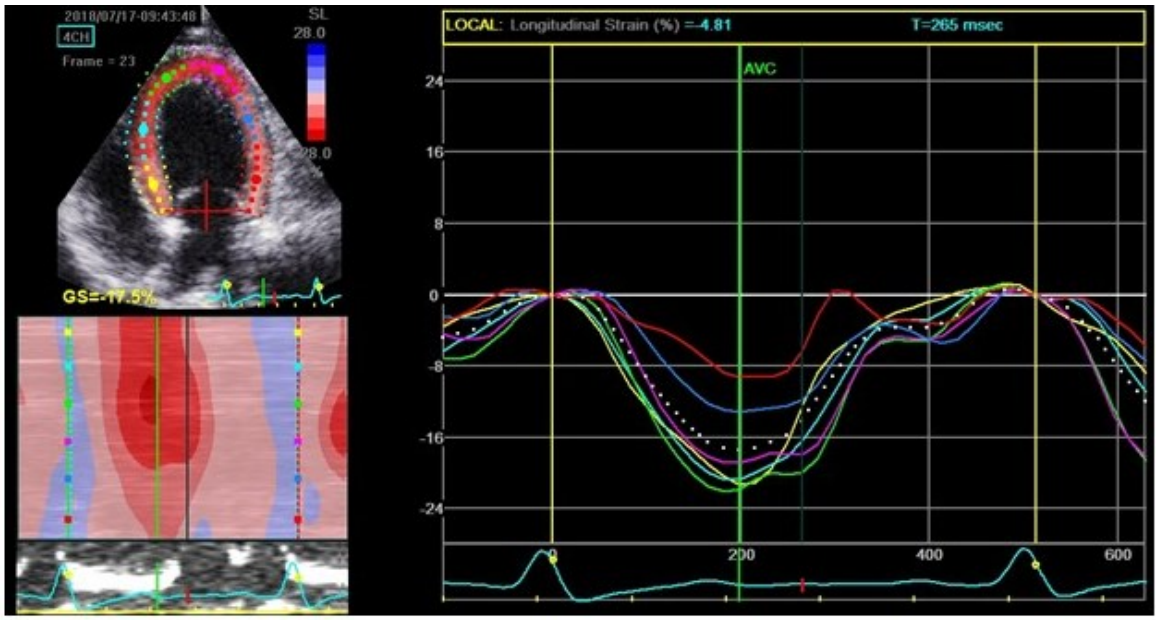

Figure 29. Left apical four-chamber view obtained in a healthy dog, and analyzed with dedicated automated software for two-dimensional speckle tracking echocardiography. In the top left portion of the image, the region of interest created by the software and adjusted by the operator can be observed. Further, a numeric value for global longitudinal strain (GS) is provided on the left of the ECG tracing, and corresponds to -17.5%. In the right portion of the image, longitudinal segmental (couloured lines) and global (white dotted line) time-strain curves, calculated by the software, are provided. Aortic valve closure (AVC) timing is observed. Used by permission of the Hospital for Small Animals of the University of Edinburgh.

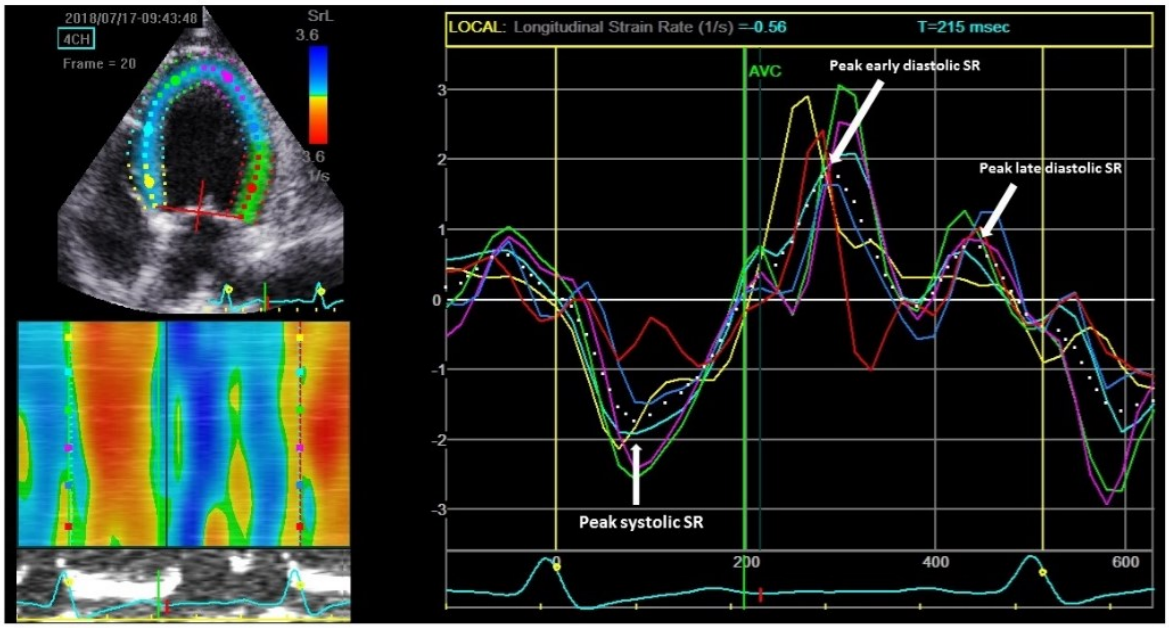

Figure 30. Left apical four-chamber view obtained in a healthy dog, and analyzed with dedicated automated software for two-dimensional speckle tracking echocardiography. In the top left portion of the image, the region of interest created by the software and adjusted by the operator can be observed. In the right portion of the image, longitudinal segmental (couloured lines) and global (white dotted line) mid-myocardial longitudinal time-strain rate (SR) curves are displayed. White arrows have been added to show appropriate timing for peak systolic, early diastolic and late diastolic SR. Used by permission of the Hospital for Small Animals of the University of Edinburgh.

Peak systolic and diastolic SR values were offered after placing the cursor at the appropriate time point along the global SR curves.

When using TomTec vendor independent software, the same technique described in the preceding section was used.

3.3.3 Measurement reliability

The intra-observer within-day and between-day measurement variabilities were determined. For this purpose, six echocardiograms obtained with Philips ultrasound system and six echocardiograms obtained with GE ultrasound system were randomly selected. The loops were subjected to repeated analyses by the same investigator (the Ph. D. student) at two different time points on a given day and on two different days, respectively.

Inter-observer measurement variability was also determined as a second experienced investigator (a board certified veterinary cardiologist for images obtained with Philips, and a veterinary cardiology resident for images obtained with GE) performed independent repeated analyses on the same six echocardiograms. Each 2-D STE variable was measured three times on the same three consecutive cardiac cycles, and the mean values were recorded and used for statistical analysis.

Again, cine loops obtained with Philips ultrasound system were analyzed with Philips specific software and TomTec vendor independent software, while those obtained with GE ultrasound system were measured with GE specific software and TomTec vendor independent software. The observers were blinded to the results of the software package not in use and previous measurements when performing strain analysis.

3.3.4 Statistical analysis

Statistical analysis was performed with SPSS 19 (IBM Corp. Released 2010. IBM SPSS Statistics for Windows, Version 19.0. Armonk, NY: IBM Corp).

Study population characteristics were analyzed using descriptive statistics and expressed as medians with the range. Distribution of the rest of variables was tested for normality using the Shapiro-Wilk test at the $\alpha = 0.05$ level. Normally distributed, variables were expressed by the mean and the SD, while median and ranges were used for non-

normally distributed variables. Subjects were assigned to one of the two following groups: Philips-cohort, or GE-cohort.

Depending on normality of data, a paired *t*-test or a Wilcoxon signed-ranked test were used to compare the 2-D STE variables obtained with vendor dependent and independent software.

Further, for each pair of values, LOA and systematic errors were assessed by calculating the mean difference (bias) and the SD of the differences by Bland-Altman analysis.

Intra- and inter-observer variability for global strain and SR values resulting from vendor dependent and independent analysis of the 6 repeated examinations obtained with either ultrasound system was quantified by means of CV. The formula CV = mean difference between measurements/average of measurements x 100% was used. Values were considered adequate for clinical use when less than 15% (Chetboul et al., 2008).

Values of *P* less than 0.05 were considered significant.

RESULTS

4. RESULTS

4.1 Study 1: Effects of a sedation protocol combining acepromazine and butorphanol on two-dimensional speckle tracking echocardiography-derived myocardial strain in healthy dogs

4.1.1 Study population

The study population comprised 18 dogs. Five were mixed-breed dogs, while represented pure breeds included Labrador Retriever (n = 5), Dalmatian (n = 3), Golden Retriever (n = 1), American Staffordshire Bull Terrier (n = 1), Irish Setter (n = 1), Spanish Podenco (n = 1), and Weimaraner (n = 1). Seven dogs were spayed females, six were sexually intact females, three were castrated males, and two were sexually intact males. The median age of the subjects was 5 years (range, 2 to 10 years), and the median body weight was 26.5 Kg (range, 16 to 48 Kg).

4.1.2 Sedation

The degree of sedation was considered adequate (see Section 2.1.2) to facilitate echocardiography in all dogs. One dog frequently panted both during the baseline examination and the sedation study.

4.1.3 Cardiovascular variables

Sedation reduced mean arterial pressure (MAP; from 91 ± 10 mmHg to 80 ± 10 mmHg) and diastolic arterial pressure (MAP; from 69 ± 12 mmHg to 59 ± 10 mmHg) by approximately 10 mmHg (**Fig. 31** and **32**, respectively; **Table 1**; $p < 0.01$). This was accompanied by a fall in heart rate (HR) of approximately 27 bpm (from 107 ± 22 bpm to 80 ± 19 bpm; **Table 1**; **Fig. 33;** $p < 0.01$)

4.1.4 Conventional echocardiography

Thirty-seven out of 44 conventional echocardiographic variables were unaffected by sedation (**Tables 1** and **2**). Only left ventricular end-diastolic volume index (EDVI), peak velocity of late transmitral diastolic flow (A wave), late diastolic velocity of the septal side of the mitral annulus (A' sep) and late diastolic velocity of the lateral side of the tricuspid

annulus (A' tric) decreased following sedation (**Fig. 34** to **36**; $p < 0.01$), while left ventricular ejection time (LVET) and E wave to A wave ratio (E/A) increased (**Fig. 38**; $p < 0.01$).

Heart rate correlated positively with A wave ($r = 0.58$; $p < 0.001$), A' sep ($r = 0.43$; $p = 0.01$), and A' tric ($r = 0.39$; $p = 0.024$). By contrast, HR correlated negatively with LVET ($r = 0.59$; $p < 0.001$), and E/A ($r = 0.61$; $p < 0.001$).

4.1.5 Two-dimensional speckle tracking echocardiography

All segments could be tracked and used for strain analysis. The FR used to analyze 2-D STE indices ranged from 60 to 90 Hz.

Fourteen out of 15 2-D STE-derived variables were unaffected by sedation (**Table 3**). These included all of the global strain variables. Only the apical lateral strain (ApL) decreased following sedation (**Fig. 39**; $p < 0.01$), but did not correlate with HR.

4.1.6 Measurement reliability

The variability of 2-D STE-derived variables was adequate for clinical use (see Section 2.1.6), with between-day CV ranging from 8.8% to 9.77%.

Table 1. Two-dimensional and M-mode echocardiographic variables (mean ± SD) before and after sedation in 18 healthy dogs.

Variable	Baseline	ACP/BUT
SAP (mmHg)	131± 10	118 ± 14
DAP (mmHg)	69 ± 12	**59 ± 10**
MAP (mmHg)	91 ± 10	**91 ± 10**
HR (bpm)	107 ± 22	**80 ± 19**
LVOT (cm)	1.8 ± 0.21	1.83 ± 0.21
ESVI (ml/m^2)	30.9 ± 6.5	29.4 ± 7.3
EDVI (ml/m^2)	65.6 ± 11.1	**59.1 ± 12.2**
EF (%)	53 ± 4	50 ± 7
LVAs (cm^2)	7.9 ± 2	7.85 ± 2.4
LVAd (cm^2)	14.1 ± 3	13.5 ± 3.6
LV-SA%	44 ± 5	42 ± 6
IVSd (cm)	1.04 ± 0.33	0.99 ± 0.14
LVIDd (cm)	4.03 ± 0.58	3.81 ± 0.45
LVPWd (cm)	0.91 ± 0.13	0.96 ± 0.12
IVSs (cm)	1.33 ± 0.2	1.31 ± 0.21
LVIDs (cm)	2.89 ± 0.51	2.8 ± 0.42
LVPWs (cm)	1.31 ± 0.18	1.36 ± 0.33
FS (%)	30 ± 6	28 ± 5
EPSS (cm)	0.32 ± 0.1	0.34 ± 0.13
LA/Ao	1.34 ± 0.19	1.35 ± 0.19

Bold values indicate statistical significance; the value differs significantly ($P<0.01$) from baseline.

ACP, acepromazine; BUT, butorphanol; SAP, systolic arterial pressure; DAP, diastolic arterial pressure; MAP, mean arterial pressure; HR, heart rate; LVOT, left ventricular outflow tract; ESVI, left ventricular end-systolic volume index; EDVI, left ventricular end-diastolic volume index; EF, left ventricular ejection fraction; LVAs, left ventricular end-systolic luminal area; LVAd, left ventricular end-diastolic luminal area; LV-SA, left ventricular shortening area; LVIDs, left ventricular systolic internal diameter; LVIDd, left ventricular diastolic internal diameter; IVSs, systolic interventricular septum; IVSd, diastolic interventricular septum; LVPWs, systolic left ventricular posterior walls size; LVPWd, diastolic left ventricular posterior walls size; FS, fractional shortening; EPSS, E-point to septal separation; LA/Ao, left atrium to aorta ratio.

Table 2. Doppler-derived echocardiographic variables (mean ± SD) before and after sedation in 18 healthy dogs.

Variable	Baseline	ACP/BUT
PA Vmax (m/s)	1.12 ± 0.27	0.99 ± 0.23
PA PG (mmHg)	5.3 ± 2.48	4.17 ± 2.17
AO Vmax (m/s)	1.66 ± 0.25	1.56 ± 0.33
AO PG (mmHg)	11.3 ± 3.68	10.2 ± 4.5
PEP (msec)	52 ± 12	57 ± 14
LVET (msec)	162 ± 18	**184 ± 27**
VTI (cm)	17.7 ± 2.86	18 ± 3.55
PEP/ET	6.67 ± 1.03	6.27 ± 1.34
SV (mL)	44.9 ± 9.6	47.9 ± 14.6
CO (L/min)	4.8 ± 1.2	3.9 ± 1.6
E wave (m/s)	0.78 ± 0.15	0.74 ± 0.13
DcT (msec)	103 ± 21	106 ± 30
A wave (m/s)	0.58 ± 0.23	**0.41 ± 0.13**
Adur (msec)	80 ± 9	87 ± 14
E/A	1.46 ± 0.41	**1.92 ± 0.43**
S lat (cm/s)	14.4 ± 6	12.7 ± 4.5
E' lat (cm/s)	12.2 ± 3.1	10.6 ± 3.3
A' lat (cm/s)	7.85 ± 2.1	6.5 ± 2
E/E' lat	0.07 ± 0.02	0.08 ± 0.02
IVRT (msec)	86 ± 36	87 ± 29
IVCT (msec)	57 ± 18	52 ± 19
S sep (cm/s)	12.3 ± 4.1	11 ± 3.3
E' sep (cm/s)	8.5 ± 2.6	7.1 ± 2
A' sep (cm/s)	7.9 ± 2.5	**5.3 ± 1.1**
S tric (cm/s)	16.2 ± 7.6	15.6 ± 4.5
E' tric (cm/s)	11.2 ± 3.8	11.6 ± 3.5
A' tric (cm/s)	11.9 ± 3.8	**7.7 ± 1.9**

Bold values indicate statistical significance; the value differs significantly ($P<0.01$) from baseline.

ACP, acepromazine; BUT, butorphanol; PA Vmax, Pulmonary artery peak velocity; PA PG, transpulmonary pressure gradient; AO Vmax, aortic peak velocity, AO PG, transaortic pressure gradient; PEP, left ventricular pre-ejection period; LVET, left ventricular ejection time; VTI, LV velocity time integral; PEP/LVET, LV pre-ejection period to ejection time ratio; SV, stroke volume; CO, cardiac output; E wave, peak velocity of early transmitral diastolic flow; DcT, E wave deceleration time; A wave, peak velocity of late transmitral diastolic flow; Adur, A wave duration; E/A, E wave to A wave ratio; S, peak systolic velocity of annulus motion; E', early diastolic velocity of annulus motion; A', late diastolic velocity of annulus motion; lat, lateral side of mitral annulus; E/E' lat, ratio of E wave velocity to E' velocity; IVCT, isometric contraction time; IVRT, isometric relaxation time; sep, septal side of mitral annulus; tric, lateral side of tricuspid annulus.

Table 3. Speckle tracking echocardiography-derived variables (mean ± SD) before and after sedation in 18 healthy dogs.

Variable (%)	Baseline	ACP/BUT
GLS	-20 ± 3.4	-20 ± 4
GCS	-26 ± 3	-25 ± 4
AntSept	-30 ± 7	-30 ± 8
Ant	-30 ± 4.7	-28 ± 5.5
Lat	-25 ± 5.7	-25 ± 7
Post	-27 ± 7	-22 ± 5.5
Inf	-27 ± 4.7	-24 ± 7
Sept	-25 ± 5.7	-24 ± 6.5
BS	-18 ± 4	-18 ± 5.2
MS	-25 ± 7.5	-22 ± 4.2
ApS	-25 ± 8	-25 ± 5.6
Apex	-23 ± 6.4	-21 ± 3.8
ApL	-22 ± 5.6	**-18 ± 4**
ML	-18 ± 5.9	-23 ± 5
BL	-20 ± 5.4	-21 ± 7

Bold values indicate statistical significance; the value differs significantly (P<0.01) from baseline.

ACP, acepromazine; BUT, butorphanol; GLS, global longitudinal strain; GCS, global circumferential strain; AntSept, anteroseptal; Ant, anterior; Lat, lateral; Post, posterior; Inf, inferior; Sept, septal; BS, basal septal; MS, midseptal; ApS, apical septal; Apex, apical; ApL, apical lateral; ML, midlateral; BL, basal lateral.

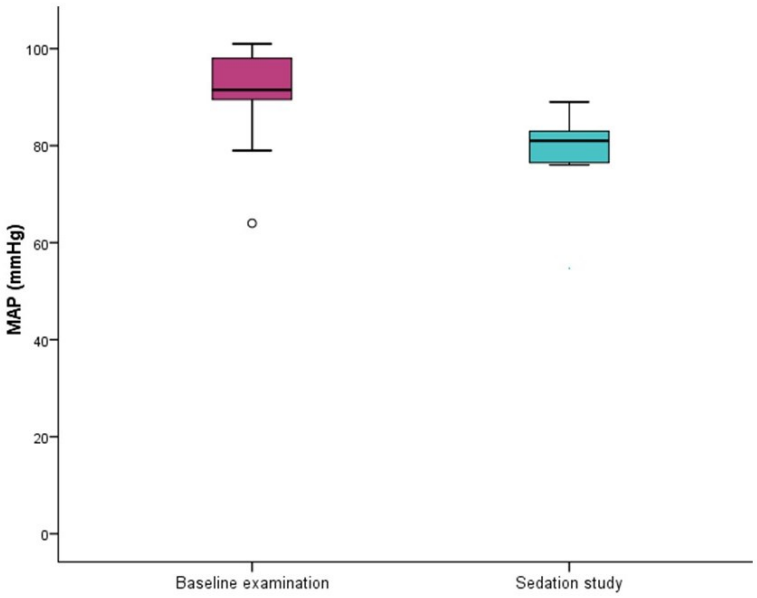

Figure 31. Change in mean arterial pressure (MAP) after sedation with a combination of acepromazine and butorphanol in 18 healthy dogs. Boxes represent the interquartile range (25th to 75th percentile). The horizontal line in each box represents the median. Whiskers represent the 5th and 95th percentiles. Outliers are plotted separately as circles. Measures obtained at baseline are displayed on the left, and those obtained after sedation on the right. The variable is significantly reduced by treatment ($p < 0.01$).

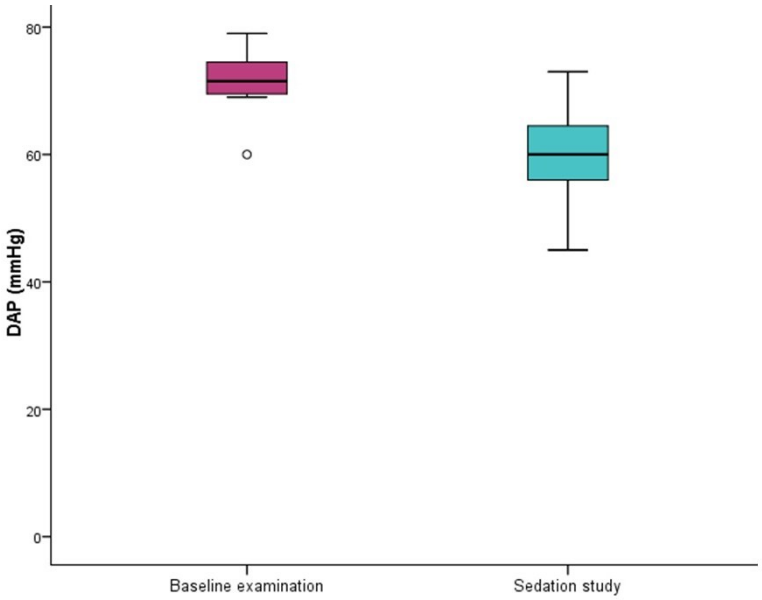

Figure 32. Change in diastolic arterial pressure (DAP) after sedation with a combination of acepromazine and butorphanol in 18 healthy dogs. Boxes represent the interquartile range (25th to 75th percentile). The horizontal line in each box represents the median. Whiskers represent the 5th and 95th percentiles. Outliers are plotted separately as circles. Measures obtained at baseline are displayed on the left, and those obtained after sedation on the right. The variable is significantly reduced by treatment ($p < 0.01$).

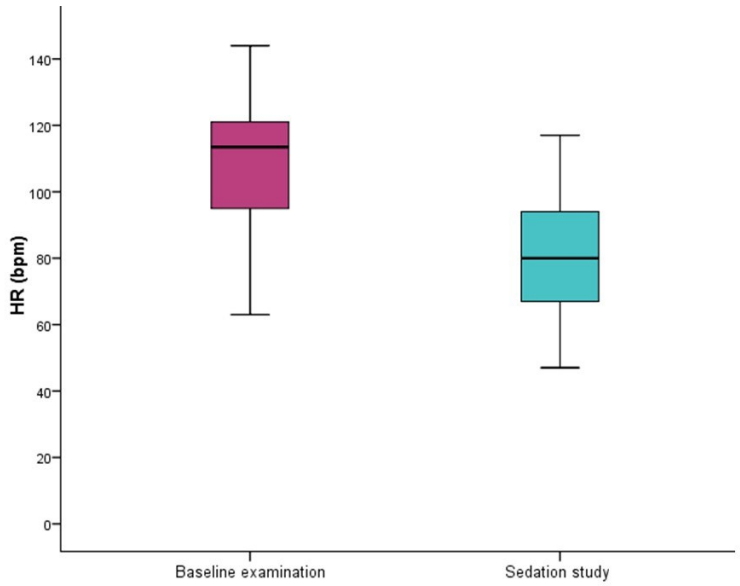

Figure 33. Change in heart rate (HR) after sedation with a combination of acepromazine and butorphanol in 18 healthy dogs. Boxes represent the interquartile range (25th to 75th percentile). The horizontal line in each box represents the median. Whiskers represent the 5th and 95th percentiles. Measures obtained at baseline are displayed on the left, and those obtained after sedation on the right. The variable is significantly reduced by treatment ($p < 0.01$).

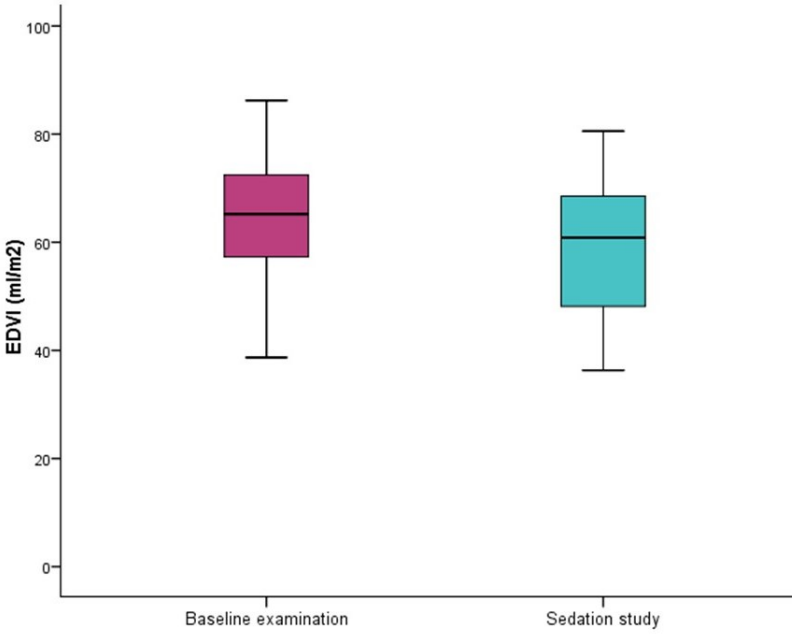

Figure 34. Change in left ventricular end-diastolic volume index (EDVI) after sedation with a combination of acepromazine and butorphanol in 18 healthy dogs. Boxes represent the interquartile range (25th to 75th percentile). The horizontal line in each box represents the median. Whiskers represent the 5th and 95th percentiles. Measures obtained at baseline are displayed on the left, and those obtained after sedation on the right. The variable is significantly reduced by treatment ($p < 0.01$).

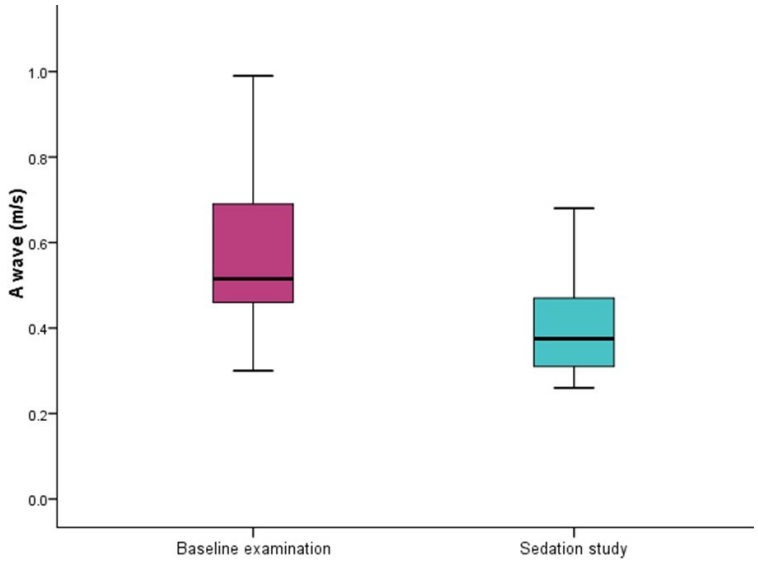

Figure 35. Change in peak velocity of late transmitral diastolic flow (A wave) after sedation with a combination of acepromazine and butorphanol in 18 healthy dogs. Boxes represent the interquartile range (25th to 75th percentile). The horizontal line in each box represents the median. Whiskers represent the 5th and 95th percentiles. Measures obtained at baseline are displayed on the left, and those obtained after sedation on the right. The variable is significantly reduced by treatment ($p < 0.01$).

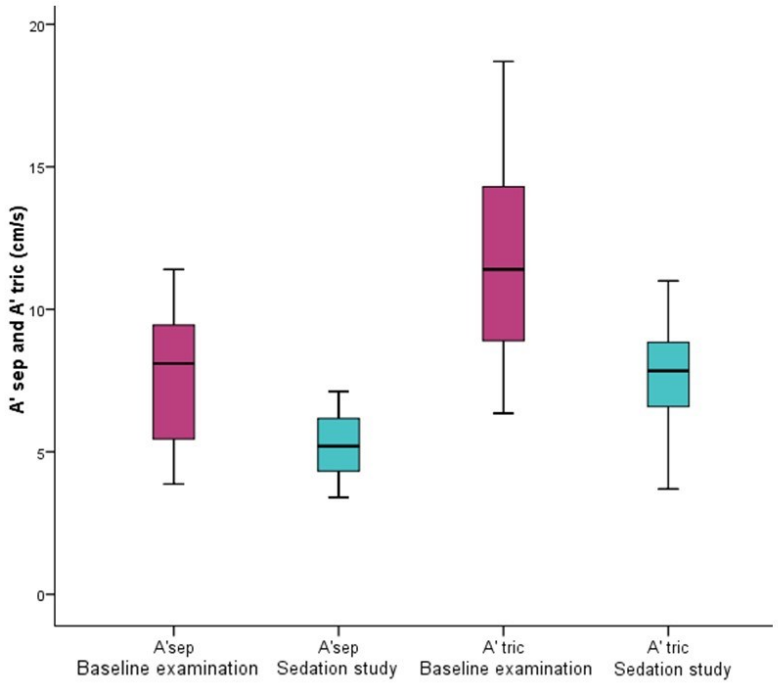

Figure 36. Change in late diastolic velocities of the septal side of the mitral annulus (A' sep) and of the lateral side of the tricuspid annulus (A' tric) after sedation with a combination of acepromazine and butorphanol in 18 healthy dogs. Boxes represent the interquartile range (25th to 75th percentile). The horizontal line in each box represents the median. Whiskers represent the 5th and 95th percentiles. Purple boxes correspond to the measures obtained at baseline, while green blue boxes to those obtained after sedation. The variables are significantly reduced by treatment ($p < 0.01$).

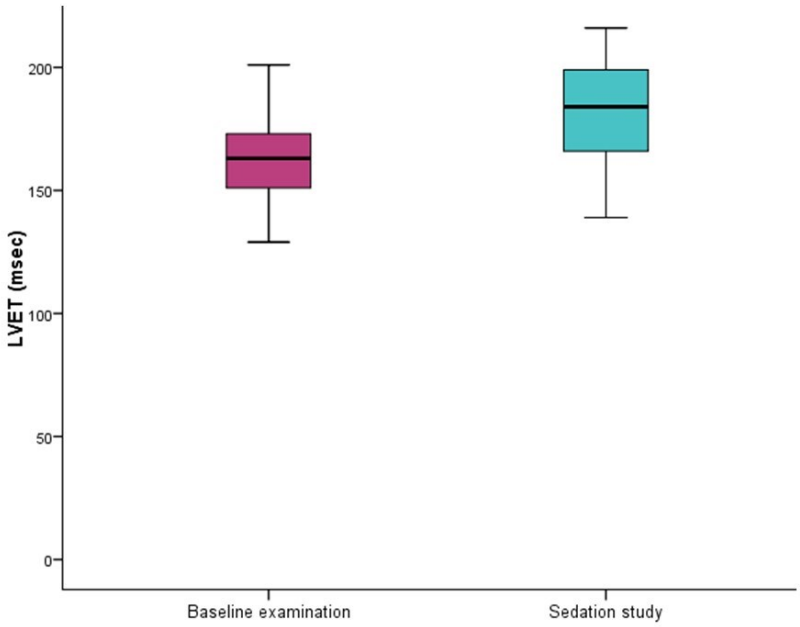

Figure 37. Change in left ventricular ejection time (LVET) after sedation with a combination of acepromazine and butorphanol in 18 healthy dogs. Boxes represent the interquartile range (25th to 75th percentile). The horizontal line in each box represents the median. Whiskers represent the 5th and 95th percentiles. Measures obtained at baseline are displayed on the left, and those obtained after sedation on the right. The variable is significantly increased by treatment ($p < 0.01$).

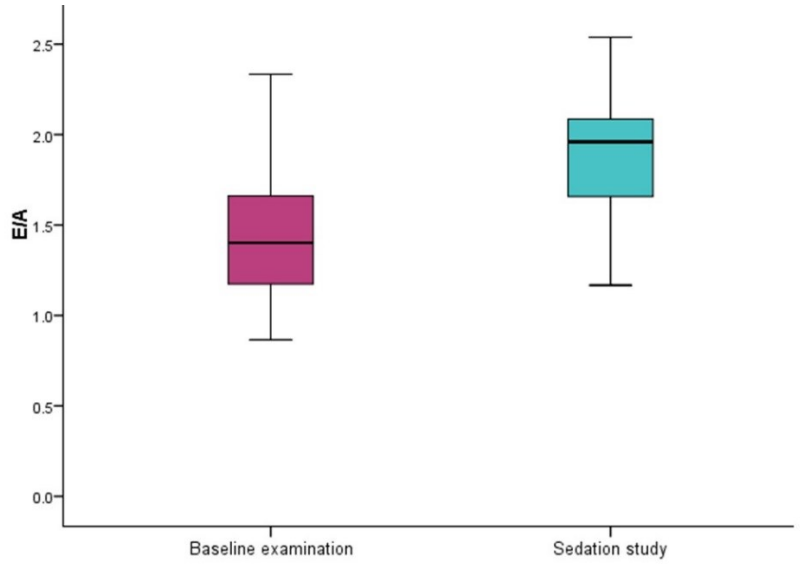

Figure 38. Change in E wave to A wave ratio (E/A) after sedation with a combination of acepromazine and butorphanol in 18 healthy dogs. Boxes represent the interquartile range (25th to 75th percentile). The horizontal line in each box represents the median. Whiskers represent the 5th and 95th percentiles. Measures obtained at baseline are displayed on the left, and those obtained after sedation on the right. The variable is significantly increased by treatment ($p < 0.01$).

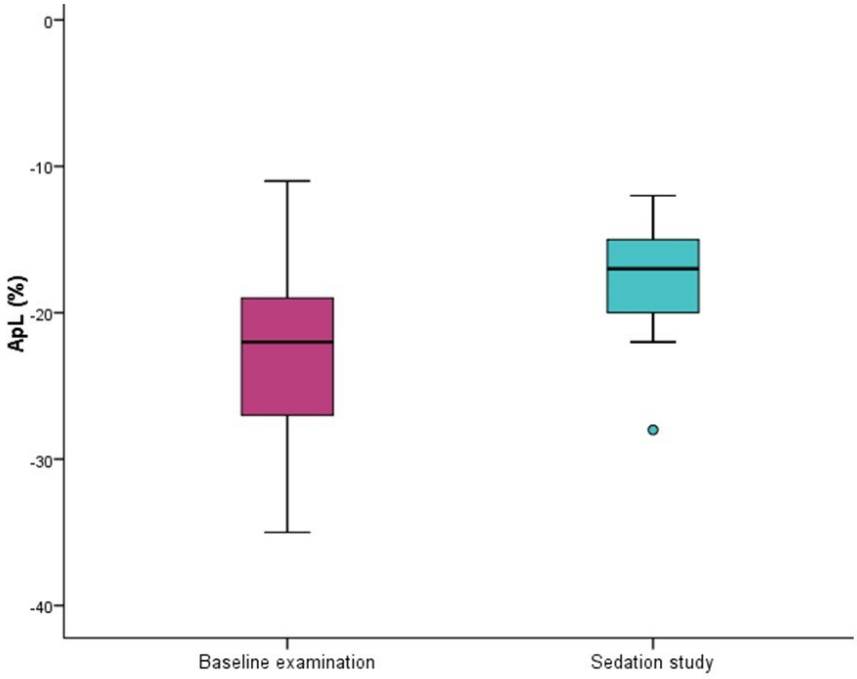

Figure 39. Change in apical lateral strain (ApL) after sedation with a combination of acepromazine and butorphanol in 18 healthy dogs. Boxes represent the interquartile range (25th to 75th percentile). The horizontal line in each box represents the median. Whiskers represent the 5th and 95th percentiles. Outliers are plotted separately as circles. Measures obtained at baseline are displayed on the left, and those obtained after sedation on the right. The variable (absolute value) is significantly decreased by treatment ($p < 0.01$).

4.2 Study 2: Use of the right parasternal four-chamber view for left ventricular longitudinal strain analysis by two-dimensional speckle tracking echocardiography in dogs

4.2.1 Study population

The initial study population comprised 62 dogs. Of these, 11 were excluded due inappropriate tracking of the apical segments from the right parasternal four-chamber RP4Ch view. Of the final study population (n = 51), 26 dogs were healthy and 25 cardiac disease.

Of the healthy dogs, five were mixed-breed, while the rest were purebred. Represented breeds comprised Labrador Retriever (n = 5), American Staffordshire Bull Terrier (n = 3), Dalmatian (n = 2), Boxer (n = 2), Spanish Podenco (n = 2), Spanish Greyhound (n = 2), Golden Retriever (n = 1), Beagle (n = 1), Bull Terrier (n = 1), Bobtail (n = 1), and Weimaraner (n = 1). Nine dogs were sexually intact females, nine were sexually intact males, seven were spayed females, and one was a castrated male. The median age of the subjects was 5.7 years (range, 1 to 12 years), and the median body weight was 26.7 Kg (range, 15 to 48 Kg). Five dogs in this group were sedated for echocardiography.

Of the dogs with cardiac disease, seven were mixed-breed, while the rest were purebred. Represented breeds comprised Bull Terrier (n = 2), Afghan Hound (n = 2), Beagle (n = 2), American Staffordshire Bull Terrier (n = 2), Golden Retriever (n = 1), Dalmatian (n = 1), Boxer (n = 1), Rottweiler (n = 1), Dogue de Bordeaux (n = 1), German Shepherd (n = 1), American Cocker Spaniel (n = 1), Standard Poodle (n = 1), Maltese (n = 1), and French Bulldog (n = 1). Nine dogs were sexually intact males, six were sexually intact females, six were spayed females, and four were castrated males. The median age of the subjects was 5.9 years (range, 3 months to 15 years), and the median body weight was 19.6 kg (range, 6 to 48 kg). The group included patients with a primary diagnosis of myxomatous mitral valve disease (MMVD; n = 9; 1 at stage B1, 6 at stage B2 and 2 at stage C based on the ACVIM classification system; Atkins et al., 2009), coexisting sub-aortic and pulmonic stenosis (n = 3), sub-aortic stenosis (n = 3), tricuspid valve dysplasia (n = 2), idiopathic dilated cardiomyopathy (n = 2), and 1 of each of hypertensive LV hypertrophy, aortic stenosis, mitral valve dysplasia, coexisting pulmonic stenosis and patent foramen ovale, pulmonic stenosis, and right bundle branch block with no identifiable structural heart disease. No dog in this group was sedated.

Healthy dogs were heavier than diseased dogs by approximately 7 Kg ($p = 0.011$). The two groups were age- and sex-matched.

4.2.2 Two-dimensional speckle tracking echocardiography

In the final study population ($n = 51$), global longitudinal strain (GLS) values obtained from the RP4Ch view differed from those obtained from the LAp4Ch view (**Fig. 40**; **Table 4**; $p < 0.05$), regardless of health status (**Fig. 41** and **42**; **Table 5**; $p < 0.05$). There were also differences in segmental strain values (**Fig. 43**; **Table 4**), and global strain rate (SR; **Fig. 44; Table 4**) depending on the view used, but these varied according to health status (**Table 5**). The mean absolute values obtained from the RP4Ch view were usually higher than LAp4Ch view values.

The Bland-Altman scattegrams comparing GLS values obtained from the RP4Ch view and the LAp4Ch view showed wide limits of agreement (**Fig. 45**). This was confirmed by the intra-class correlation coefficients (ICC), which demonstrated only a moderate degree of congruence between repeated measurements obtained from the two views in the entire population (ICC = 0.717), and within both groups of healthy (ICC = 0.737) and diseased (ICC = 0.711) dogs.

4.2.3 Measurement reliability

The reproducibility of global strain values obtained from the RP4Ch view was high, as demonstrated by CV of less than 6% (**Table 6**). Strain rate values were also within clinically acceptable limits (see Section 2.2.4; **Table 6**). By contrast, segmental strain indices had variable reproducibility, with CV often exceeding 15%.

Intra-class correlation coefficients (ICC) for GLS values showed an excellent degree of congruence between repeated measurements obtained from the RP4Ch view by the same investigator at different time points on the same day (ICC = 0.968) and on two different days (ICC = 0.989), and by two different investigators (ICC = 0.987).

Table 4. Mean ± SD values for two-dimensional speckle tracking echocardiography-derived longitudinal strain and strain rate obtained from the left apical and the right parasternal four-chamber views in a group of 51 dogs including healthy subjects and patients with various cardiac diseases.

Variable	LAp4Ch	RP4Ch
GLS (%)	–20.6 ± 4.4	**–23.8 ± 5.1**
BS (%)	–18.6 ± 6.3	**–20.9 ± 6**
MS (%)	–24.9 ± 7.3	–24.7 ± 6.1
ApS (%)	–23.9 ± 7.7	**–28.2 ± 7.4**
Apex (%)	–22.6 ± 6	**–27.3 ± 6.5**
ApL (%)	–21.6 ± 6.2	**–27.1 ± 6.9**
ML (%)	–20.1 ± 6.7	–22.6 ± 6.8
BL (%)	–21.1 ± 6.7	–22.5 ± 6.5
Peak S SR (1/s)	-2.14 ± 0.7	**-2.43 ± 0.55**
Peak E diastolic SR(1/s)	1.8 ± 0.59	**2.25 ± 0.61**
Peak A diastolic SR(1/s)	1.43 ± 0.58	1.35 ± 0.55

Bold values indicate statistical significance; the value differs significantly ($P<0.05$) from the one obtained from the standard LAp4Ch view.

LAp4Ch, left apical four-chamber view; RP4Ch, right parasternal four-chamber view; GLS, global longitudinal strain; BS, basal septal; MS, midseptal; ApS, apical septal; Apex, apical; ApL, apical lateral; ML, midlateral; BL, basal lateral; S, systolic; SR, Strain rate; E, Early diastolic; A, late diastolic.

Table 5. Mean ± SD values for two-dimensional speckle tracking echocardiography-derived longitudinal strain and strain rate obtained from the left apical and the right parasternal four-chamber views in a group of 51 dogs including healthy subjects and patients with various cardiac diseases.

	Healthy group (n=26)		**Diseased group (n=25)**	
Variable	**LAp4Ch**	**RP4Ch**	**LAp4Ch**	**RP4Ch**
GLS (%)	–20.8 ± 4	**–23.8 ± 4**	–20.4 ± 4.9	**–23.8 ± 6.1**
BS (%)	–18.5 ± 7.1	–20 ± 5.6	–18.7 ± 5.3	**–21.9 ± 6.4**
MS (%)	–24.9 ± 7.3	–25.5 ± 6.1	–23.4 ± 9.1	–28.6 ± 7.9
ApS (%)	–24.4 ± 6.3	**–27.7 ± 6.9**	–21.8 ± 7.1	**–27.7 ± 6.8**
Apex (%)	–23.4 ± 4.7	**–26.9 ± 6.3**	–20.6 ± 6.5	**–27.4 ± 7.1**
ApL (%)	–22.6 ± 5.9	**–26.6 ± 6.8**	–21.8 ± 6.9	**–21.8 ± 8.1**
ML (%)	–19.7 ± 6.4	**–23.5 ± 5.3**	–21 ± 7.4	–22.4 ± 6.6
BL (%)	–21.3 ± 6.2	–22.7 ± 6.4	–21.2 ± 6.8	–22.5 ± 6.5
Peak S SR (1/s)	-2.3 ± 0.74	-2.42 ± 0.49	-1.99 ± 0.6	**-2.43 ± 0.6**
Peak E diastolic SR(1/s)	1.94 ± 0.48	2.2 ± 0.56	1.67 ± 0.67	**2.3 ± 0.67**
Peak A diastolic SR(1/s)	1.37 ± 0.43	1.25 ± 0.55	1.49 ± 0.71	1.47 ± 0.54

Bold values indicate statistical significance; the value differs significantly ($P<0.05$) from the one obtained from the standard LAp4Ch view.

LAp4Ch, left apical four-chamber view; RP4Ch, right parasternal four-chamber view; GLS, global longitudinal strain; BS, basal septal; MS, midseptal; ApS, apical septal; Apex, apical; ApL, apical lateral; ML, midlateral; BL, basal lateral; S, systolic; SR, Strain rate; E, Early diastolic; A, late diastolic.

Table 6. Intra-observer (within-day and between-day) and inter-observer variability (coefficients of variation in %) of two-dimensional speckle tracking echocardiography-derived longitudinal strain and strain rate obtained from the left apical and the right parasternal four-chamber views in six dogs.

	Intra-observer (Within-day) CV (%)		**Intra-observer (Between-day) CV (%)**		**Intra-observer (Between-day) CV (%)**	
Variable	**LAp4Ch**	**RP4Ch**	**LAp4Ch**	**RP4Ch**	**LAp4Ch**	**RP4Ch**
GLS	5.6	5.1	3.1	1.4	3.2	2.1
BS	16.9	19.6	16.2	6.6	6.6	8.5
MS	10.4	16.3	20.5	7.1	17.2	12.4
ApS	9.1	9.8	9.6	14.5	17.4	9.7
Apex	7.3	8.7	6.4	1.1	10	6.5
ApL	14.1	13.3	9.7	4.8	5.3	7.6
ML	2.3	17.4	14.1	8.8	14.3	21.7
BL	15.6	16.9	10.6	10.2	17.2	16.6
Peak S SR	4.4	9.4	8.1	6.3	7.8	4
Peak E diastolic SR	10.5	10.3	10.8	9.3	8.8	3.6
Peak A diastolic SR	13.6	14.2	11	8.5	14.2	13.1

LAp4Ch, left apical four-chamber view; RP4Ch, right parasternal four-chamber view; GLS, global longitudinal strain; BS, basal septal; MS, midseptal; ApS, apical septal; Apex, apical; ApL, apical lateral; ML, midlateral; BL, basal lateral; S, systolic; SR, Strain rate; E, Early diastolic; A, late diastolic.

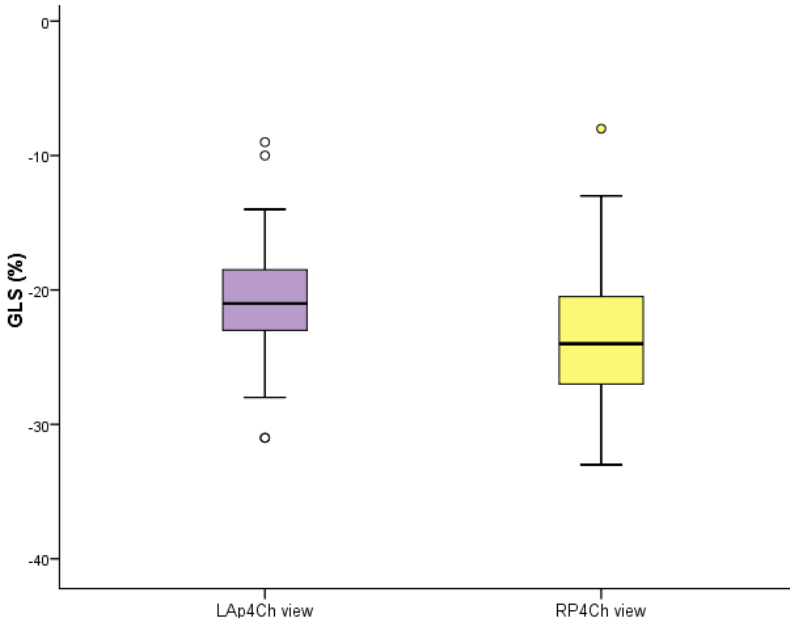

Figure 40. Global longitudinal strain (GLS) obtained from the left apical four-chamber (LAp4Ch) and right parasternal four-chamber (RP4Ch) views in a population 51 dogs, including healthy subjects and patients with various cardiac diseases. Boxes represent the interquartile range (25th to 75th percentile). The horizontal line in each box represents the median. Whiskers represent the 5th and 95th percentiles. Outliers are plotted separately as circles. Measures obtained from the LAp4Ch view are displayed on the left, and those obtained from the RP4Ch view on the right. Mean absolute values from the RP4Ch view are significantly higher ($p < 0.05$).

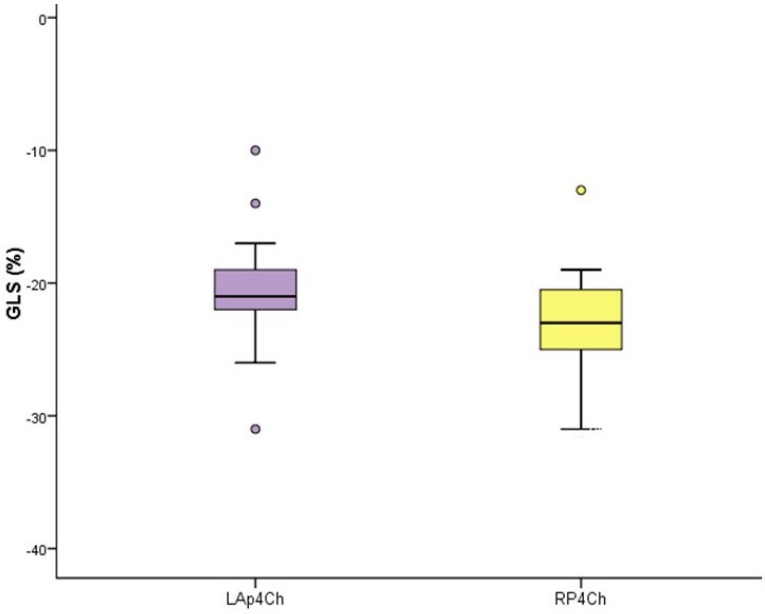

Figure 41. Global longitudinal strain (GLS) obtained from the left apical four-chamber (LAp4Ch) and right parasternal four-chamber (RP4Ch) views in 26 healthy dogs. Boxes represent the interquartile range (25th to 75th percentile). The horizontal line in each box represents the median. Whiskers represent the 5th and 95th percentiles. Outliers are plotted separately as circles. Measures obtained from the LAp4Ch view are displayed on the left, and those obtained from the RP4Ch view on the right. Mean absolute values from the RP4Ch view are significantly higher ($p < 0.05$).

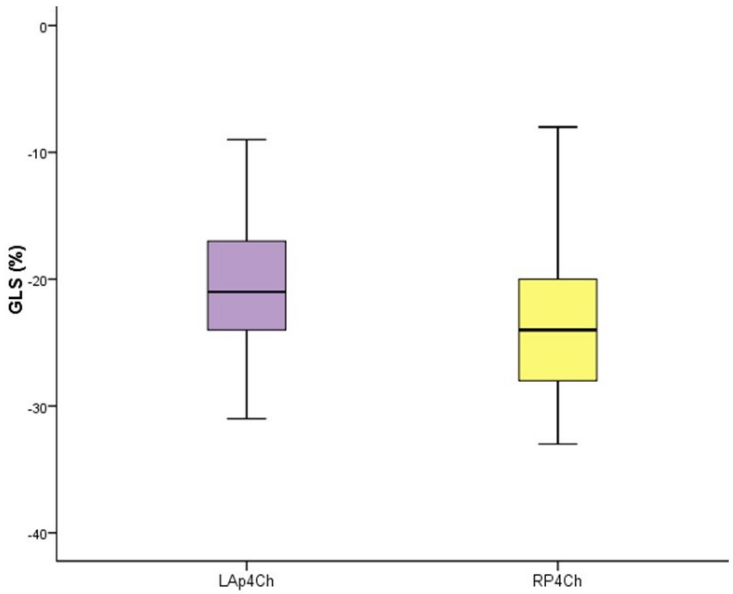

Figure 42. Global longitudinal strain (GLS) obtained from the left apical four-chamber (LAp4Ch) and right parasternal four-chamber (RP4Ch) views in 25 dogs with various cardiac diseases. Boxes represent the interquartile range (25th to 75th percentile). The horizontal line in each box represents the median. Whiskers represent the 5th and 95th percentiles. Measures obtained from the LAp4Ch view are displayed on the left, and those obtained from the RP4Ch view on the right. Mean absolute values from the RP4Ch view are significantly higher ($p < 0.05$).

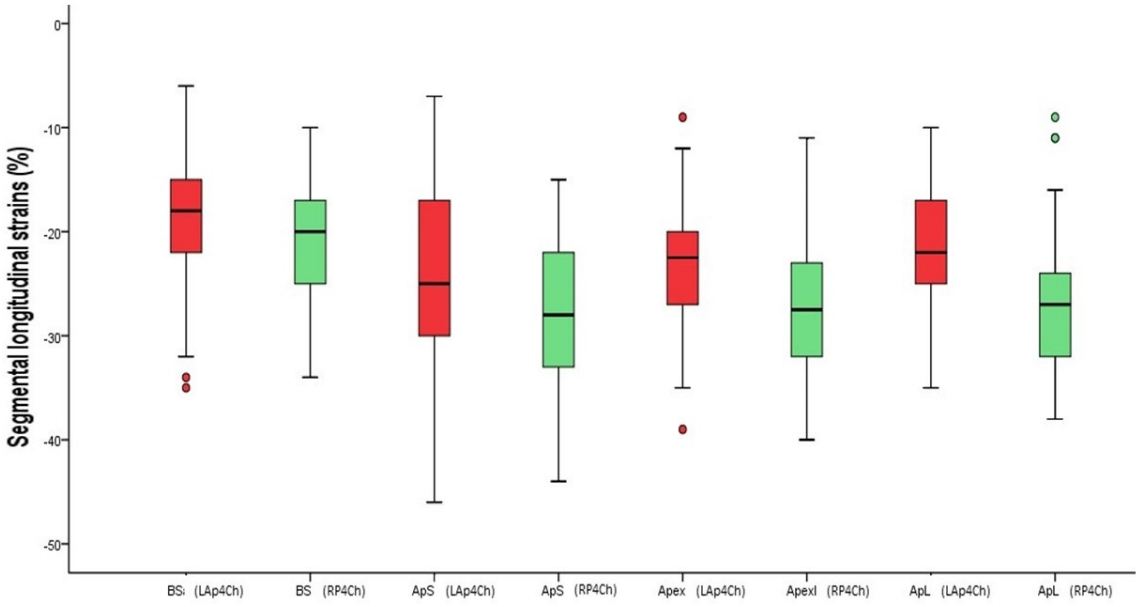

Figure 43. Segmantal longitudinal strains obtained from the left apical four-chamber (LAp4Ch) and right parasternal four-chamber (RP4Ch) views in a population 51 dogs, including healthy subjects and patients with various cardiac diseases. Boxes represent the interquartile range (25th to 75th percentile). The horizontal line in each box represents the median. Whiskers represent the 5th and 95th percentiles. Outliers are plotted separately as circles. Red boxes correspond to measures obtained from the LAp4Ch view, while green boxes to those obtained from the RP4Ch view. Represented segments comprise the basal septal (BS), apical septal (ApS), apical (Apex) and apical lateral (ApL). Mean absolute values for each segment represented are significantly higher when obtained from the RP4Ch ($p < 0.05$).

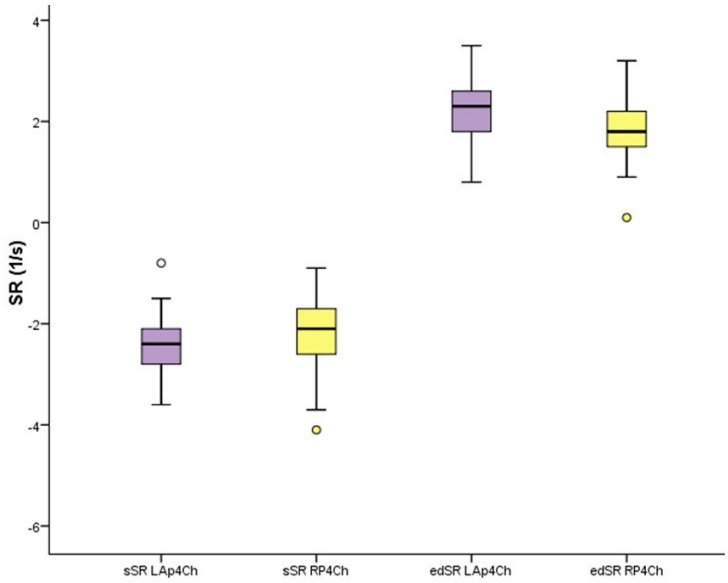

Figure 44. Strain rates (SR) obtained from the left apical four-chamber (LAp4Ch) and right parasternal four-chamber (RP4Ch) views in a population of 51 dogs, including healthy subjects and patients with various cardiac diseases. Boxes represent the interquartile range (25th to 75th percentile). The horizontal line in each box represents the median. Whiskers represent the 5th and 95th percentiles. Outliers are plotted separately as circles. Purple boxes correspond to measures obtained from the LAp4Ch view, while yellow boxes to those obtained from the RP4Ch view. Represented SR are peak systolic SR (sSR) and early diastolic SR (edSR). Mean absolute values for each segment represented are significantly higher when obtained from the RP4Ch ($p < 0.05$).

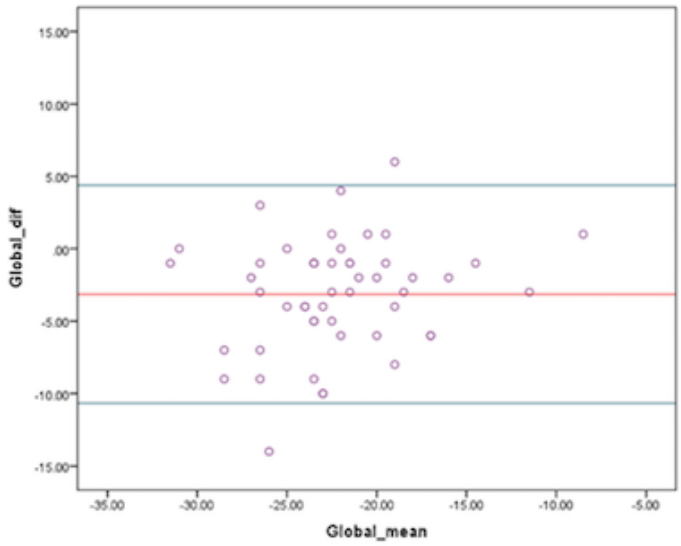

Figure 45. Bland-Altman plots for global longitudinal strain (GLS, %) in a group of 51 dogs, comprising 26 healthy animals and 25 animals with various cardiac diseases. The differences of the GLS values, obtained from the right parasternal four-chamber (RP4Ch) and left apical four-chamber (LAp4Ch) views, are plotted against average values from both views. The mean differences (red middle line) and the range containing the mean of the differences ± 1.96 SD (blue lines) are shown.

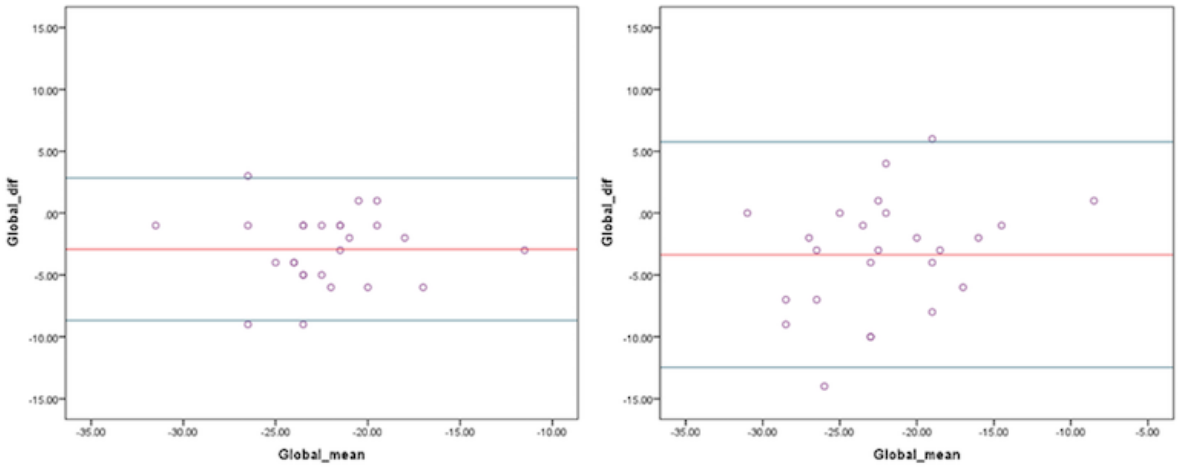

Figure 46. Bland-Altman plots for global longitudinal strain (GLS, %) in two groups of dogs, one comprising 26 healthy dogs and the other 25 dogs with various cardiac diseases. The graph on the left displays healthy dogs, while the one the right cardiovascularly diseased dogs. In each graph, the differences of the GLS values, obtained from the right parasternal four-chamber (RP4Ch) and left apical four-chamber (LAp4Ch) views, are plotted against average values from both views. The mean differences (red middle line) and the range containing the mean of the differences ± 1.96 SD (blue lines) are shown.

4.3 Study 3: Inter-software variability of two-dimensional speckle tracking-derived parameters in dogs

4.3.1 Study population

The initial study population comprised 96 dogs. Of these, 12 were excluded from the comparative study among software as TomTec vendor independent software could not preform reliable analysis. The final study population comprised 84 dogs, divided in two cohorts, as detailed below.

The Philips-cohort comprised 44 dogs. Of these, 14 were mixed-breed, while the rest were purebred. Represented breeds comprised Labrador Retriever (n = 4), American Staffordshire Bull Terrier (n = 3), German Shepherd dog (n = 3), Doberman Pinscher (n = 3), Spanish Greyhound (n = 2), Yorkshire Terrier (n = 2), Cavalier King Charles Spaniel (n = 2), Spanish Water dog (n = 2), Boxer (n = 1), Dalmatian (n = 1), Spanish Podenco (n = 1), Golden Retriever (n = 1), Beagle (n = 1), Pomeranian (n = 1), Fox Terrier (n = 1), Spanish Mastiff (n = 1), and Standard Poodle (n = 1). Eighteen dogs were sexually intact males, twelve were spayed females, ten were sexually intact females, and four were castrated males. The median age of the subjects was 6.5 years (range, 1 to 17 years), and the median body weight was 21 Kg (range, 3 to 48 Kg). Twenty-three dogs were cardiovascularly healthy, while 21 had cardiac disease. The latter were patients with a primary diagnosis of myxomatous mitral valve disease (MMVD; n = 14; 4 at stage B1, 5 at stage B2 and 5 at stage C based on the ACVIM classification system; Atkins et al., 2009), idiopathic dilated cardiomyopathy (DCM; n = 2), coexisting mild sub-aortic and pulmonic stenosis (n = 2), and 1 of each of mild sub-aortic stenosis, hypertensive LV hypertrophy and right auricular hemangiosarcoma.

The GE-cohort comprised 40 dogs. Of these, four were mixed-breed, while the rest were purebred. Represented breeds comprised Labrador Retriever (n = 8), German Shepherd dog (n = 4), Golden Retriever (n = 3), Whippet (n = 3), English Springer Spaniel (n = 2), Newfoundland (n = 1), Staffordshire Bull Terrier (n = 1), Japanese Akita (n = 1), Bearded Collie (n = 1), Boxer (n = 1), Basset Hound (n = 1), Miniature Schnauzer (n = 1), Lakeland Terrier (n = 1), Flatcoated Retriever (n = 1), Chihuahua (n = 1), Border Collie (n = 1), Lhasa Apso (n = 1), Cockerpoo (n = 1), Spanish Greyhound (n = 1), Beagle (n = 1), and Cairn Terrier (n = 1). Seventeen dogs were spayed females, 13 were castrated males, nine were sexually intact males, and one was a sexually intact female. The median age of the

subjects was 7 years (range, 6 months to 14 years), and the median body weight was 21.2 Kg (range, 1.3 to 47.5 Kg). Eighteen dogs were cardiovascularly healthy, while 22 had cardiac disease. The latter were patients with a primary diagnosis of MMVD (n = 8; 5 at stage B1 and 3 at stage B2 based on the ACVIM classification system; Atkins et al., 2009), idiopathic DCM (n = 4), left-to-right shunting patent ductus arteriosus (n = 3), severe pulmonic stenosis (n = 3), tricuspid valve dysplasia (n = 2), and 1 of each of mild sub-aortic stenosis and pericardial hemangiosarcoma.

4.3.2 Two-dimensional speckle tracking echocardiography

In the final study population (n = 84), data were mostly non-normally distributed, and were therefore expressed as medians and ranges.

4.3.2.1 Two-dimensional speckle tracking echocardiography-derived analysis of images obtained with Philips ultrasound system

In 11 dogs, vendor independent software could not perform reliable deformation analysis.

In the final cohort (n = 44), three out of four echocardiographic variables obtained with vendor specific software differed from those obtained with vendor independent software (**Table 7**). Mean absolute values for global longitudinal strain (GLS), peak systolic strain rate (SR), and peak late diastolic SR obtained with vendor specific software were higher than those obtained with vendor independent software (**Fig. 47** to **49**; **Table 7**; $p < 0.05$).

The Bland-Altman scattegrams comparing values obtained with vendor specific software and with vendor independent software showed wide limits of agreement (**Fig. 50**). For GLS values, the Bland-Altman plot showed a mean difference of -0.9%, with a range in strain values of – 6.5 % to + 4.7 % (95% LOA). For systolic SR, the mean difference was -0.3 1/s, with a range in SR values of -1.5 1/s to + 0.9 1/s (95% LOA). For early diastolic SR, the mean difference was 0.1 1/s, with a range in SR values of -1.5 1/s to + 1.7 1/s (95% LOA). For late diastolic SR, the mean difference was 0.7 1/s, with a range in SR values of -0.5 1/s to + 1.9 1/s (95% LOA).

4.3.2.2 Two-dimensional speckle tracking echocardiography-derived analysis of images obtained with General Electric ultrasound system

In one dog, vendor independent software could not perform reliable deformation analysis.

In the final cohort (n = 40), all the echocardiographic variables obtained with vendor specific software differed from those obtained with vendor independent software (**Table 7**). Mean absolute values for mid-myocardial strain obtained with GE software were lower than mean absolute endocardial values obtained with TomTec (**Fig. 51**; p = 0.006). By contrast, mean absolute endocardial values obtained with GE were higher than those obtained with TomTec (**Fig. 51**; p < 0.001). Peak systolic strain rate (SR), peak early diastolic SR and peak late diastolic SR obtained with vendor specific software were lower than those obtained with vendor independent software (**Table 7**; p < 0.05).

The Bland-Altman scattegrams comparing values obtained with vendor specific software and with vendor independent software showed wide limits of agreement (**Fig. 52** and **53**). The mean difference between mid-myocardial strain values obtained with GE software and endocardial strain values obtained with TomTec software was 1.3%, with a range in strain values of – 4.4 % to + 7 % (95% LOA; **Fig. 52**). The mean difference between endocardial strain values obtained with GE software and TomTec software was -2.6 %, with a range in strain values of – 8.9 % to + 3.7 % (95% LOA; **Fig. 52**).

For systolic SR values, the Bland-Altman plot showed a mean difference of -0.2 1/s, with a range in SR values of – 1.4 1/s to + 1.8 1/s (95% LOA). For early diastolic SR, the mean difference was 0.7 1/s, with a range in SR values of -1.7 1/s to + 3.1 1/s (95% LOA). For late diastolic SR, the mean difference was 0.3 1/s, with a range in SR values of – 0.7 1/s to + 1.3 1/s (95% LOA).

4.3.3 Measurement reliability

The reproducibility of global strain values was high for each software, as demonstrated by CV of less than 10%. Systolic SR values were also within clinically acceptable limits (see Section 2.3.4). By contrast, diastolic SR had variable reproducibility, with CV reaching up to 18.7 %.

Table 7. Median (and range) values for two-dimensional speckle tracking echocardiography-derived longitudinal strain and strain rate obtained with vendor-dependent and vendor independent software in 84 dogs, sub-divided in two cohorts according to the ultrasound system employed to obtain the echocardiograms analyzed, and including both cardiovascularly healthy dogs and dogs with various cardiac diseases.

	Philips cohort (n = 44)			**GE cohort (n = 40)**		
Variable	**Philips**	**TomTec**	**P value**	**GE**	**TomTec**	**P value**
GLS (%)	- 21 (-33 to -14)	-19.5 (-39 to -11)	0.020	- 17.5 (-27.5 to -9.5)	-18.8 (-28.9 to -4.3)	0.006
Endo (%)				- 21.7 (-32.3 to -11.4)	[-18.8 (-28.9 to -4.3)]	<0.001
Peak S SR (1/s)	- 2.2 (-3.2 to -1.4)	-1.8 (-4.4 to -0.7)	0.005	- 1.8 (-2.9 to -0.3)	-1.8 (-2.9 to -0.4)	<0.001
Peak E diastolic SR (1/s)	2.1 (0.1 to 3.4)	2 (0.6 to 5.4)	0.357	1.6 (0.5 to 5)	1.2 (0.4 to 4)	<0.001
Peak A diastolic SR (1/s)	1.5 (0.7 to 3.5)	0.9 (0.3 to 2.4)	<0.001	1 (0.6 to 2.3)	0.7 (0.3 to 2.3)	0.003

Values are considered different, with statistical significance, when $P<0.05$.

GE, General Electric; GLS, global longitudinal strain; Endo, endocardial strain (obtained with GE software); S, systolic; SR, Strain rate; E, Early diastolic; A, late diastolic.

Table 8. Intra-observer (within-day and between-day) and interobserver variability (coefficients of variation in %) of two-dimensional speckle tracking echocardiography-derived longitudinal strain and strain rate obtained with Philips (vendor-specific) and TomTec (vendor independent) software in six dogs, whose echocardiograms were obtained with Philips ultrasound system.

	Intra-observer (Within-day) CV (%)		**Intra-observer (Between-day) CV (%)**		**Intra-observer (Between-day) CV (%)**	
Variable	**Philips**	**TomTec**	**Philips**	**TomTec**	**Philips**	**TomTec**
GLS	3.5	5.6	3.1	9.5	8	3.9
Peak S SR	7.4	8.6	6.2	9.8	7.8	5.7
Peak E diastolic SR	11.3	5.8	9.3	16.9	8.8	11.1
Peak A diastolic SR	14.2	13.1	8.5	18.7	14.2	17.3

CV, coefficients of variation; GLS, global longitudinal strain; S, systolic; SR, Strain rate; E, Early diastolic; A, late diastolic.

Table 9. Intra-observer (within-day and between-day) and inter-observer variability (coefficients of variation in %) of two-dimensional speckle tracking echocardiography-derived longitudinal strain and strain rate obtained with General Electric (GE; vendor-specific) and TomTec (vendor independent) software in six dogs, whose echocardiograms were obtained with GE ultrasound system.

	Intra-observer (Within-day) CV (%)		**Intra-observer (Between-day) CV (%)**		**Intra-observer (Between-day) CV (%)**	
Variable	**GE**	**TomTec**	**GE**	**TomTec**	**GE**	**TomTec**
GLS	2.8	6.2	5.5	3.8	6.8	7.1
Endo	2.9		7.4		9.9	
Peak S SR	6.9	8.9	8.1	6.8	7.6	15.1
Peak E diastolic SR	4.1	11.1	10.8	4.7	11.7	16.2
Peak A diastolic SR	6	10.9	11	16.9	17.1	11.6

CV, coefficients of variation; GE, General Electric; GLS, global longitudinal strain; Endo, endocardial strain (obtained with GE software); S, systolic; SR, Strain rate; E, Early diastolic; A, late diastolic.

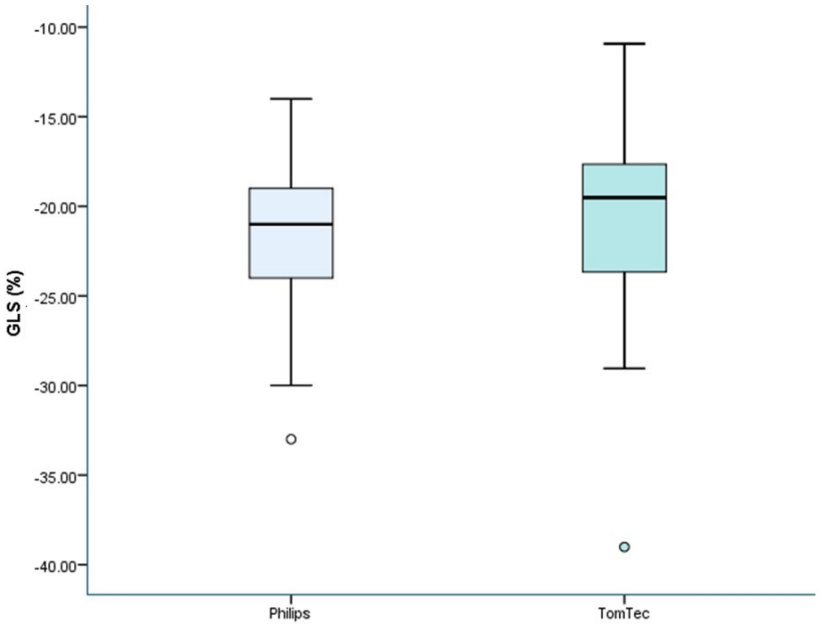

Figure 47. Global longitudinal strain (GLS) obtained with vendor specific software (Philips) and vendor independent software (TomTec) in a population of 44 dogs, including healthy subjects and patients with various cardiac diseases. Boxes represent the interquartile range (25th to 75th percentile). The horizontal line in each box represents the median. Whiskers represent the 5th and 95th percentiles. Outliers are plotted separately as circles. Measures obtained with Philips are displayed on the left, while those obtained with TomTec on the right. Mean absolute values obtained with Philips view are significantly higher than those obtained with TomTec (p = 0.020).

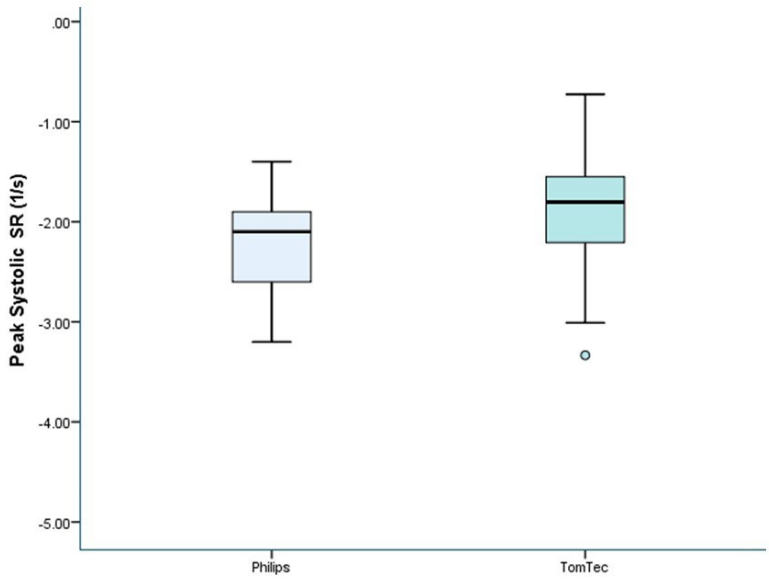

Figure 48. Peak systolic strain rate (SR) obtained with vendor specific software (Philips) and vendor independent software (TomTec) in a population of 44 dogs, including healthy subjects and patients with various cardiac diseases. Boxes represent the interquartile range (25th to 75th percentile). The horizontal line in each box represents the median. Whiskers represent the 5th and 95th percentiles. Outliers are plotted separately as circles. Measures obtained with Philips are displayed on the left, while those obtained with TomTec on the right. Mean absolute values obtained with Philips view are significantly higher than those obtained with TomTec (p = 0.005).

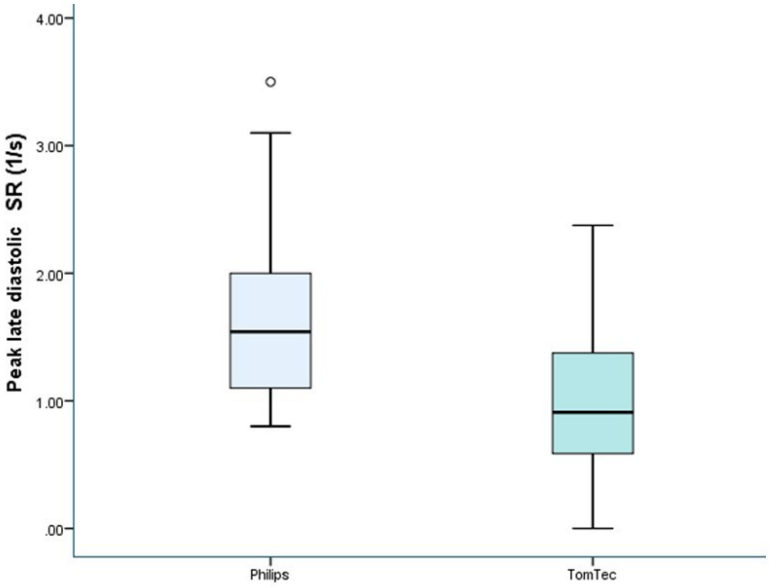

Figure 49. Peak late diastolic strain rate (SR) obtained with vendor specific software (Philips) and vendor independent software (TomTec) in a population of 44 dogs, including healthy subjects and patients with various cardiac diseases. Boxes represent the interquartile range (25th to 75th percentile). The horizontal line in each box represents the median. Whiskers represent the 5th and 95th percentiles. Outliers are plotted separately as circles. Measures obtained with Philips are displayed on the left, while those obtained with TomTec on the right. Mean absolute values obtained with Philips view are significantly higher than those obtained with TomTec ($p < 0.00$

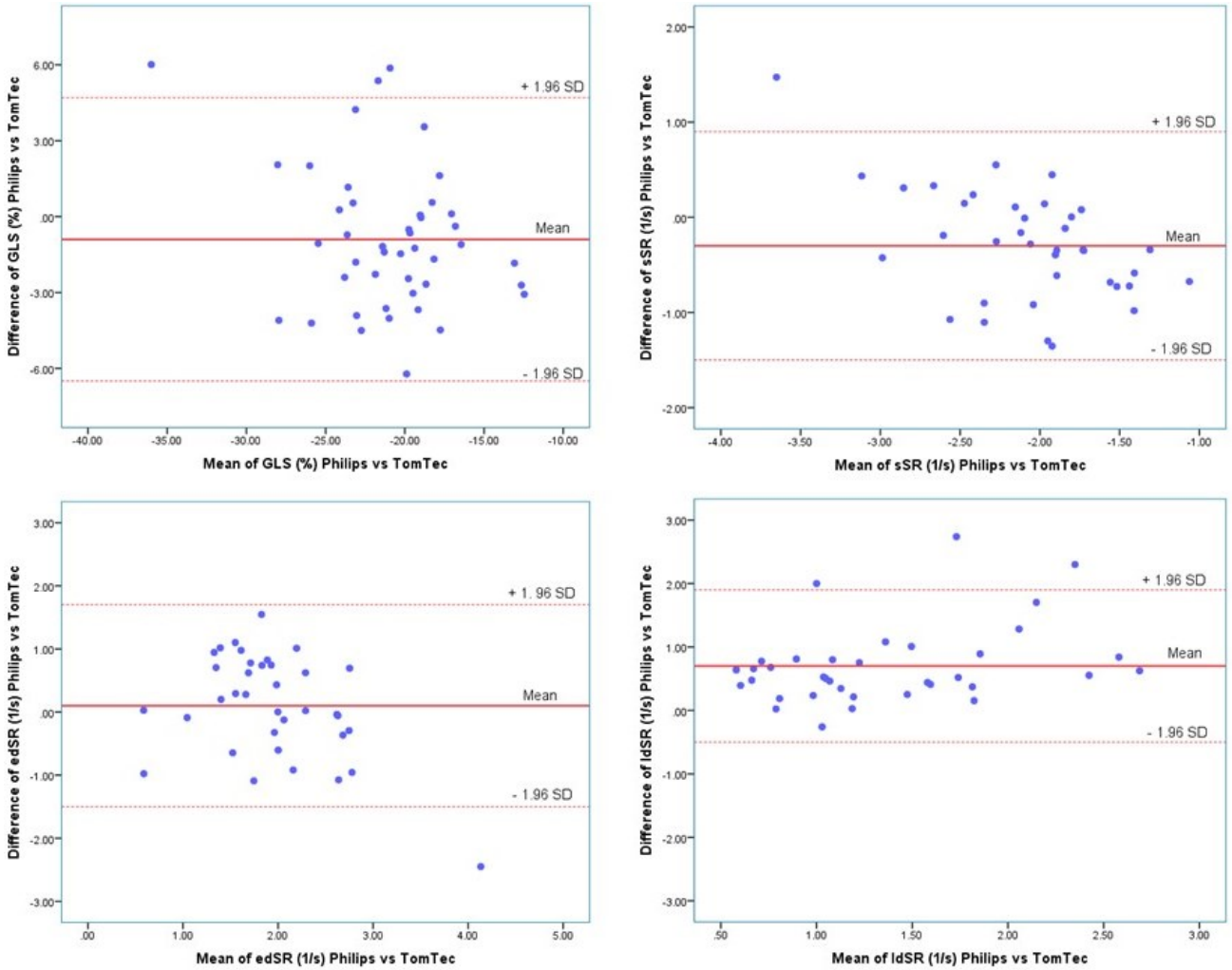

Figure 50. Bland-Altman plots for global longitudinal strain (GLS), peak systolic strain rate (sSR), early diastolic strain rate (edSR) and late diastolic strain rate (ldSR) in a group of 44 dogs, comprising healthy animals and animals with various cardiac diseases. The differences of the above values, obtained wi Philips software (Vendor 1), are plotted against average values from TomTec vendor independent software (Vendor Independent). The mean differences (red middle line) and the range containing the mean of the differences ± 1.96 SD (red dotted lines) are shown.

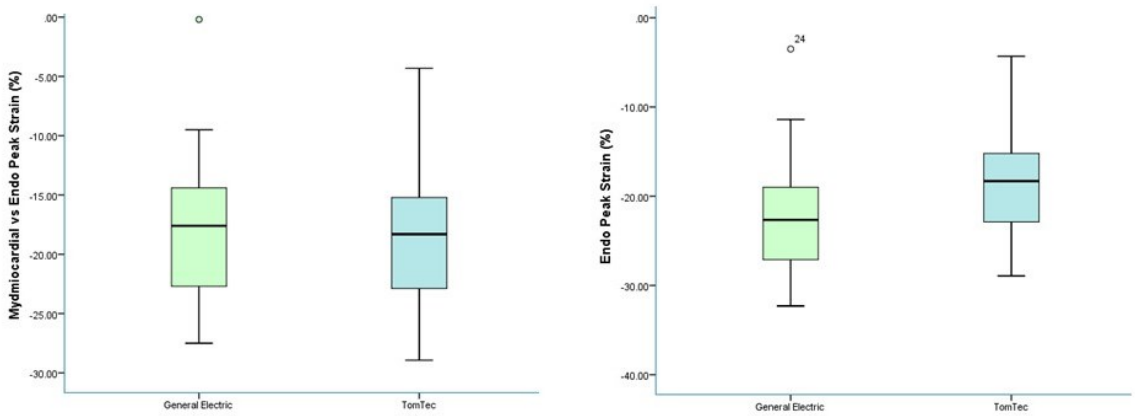

Figure 51. Global longitudinal strain obtained with vendor specific software [General Electric (GE)] and vendor independent software (TomTec) in a population of 40 dogs, including healthy subjects and patients with various cardiac diseases. The graph on the left displays midmyocardial strain obtained with GE (green box) and endocardial strain obtained with TomTec (blue box). The graph on the right displays endocardial strain obtained with GE (green box) and endocardial strain obtained with TomTec (blue box). Boxes represent the interquartile range (25th to 75th percentile). The horizontal line in each box represents the median. Whiskers represent the 5th and 95th percentiles. Outliers are plotted separately as circles. Mean absolute midmyocardial values obtained with GE are significantly lower than mean absolute endocardial values obtained with TomTec ($p = 0.006$). Mean absolute endocardial values obtained with GE are significantly higher than those obtained with TomTec ($p < 0.001$).

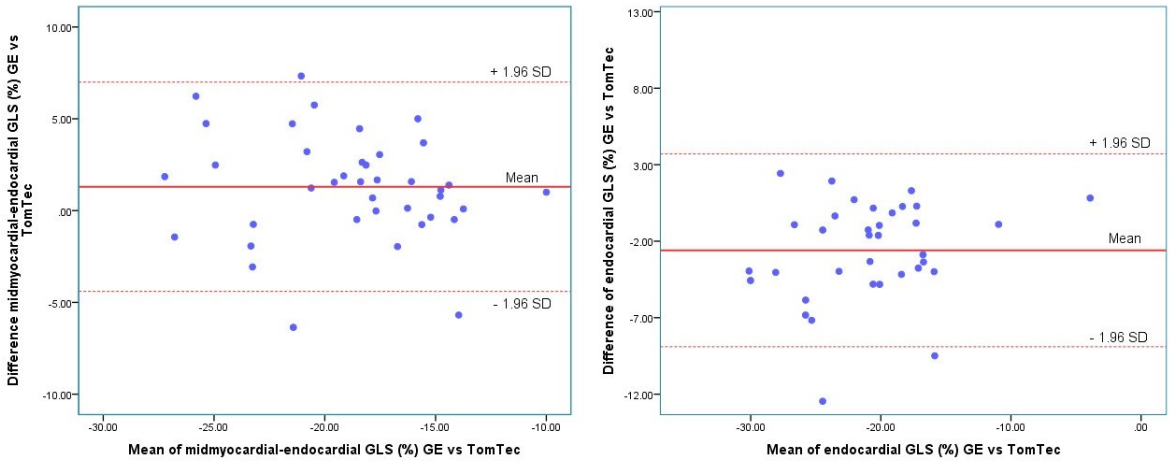

Figure 52 – Bland-Altman plots for global longitudinal strain (GLS) obtained with vendor specific software General Electric (GE)] and vendor independent software (TomTec) in a population of 40 dogs, including healthy subjects and patients with various cardiac diseases. The graph on the left displays the comparison between midmyocardial strain obtained with GE and endocardial strain obtained with TomTec. The graph on the right displays the comparison between endocardial strain obtained with GE and endocardial strain obtained with TomTec. The differences of the above values, obtained with GE-specific software, are plotted against average values from vendor independent software (TomTec). The mean differences (red middle line) and the range containing the mean of the differences ± 1.96 SD (red dotted lines) are shown.

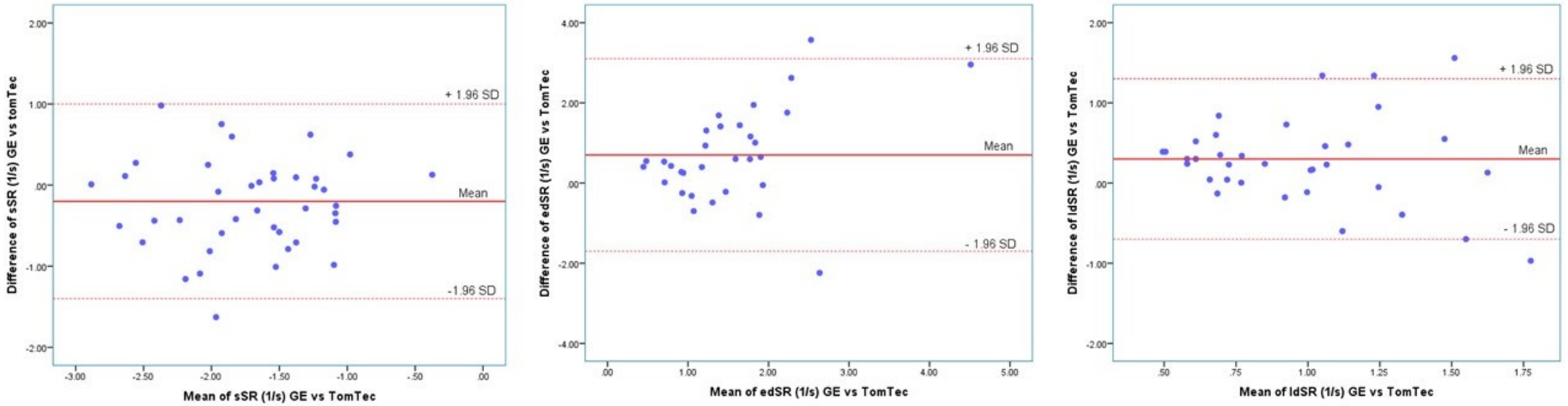

Figure 53 – Bland-Altman plots for peak systolic strain rate (sSR), early diastolic strain rate (edSR) and late diastolic strain rate (ldSR) obtained with General Electric (GE) specific software and TomTec vendor independent software in a population of 40 dogs, including healthy subjects and patients with various cardiac diseases. The graph on the left displays sSR, the one in the middle between edSR, and the one on the left between ldSR, each obtained with Vendor 2 and Vendor Independent. The differences of the above values, obtained with Vendor 2, are plotted against average values from Vendor Independent. The mean differences (red middle line) and the range containing the mean of the differences ± 1.96 SD (red dotted lines) are shown.

DISCUSSION

5. DISCUSSION

The experiments conducted focused on different aspects of two-dimensional (2-D) speckle tracking echocardiography (STE) in dogs, and aimed at improving its applicability and correct interpretation in the canine species. Firstly, the effects of a combination of acepromazine (ACP) and butorphanol (BUT) on 2-D STE-derived strain values, obtained in healthy dogs, were evaluated. The results indicated that a combination of ACP (0.02 mg/Kg) and BUT (0.2 mg/Kg) administered intramuscularly (IM) provides adequate sedation to facilitate echocardiography, with only a minor influence on 2-D STE-derived variables, when the scans are performed 30 to 40 minutes after treatment. Secondly, the use of the right parasternal four-chamber view (RP4Ch) view for the assessment of longitudinal strain and strain rate (SR) by use of 2-D STE was investigated in healthy dogs and dogs with cardiac disease. The results indicated that it is feasible to use this view to measure the aforementioned variables. However, the values obtained cannot be used interchangeably with those obtained from the standard left apical four-chamber (LAp4Ch) view. Thirdly, different 2-D STE software for longitudinal strain analysis were compared in dogs with and without cardiac disease. The results indicated that feasibility is not uniform across software methods, despite the use of good quality images and relatively high frame rate (FR). Furthermore, statistically significant differences between software exist for global longitudinal strain (GLS) and SR measurements. Overall, the reproducibility of GLS measurements was good, and superior to that of SR. A thorough discussion of the results of each study can be found hereafter.

The majority of the 2-D STE-derived variables investigated in Study 1 were not significantly affected by sedation. In particular, no significant differences in global strain indices were found, and only one out of seven segmental strain values [apical lateral strain (ApL)] decreased significantly after sedation. The lack of a significant effect on global values is probably more interesting than the change in one segmental variable, as the former are more often used, and accurately represent the entire left ventricular (LV) deformation (Smith et al., 2012). A study comparing strain parameters attained with recently released software from two manufacturers, including the one employed in Study 1, showed good agreement for GLS but not for segmental values (Castel et al., 2014). It seems, therefore, that the use of GLS could be preferable for clinical purposes.

In Study 1, the segmental longitudinal strain values measured were not comparable to those of a previous investigation where different equipment and segmentation were used

(Wess et al., 2011). Importantly, the software employed in Study 1 segments the LV into seven regions, and so is different from other software, which divide the LV into six regions. The latter difference mainly involves the apical region, where the only segment affected by sedation in Study 1 is found, meaning that the results could be different if another platform is used. Lastly, the method of segmentation used by the systems currently available is based on the human anatomy of the LV, which is not necessarily representative of the canine LV (Smith et al., 2012). The software are, in fact, developed to provide the best agreement with the available anatomic human data, and to reflect the coronary perfusion territories, based on the clinical application in this species. The use of global values may therefore be more applicable in veterinary medicine.

Cardiovascular parameters were also assessed in Study 1 to assist in the interpretation of the effects of sedation on 2-D STE-derived variables. A mild but significant decrease in diastolic and mean arterial blood pressure was observed after sedation, and hypotension was recorded in two dogs, characterized by a systolic arterial pressure (SAP) less than 90 mm Hg in one dog, and by a mean arterial pressure (MAP) less than 70 mm Hg in another dog. Furthermore, a significant reduction in heart rate (HR) was registered after ACP/BUT treatment, and three out of 18 dogs showed bradycardia (HR less than 60 bpm).

The administration of different combinations of ACP/BUT has been previously associated with transient reductions in arterial blood pressure and/or HR in dogs (Cornick & Hartsfield, 1992; Kojima et al., 1999; Kojima et al., 2002; Monteiro, Junior, Assis, Campagnol, & Quitzan, 2009). However, it is difficult to attribute a specific cardiovascular effect to either drug alone when combinations are employed (Cornick & Hartsfield, 1992). In healthy dogs, a decrease in HR and SAP and/or MAP has been reported with ACP alone (Cornick & Hartsfield, 1992; Monteiro et al., 2009; Page et al., 1993; Saponaro et al., 2013). Depression of the hypothalamic vasomotor center and peripheral alpha1-adrenoceptor blockade could be responsible for the decrease in systemic arterial blood pressure, while a central vagal effect may be responsible for the reduction in HR (Greene, Hartsfield, & Tyner, 1990; Monteiro et al., 2009). Similar effects have been observed with BUT alone, with blood pressure affected through decreased peripheral vascular tone, and HR through vagal stimulation (Cornick & Hartsfield, 1992; Greene et al., 1990; Monteiro et al., 2009; Trim, 1983).

In healthy dogs, hypotension (SAP < 90 mmHg and MAP < 70 mmHg) has not been reported following either ACP or BUT when these drugs were given alone, but the reported effects of different ACP/BUT combinations vary (Greene et al., 1990; Kojima et al., 2002; Monteiro et al., 2009; Takano et al., 2011; Trim, 1983). More specifically, when ACP was administered 15 minutes before BUT, either intravenously (IV) or IM, hypotension was not observed (Greene et al., 1990; Monteiro et al., 2009). However, mild systemic and pulmonary arterial hypotension were described after simultaneous IM administration of ACP/BUT (Kojima et al., 2002). The results of these previous investigations do not seem to suggest that the use of a particular route of administration or dosage is determinant, and it is unclear whether hypotension can be fully avoided if ACP and BUT are administered separately, leaving a certain amount of time between treatments. However, this seems impractical for clinical purposes, as multiple injections would be needed, and echocardiography might be delayed. In any case, the reduction in arterial blood pressure observed during Study 1 was transient, and mostly mild, and the sedation protocol employed was therefore deemed adequate to facilitate echocardiography in healthy dogs. However, its impact in animals with cardiac disease could be more serious, and its use is discouraged until further investigation is carried out.

Regarding the effects of the sedation on HR, bradycardia was commonly observed in a previous investigation after 0.1 mg/Kg or 0.4 mg/Kg of BUT were given IV in healthy dogs, and this was registered up to 60 minutes after injection, although it was easily reversible with verbal stimulation (Trim et al., 1983). In a later investigation in halothane-anesthetized dogs, IV administration of BUT (0.2 mg/Kg) caused a clinically relevant reduction in HR, and the authors suggested that the concurrent use of an anticholinergic agent could be a possible strategy to prevent the phenomenon (Greene et al., 1990). Similarly, the use of ACP prior to opioid administration was advocated in another study, and ACP (0.22 mg/Kg) prior to BUT administration (0.22 mg/Kg), either IV or IM, proved useful to reduce the incidence of bradycardia, with no significant difference in HR recorded between the two routes of administration (Cornick & Hartsfield, 1992). However, in a later investigation, bradycardia was observed after IV BUT (0.15 mg/Kg), despite pretreatment with ACP (0.05 mg/Kg; Monteiro et al, 2009). Therefore, based on the results of Study 1 and of previous investigations, bradycardia is a possible side effect of ACP/BUT in healthy dogs, regardless of routes of administration and dosages.

Conventional echocardiographic parameters were also assessed in Study 1 to assist in the interpretation of possible changes in 2-D STE-derived parameters. Six measurements

were significantly affected by treatment, including left ventricular end-diastolic volume index (EDVI), left ventricular ejection time (LVET), peak velocity of late transmitral diastolic flow (A wave), E wave to A wave ratio (E/A), late diastolic velocity of the septal side of the mitral annulus (A' sep) and late diastolic velocity of the lateral side of the tricuspid annulus (A' tric). The decrease in EDVI could suggest a reduction in preload, which could be secondary to diminished vascular resistance caused by the drugs used, as mentioned above. The increase in LVET could have been secondary to the reduction in HR, supported by the moderate, negative correlation between the two variables. However, this would relate to an increase in preload, not supported by the change in EDVI. On the other hand, both increased and decreased afterload can prolong LVET (Boon, 2011). In the intact heart, complex hemodynamic and reflex changes occur with changes in arterial pressure (Nakamura, Wiegner, Gaasch, & Bing, 1983), and it can be difficult to identify a unique cause of change in systolic time intervals. However, decrease in afterload could well contribute to LVET prolongation, as supported by the decrease in MAP and DAP observed, and related to diminished vascular resistance. The reduction in A wave and subsequent increase in E/A ratio could again indicate a reduced preload. In fact, while a moderate positive correlation between HR and A wave, and a strong negative correlation between HR and E/A were found, slow HR is expected to increase A flow velocity (Boon, 2011). A wave reduction, associated with decreased HR, has been also reported after sedation with a combination of ACP and buprenorphine in healthy beagles (Takano et al., 2011).

Few pulsed-wave TDI variables (A' sep and A' tric) investigated in Study 1 were significantly reduced by sedation. In clinically healthy dogs, preload can affect pulsed-wave TDI variables, and a reduction in velocity can follow a decrease in preload, while these parameters seem to be unaffected by HR (Boon, 2011). However, positive correlations between HR and both A' sep and A' tric were registered, and even if this observation could be spurious, a contribution of HR to their reduction cannot be completely excluded.

The small decrease in ApL observed in Study 1 after sedation could have also been provoked by the above suggested decrease in preload. Deformation indices have been reported to be at least partially load independent in healthy, awake dogs (Chetboul et al., 2007). However, load independency of 2-D STE-derived strain was not supported by the results of other studies (Culwell et al., 2011; Zois et al., 2013). A decrease in strain may also result from vagal stimulation and a consequential prolongation of the R-R interval (Takano et al., 2010). However, in Study 1, no correlation between ApL and HR was found. The previously reported influence of HR on canine 2-D STE-derived strain indices vary. In

healthy, anesthetized dogs, pacing rates of 120, 140, 160, and 180 bpm did not result in significant differences in longitudinal, circumferential, and radial strain values (Suzuki et al., 2013c). However, significant correlations between HR and 2-D STE-derived indices have been found in other studies (Smith et al., 2012; Suzuki et al., 2013a; Takano et al., 2010; Zois et al., 2012; Zois et al., 2013).

Overall, most of the results observed in Study 1 seem to indicate that the sedation protocol used causes a reduction in preload, and possibly afterload. In healthy cats, sedation with ACP/BUT also caused echocardiographic changes in conventional echocardiographic variables ascribable to reduced preload (Ward et al., 2012). However, in the study by Ward and colleagues, as in Study 1, the effects of the sedation were considered mild and not clinically meaningful. Furthermore, the main objective of Study 1 was to investigate the effects of sedation on 2-D STE-derived parameters, and the majority of these variables were not significantly affected by sedation. In healthy beagles, the few changes in conventional echocardiographic variables, including EDVI and A wave, caused by a combination of ACP and buprenorphine were not considered severe enough to alter interpretation of the results, and no significant effects on 2-D STE-derived variables was demonstrated (Takano et al., 2011). In healthy cats, a combination of ACP and buprenorphine did not have a significant influence on 2-D STE-derived variables (Takano et al., 2015).

Therefore, despite the mild changes in echocardiographic parameters mentioned above, and mainly involving conventional parameters, the sedation protocol employed in Study 1 was deemed adequate to facilitate echocardiography in healthy dogs. The operator could comfortably perform a quality diagnostic examination, and the dogs maintained lateral recumbency voluntarily with only minimal restraint. Furthermore, except in one out of 18 dogs that continued panting, most breathed calmly, with negligible respiration artifact. The latter is important for the reliability of strain analysis by 2-D STE, as tracking errors due to breathing artifacts can occur (Griffiths et al., 2011).

The LAp4Ch view, used for longitudinal strain analysis in dogs, has been associated with tracking errors due to breathing artifact and dropout, especially involving the free LV wall (Griffiths et al., 2011; Wess et al., 2011). While good quality four-chamber images can be difficult to obtain from the left parasternal apical location in some dogs, especially if deep-chested (Dukes-McEwan, 2002), the conformation of the canine thorax allows their attainment from the right parasternal location in most dogs (Dukes-McEwan, 2002; Thomas

et al., 1993). Therefore, to assess whether actions other than sedation could help in performing reliable strain analysis in cases where strain data is invalid, the feasibility of the RP4Ch view for longitudinal strain and SR analysis was assessed in Study 2. Both healthy and diseased dogs were included, because the use of sedation might be sub-optimal in dogs with cardiac disease, and a different approach to improve 2-D STE reliability might be preferred.

The results of Study 2 indicated that the RP4Ch view can be feasible to measure longitudinal strain and SR. However, the measurements obtained from the two views are not interchangeable, as demonstrated by significant differences between the majority (seven out of 11) of 2-D STE-derived variables. Because most of these differences persisted when sub-analysis of the groups of healthy and diseased dogs was performed, the discrepancy observed did not seem to be influenced by the presence or absence of cardiac disease. However, only a few subjects were available for each disease subcategory, and so the effects of a specific pathology were not able to be evaluated.

The RP4Ch view, often considered less technically demanding to obtain than the LAp4Ch view, has been previously compared with the latter for the evaluation of other parameters of LV function (Dukes-McEwan, 2002; Wess, Mäurer, Simak, & Hartmann, 2010). In a study including healthy dogs of different breeds, the RP4Ch view maximized ejection fraction and LV volumes, measured with the length-area method, compared with the LAp4Ch view (Dukes-McEwan, 2002). On the other hand, good agreement between the two projections was found in another study including Doberman Pinschers only, and measuring LV volume via the modified Simpson's method of discs (Wess, Mäurer, et al., 2010).

In humans, longitudinal deformation of the LV is evaluated via 2-D STE by integrating values obtained from the apical two-chamber, four-chamber and five-chamber views (Blessberger & Binder, 2010). Furthermore, segmentation models that allow the assignment of individual segments to specific coronary artery territories are used (Cerqueira et al., 2002). In dogs, only one plane is generally analyzed, and the standard LAp4Ch view is typically chosen for this purpose. Long-axis function of segments present in other planes is usually ignored, as myocardial infarcts leading to regional dysfunction are uncommon in dogs, compared with humans (Wess, Mäurer, et al., 2010). Additionally, pacemaker optimization and cardiac resynchronization therapy are not currently performed in dogs in

the clinical setting, and therefore inter- and intra-ventricular dyssynchrony are not routinely assessed (Estrada & Chetboul, 2006; Gorcsan & Tanaka, 2011; Griffiths et al., 2011).

Depending on the species, the use of specific echocardiographic planes might be recommended based on peculiar anatomic characteristics (Abduch et al., 2014), and this also applies to long-axis function assessment by 2-D STE. For this purpose, the LAp4Ch view is typically chosen in cats (Silva et al., 2013; Sugimoto et al., 2015; Suzuki et al., 2017), as it is in dogs. A subxiphoid approach providing an apical four-chamber view has been chosen in pigs (Ishikawa et al., 2015), while left parasternal long-axis planes in mice, rats and rabbits (Kusunose et al., 2012), and sagittal long-axis planes in zebrafish are used (Hein et al., 2015). In horses, a modified four-chamber view obtained by adjusting the standard RP4Ch view is employed (Decloedt et al., 2011, 2012; Schefer et al., 2010; Schwarzwald et al., 2009). Similarly, the RP4Ch view has been adopted for this purpose in goats, in which the right parasternal approach is considered to be the only reliable one for transthoracic echocardiography, as in other ruminants (Abduch et al., 2014; Berli et al., 2015).

Study 2 demonstrated the ability of 2-D STE to quantify, also in dogs, LV longitudinal strain and SR from the RP4Ch view in dogs. A good quality four-chamber image can be attained in most dogs from the right parasternal location (Dukes-McEwan, 2002; Thomas et al., 1993), and the use of this view might therefore be considered when the images obtained from the left apical approach are of suboptimal quality, or strain data are not deemed reliable. However, 2-D STE performed from the LAp4Ch view has been validated in healthy anesthetized subjects against sonomicrometry, and demonstrated to provide accurate measurements of LV dimensions and strains (Amundsen et al., 2006). Therefore, routinely, 2-D STE should still be performed on the LAp4Ch view. Additionally, Study 2 showed that the RP4Ch view is not always a viable alternative to the LAp4Ch view, as out of sector motion of the apical segments can occur, also invalidating strain data in some dogs. In fact, in a relevant proportion of cases (approximately 18% of the initial population), the epicardial portion of the apical segments ceased to be visible at least partially during diastole. In horses and humans, the apical regions obtained from parasternal views are excluded if there are difficulties in fully including them within the sector arc (Decloedt et al., 2011; Forsha et al., 2015). The same may be necessary in those dogs where the apex is not entirely imaged, or, if a more conservative practice is desired, the measurements from the entire LV should be discarded.

If the RP4Ch view is employed, this should be recorded, and taken into account when serial results obtained from the same individual are compared. A difference related to the use of different projections could be misinterpreted as a real change in cardiac function. Furthermore, in light of the significant differences in strain measurements between the two views found in Study 2, reference ranges derived from the standard apical view should not be used to interpret values obtained from the RP4Ch view.

The differences between echocardiographic views observed in Study 2 could suggest that different segments of the LV are imaged, even if both views display four-chamber planes. Each myocardial region creates its individual pattern of speckles (Hein et al., 2015), and it is reported that the RP4Ch view does not include the true apical region in animals (Abduch et al., 2014). Another explanation could be a difference in tracking quality, related to the different orientation of the heart within the plane in the two views.

In children, standard windows were compared to those obtained from near-orthogonal planes, and significantly different values were found, suggesting that angle insonation and target depth may exert an influence on 2-D STE-derived peak systolic longitudinal strain (Forsha et al., 2015). Despite strain analysis being theoretically angle-independent, the use of echocardiography to perform it would introduce angle and depth dependence (Forsha et al., 2015). Speckle tracking works better along the ultrasound beam than across beams, and because lateral resolution decreases with depth, tracking across beams works better in areas adjacent to the transducer (Forsha et al., 2015; Støylen, 2015; Voigt et al., 2015). Image acquisition from different windows can change the ratio of axial to lateral resolution in a given myocardial segment, and can result in a change in image quality of that segment as lateral resolution is inferior to axial resolution (Forsha et al., 2015; Støylen, 2015). Therefore, longitudinal strain values obtained from alternative imaging windows or off-axis apical windows should not be used interchangeably with those derived from the standard apical window (Forsha et al., 2015), as also supported by the results of Study 2.

Additionally, Study 2 showed that global longitudinal strain parameters obtained from the RP4Ch view usually have lower variability than segmental strain values. While CV were always less than 10% for GLS and global longitudinal SR parameters, repeatability and reproducibility were less acceptable for some segmental strain measurements, with the highest variability relating to the basal septal segment (within-day intra-observer CV 19.6%) and the midlateral segment (inter-observer CV 21.7%). Neither of the two views clearly

performed better, and high variability was also identified when assessing some of the same and some additional segments from the LAp4Ch view. This finding does not seem particularly alarming, and confirms what has already been discussed above, regarding the possible better applicability of global strain analysis in veterinary medicine. The consistency and reproducibility of GLS in Study 2 was also confirmed by the ICC, which showed an excellent degree of congruence between repeated measurements obtained from the RP4Ch view.

Due to the higher reproducibility of global values compared with segmental ones demonstrated in Study 2, only the former were included in Study 3. Inter-software variability may represent an additional source of variability in the analysis of 2-D STE-derived deformations parameters, and therefore, variables as reproducible as possible should be investigated in order to limit measurement error. Furthermore, as previously mentioned, different segmentation models were used by the different software, making comparison between them impractical.

The results of Study 3 indicated that feasibility is not uniform across software methods, despite the use of good quality images and high FR. In fact, even if a prospective image acquisition protocol for 2-D STE strain analysis was used, TomTec vendor independent software could not reliably analyze images from 20% (11/55) of the dogs initially included in the Philips-cohort.

The independent platform uses DICOM files instead of raw data, the former having lower image quality and FR compared with the latter, which is used by the vendor dependent software (van Everdingen et al., 2017). Poor image quality can hinder accurate speckle tracking by directly affecting spatial resolution, while low FR can impede reliable strain analysis by influencing temporal resolution (van Everdingen et al., 2017). Therefore, the use of DICOM files could provide a possible explanation to the lower feasibility of the vendor independent software, especially compared to Philips software.

Good image quality represented a criterion for inclusion of dogs in Study 3, and appeared equal in the two cohorts upon subjective assessment. However, most of the images obtained with General Electric (GE) ultrasound system could be reliably analyzed by vendor independent software, despite the same acquisition FR range being used in the two cohorts. While it is possible that small differences in image quality might have been overlooked, an explanation for the variable feasibility of TomTec software could be the

different technology of the ultrasound systems used for image acquisition. Temporal and spatial resolution, filter settings and other post-processing effects may vary among ultrasound machines, influencing image characteristics (Farsalinos et al., 2015).

In people, acquisition FR above 30 Hz, and ideally around 50 Hz, are advised for 2-D STE-derived strain analysis (Blessberger & Binder, 2010). Frame rates above 60 Hz were employed in Study 3, as in Study 1 and 2, because dogs usually have higher HR compared with humans. The choice seemed appropriate, at least for raw format image analysis, as all the echocardiographic images included could be analyzed with vendor specific software in the three studies.

Accuracy of 2-D STE-derived strain analysis can also be affected by HR, and high HR at conventional FR might cause underestimation of GLS (D'hooge et al., 2016). In anesthetized dogs, strain parameters did not differ significantly at pacing rates between 120 and 180 bpm, when FR was increased with increasing HR (Suzuki et al., 2013c). In Study 3, FR was maintained within a pre-established range, but was not systematically set according to HR. Therefore, it might be possible that this resulted in inadequate FR for some of the images, once exported to the DICOM format. Previous studies have demonstrated that lower strain measurements can be obtained if DICOM data are compressed at 30 frames/sec, however, reliable analysis can still be performed (Risum et al., 2012). While data compression, ultrasound technology, FR and HR could all have an influence on strain measurements, the source of the dissimilar feasibility of vendor independent analysis observed in Study 3 remains unclear.

When strain analysis was feasible, intra-observer and inter-observer agreement on GLS values were good using each software in Study 3, as observed in Study 1 and 2, and similar to previous studies in people (D'hooge et al., 2016). Variability of systolic SR was also acceptable, as the highest CV obtained was 15.1 %. However, diastolic SR indices showed an overall poorer reproducibility. In most cases, the software displayed SR measurements only after a cursor was placed by the investigator at the appropriate time point over the global SR curve, while GLS values were provided automatically, potentially adding a source of variability. Semi-automatic user guidance and different user interaction may have a substantial impact on measurement variability between software, especially for SR data (Farsalinos et al., 2015; Voigt et al., 2015). Furthermore, time-dependent parameters such as SR might be more demanding and require higher FR, compared with

strain (Voigt et al., 2015). Regardless of the cause for higher SR variability, GLS was the most reproducible longitudinal strain index in Study 3.

In Study 3, peak strain measurements were included, as each software provide them by default, and are therefore more likely to be used in clinical veterinary practice in the absence of specific guidelines. However, the Industry Strain Standardization Taskforce advocates the use of end-systolic strain values as default parameters to describe myocardial deformation (Voigt et al., 2015).

When the 2-D STE software investigated in Study 3 were compared, statistically significant differences in longitudinal strain and SR parameters were found, and in some individual patients, measurements varied considerably. In fact, repeat GLS measurements obtained in the same patient with vendor dependent and independent software could vary up to 5.6-5.7 strain units. Therefore, when different post-processing software are used, a change in GLS of less than 6 % could still be due to inter-software variability, instead of reflecting a true change in systolic function. This can have a significant clinical impact, considering that one of the main uses of GLS, at least in people, is to track subclinical changes in LV function through serial echocardiographic examinations (Costa et al., 2014).

Regrettably, the source of discordance between software found in Study 3 could not be further investigated, as a gold-standard technique for deformation imaging, such as sonomicrometry, was not available, as has occurred in previous studies (van Everdingen et al., 2017). Discrepancies between software from different manufacturers can be mainly attributed to differences in 2-D STE algorithms (van Everdingen et al., 2017). Since the appointment of the EACVI/ASE Industry Strain Standardization Taskforce, overall improvements in variation across vendors have taken place (Costa et al., 2014; Shiino et al., 2017). However, most software are not open-source, and there remains a lack of published validation (van Everdingen et al., 2017). Hopefully improvements will continue. However, due to the significant costs that renewing dedicated software might incur, older versions might be in use for a considerable period, at least in the veterinary setting, and inter-software variability will have to be seriously taken into account.

To ensure a broad spectrum of strain values, and provide useful results for the clinical setting, Study 3 involved a mixed population of dogs with and without myocardial disease, similarly to Study 2. Left ventricular function ranged from severely reduced, as in DCM cases, to enhanced, as in some dogs with advanced compensated MMVD. However,

left ventricular function does not seem to have a significant impact on longitudinal strain variability (Risum et al., 2012).

An important source of inter-software variability can be related to layer-specific strain analysis. Software packages can interrogate different myocardial layers. As well as deformations measured over the entire cardiac wall, endocardial, midline and epicardial strain values can all potentially be obtained (D'hooge et al., 2016). A longitudinal strain gradient exists, with lower values obtained when the epicardial layer is approached (Waldman, Fung, & Covell, 1985; Nagata et al., 2017). This is possibly due to differences in coronary perfusion and metabolism, and higher end-diastolic wall stress at the endocardium (Nagata et al., 2017). The vendor independent software employed in Study 3 analyzes either the endocardial or the epicardial layers, but epicardial data were discarded as the analysis was not deemed reliable. On the other hand, the version of Philips software employed incorporates a weighted average of the deformation across the myocardium in strain calculation, with the weighting greatest at the endocardium, as stated by the instructions. Finally, the version of GE software employed can measure mid-myocardial, endocardial and epicardial strain, the former being those included in Study 3.

While use of strain data taken at different layers might seem a plausible explanation for the inter-software variability encountered, the results of Study 3 do not entirely support this hypothesis. In fact, significant differences were still found between the measurements obtained at the endocardial layer with the two software packages used in the GE-cohort. Furthermore, endocardial strain values should be higher than transmural ones (D'hooge et al., 2016), while the contrary was observed in the Philips-cohort. Therefore, use of strain data taken at different layers does not appear to be the only cause of the inter-software variability found in Study 3.

The EACVI/ASE Inter-Vendor Comparison Study revealed statistically significant differences between GLS strain obtained from the endocardial layer with nine different software packages (Farsalinos et al., 2015). On the other hand, a similar comparison as that done in Study 3 for the Philips-cohort, between software measuring transmural vs. endocardial strain, showed small and non-significant differences in 2-D STE-derived parameters (van Everdingen et al., 2017). The results of investigations regarding between-layer strain comparability appear therefore conflicting. While layer specific strain measurements can all be employed, the user should report which one has been measured (Farsalinos et al., 2015), and they should not be compared without care. However, this was

done in Study 3 to aid in the assessment of strain indices potentially obtained in clinical situations, as commonly used software were investigated, and the parameters examined were mostly those provided by default.

5.1 Limitations

Overall, the number of dogs included in each study was relatively limited.

In Study 1, large effects were considered the most relevant, and therefore 18 dogs were deemed enough to provide an adequate power; however, the sample size needed to reach a high statistical power at medium or small effect size was larger. Furthermore, only middle to large-sized dogs were investigated, and the dogs included differed significantly in terms of sex and age, so that our results may not apply to the overall dog population. The dogs' weight range (15 to 50 Kg) was preselected based on the frequency range of the probe available for attainment of images for strain analysis. Also, middle and large-sized dogs are predisposed to cardiomyopathies such as DCM, where strain measurement can be especially useful. Another limitation of Study 1 relates to the fact that the subjects included were healthy dogs. Sedation may influence echocardiographic variables differently in the presence of cardiac disease, and potentially cause unexpected adverse effects, other than those observed in Study 1. Finally, the results obtained may differ from those obtained by use of another software system, as demonstrated by Study 3.

In Study 2 and 3, each group of dogs included consisted of several canine breeds with a wide range of weights and age. Furthermore, dogs with cardiovascular disease had various cardiac pathologies. It was therefore not possible to exclude that variables such as breed, weight, age, or a specific cardiac pathology, had a determinant influence on the results. Being clinical studies however, it was not possible to better control for the status of the dogs included, and at the same time, a broad range of strain values was desired. Another limitation of both experiments was that some of the dogs with cardiac disease received medication, with some of the treatments administered possibly affecting LV function. However, each patient acted as his/her own control, as a paired sample design was used, so that the inclusion of treated patients was not deemed incautious.

Additionally, in Study 2, the effects of small variations in image quality, cardiac cycles, HR, and FR, were not statistically evaluated. Heart rate did not appear to vary significantly during the scans, and only cardiac cycles with stable sinus rhythms were

analyzed; furthermore, we attempted to minimize these confounders by maintaining FR within a narrow range (60–90 Hz), and choosing patients with good image quality and acoustic windows. However, their partial contribution to the results cannot be completely excluded. Another limitation could be the sedation employed in a small number of subjects. However, only healthy subjects were sedated, and with the same protocol used in Study 1, shown not to affect significantly 2-D STE-derived parameters significantly in such subjects. Additionally, the results obtained may differ from those obtained by use of another software system, as demonstrated by Study 3.

In Study 3, an additional limitation was that each dog underwent echocardiographic examination by a single ultrasound system depending on the location. Regrettably, this was unavoidable due to the availability of each University, but ideally, dogs would undergo echocardiography by both ultrasound systems, and vendors could be directly compared. Another limitation was the use of an earlier version of Philips software. Significant differences in GLS values were found when comparing this version with a more recent one available (Nagata et al., 2015), and improved inter-vendor agreement was found when using the latest versions of different software (Shiino et al., 2017).

CONCLUSIONS

6. CONCLUSIONS

1. In healthy dogs, the intramuscular administration of a combination of acepromazine (0.02 mg/Kg) and butorphanol (0.2 mg/Kg) provided an adequate degree of sedation to facilitate echocardiography and the attainment of good quality images for strain analysis by two-dimensional (2-D) speckle tracking echocardiography (STE), when the scans were performed 30 to 40 minutes after treatment.

2. In healthy dogs, the sedation protocol mentioned above exerted only a minor influence on 2-D STE-derived echocardiographic variables, and could thus be used in uncooperative dogs without altering significantly the results of strain analysis.

3. Transient bradycardia was the most common side effect observed in healthy dogs after the administration of the sedation protocol mentioned above. Hypotension also occurred in a minority of dogs.

4. The right parasternal four-chamber (RP4Ch) view was feasible for the assessment of longitudinal strain and strain rate (SR) by use of 2-D STE in cardiovascularly healthy and diseased dogs.

5. The values obtained from the RP4Ch view were significantly different from those obtained from the standard left apical four-chamber view, and should not be used interchangeably.

6. Out of sector motion of the apical segments invalidated strain data in a few dogs when the RP4Ch view was used. Only loops where the entire LV is imaged throughout the cardiac cycle should be used for analysis, or the apical segments should be excluded if they cease to be visible at any moment.

7. Global longitudinal parameters showed good repeatability and reproducibility, while segmental strains were less reliable from each view interrogated. Furthermore, the reproducibility of global longitudinal strain (GLS) was superior to that of SR. Therefore, the use of strain analysis for global assessment of cardiac function appeared more applicable in dogs than for interrogation of myocardial segmental activity, especially by means of GLS measurement.

8. Feasibility of strain analysis was not uniform across software, and statistically significant inter-software variability in GLS and SR measurements was demonstrated, warranting care when comparing serial measurements or consulting reference values if different software have been used.

SUMMARY/RESUMEN

SUMMARY

Two-dimensional (2-D) speckle tracking echocardiography (STE) is a relatively new imaging technique, introduced in veterinary medicine to aid the assessment of cardiac function. The experiments conducted during the Ph. D. focused on different aspects of 2-D STE in dogs, and aimed at improving its applicability and correct interpretation in the canine species.

Firstly, the effects of a combination of acepromazine (ACP; 0.02 mg/Kg) and butorphanol (BUT; 0.2 mg/Kg) on 2-D STE-derived strain values, obtained in 18 healthy middle and large-sized adult dogs, were evaluated. Left ventricular circumferential and longitudinal global and segmental strains were derived via 2-D STE, and comparison between parameters, obtained prior to and after sedation was performed. Between-day measurement variability was also assessed. The results indicated that the combination of ACP and BUT employed, administered intramuscularly, provides adequate sedation to facilitate echocardiography in healthy dogs when the scans are performed 30 to 40 minutes after treatment, with only a minor influence on 2-D STE variables. In fact, global strain values were not affected by sedation, and only one segmental (apical lateral) strain value decreased significantly. However, systemic arterial pressure and heart rate also decreased, and use of the same sedation protocol in cardiovascularly diseased dogs should be considered with care as undesirable effects could occur.

Secondly, the use of the right parasternal four-chamber (RP4Ch) view for the assessment of LV longitudinal strain and strain rate (SR) by 2-D STE, usually performed on left apical four-chamber (LAp4Ch) views, was investigated. Twenty-six healthy dogs and 25 dogs with various cardiac diseases were examined. Longitudinal global and segmental strains and global SR of the LV were obtained through 2-D STE by use of RP4Ch and LAp4Ch views. Feasibility and reproducibility of the RP4Ch view were investigated, and strain and SR values obtained from the two views were compared. The results indicated that the RP4Ch view is feasible to measure the variables aforementioned. However, out-of-sector motion of the apical segments can invalidate strain data in some dogs. Furthermore, significant differences between the values obtained from this view and the LAp4Ch view were found, and therefore they should not be used interchangeably.

Thirdly, the intersoftware variability of longitudinal global strain and SR measurements derived from 2-D STE in dogs with and without cardiac disease was assessed. Echocardiographic images were obtained from two cohorts of dogs. The first cohort included 44 dogs (23 cardiovascularly healthy, 21 with cardiac disease), imaged with a Philips ultrasound system, while the second cohort included 40 dogs (18 cardiovascularly

healthy, 22 with cardiac disease), imaged with a General Electric ultrasound system. Echocardiographic images in each cohort were analyzed with vendor specific 2-D STE software, and with TomTec vendor independent software. Global longitudinal strain and SR values obtained with different software from the same LAp4Ch views were compared. Intra- and inter-observer variability was determined, and intersoftware agreement assessed. The results indicated that feasibility is not uniform across software methods, despite the use of good quality images and relatively high frame rate. Furthermore, significant differences among software were found for strain and SR measurements, and longitudinal global strain in a single patient could vary up to 5.7 units. Therefore, care should be taken when referring to published ranges of normality, or comparing serial measurements in the same patient, as changes in longitudinal global strain < 6 % might still be within measurement error when different post-processing software are used.

Overall, the experiments showed a high reproducibility of longitudinal global measurements, superior to that of segmental strains and global SR.

RESUMEN

ANTECEDENTES: La ecocardiografía bidimensional (2-D) con rastreo de marcas o *speckle tracking* (ST) es una técnica de reciente desarrollo, introducida como prueba adicional para la evaluación de la función cardíaca y basada en el análisis de deformación miocárdica. En medicina veterinaria esta técnica se ha validado en perros sanos y empleado en algunos estudios sobre las cardiopatías más comunes, aunque su uso aún no es frecuente en la práctica clínica. Los experimentos llevados a cabo durante el doctorado se enfocaron en aspectos inexplorados de la ecocardiografía 2-D ST en perros, con el objetivo de mejorar su aplicabilidad y correcta interpretación.

El uso de tranquilizantes o sedantes puede ser necesario para facilitar la realización de ecocardiografías en pequeños animales y obtener imágenes ecográficas de calidad. El protocolo sedante ideal para procedimientos diagnósticos en medicina cardiovascular debe reducir la ansiedad del paciente, proporcionar una inmovilización adecuada y a la vez preservar las condiciones hemodinámicas tanto como sea posible. En la actualidad no hay muchos datos disponibles sobre la influencia de la sedación en variables derivadas de la ecocardiografía 2-D ST en perros, aunque es importante utilizar protocolos que no alteren significativamente sus resultados, garantizando una correcta interpretación de la prueba.

Para la evaluación de la deformación longitudinal del ventrículo izquierdo (VI) se utiliza la proyección apical izquierda de cuatro cámaras (LAp4Ch) en perros, así como en humanos y en gatos. Sin embargo, esta proyección no siempre es fácil de obtener, y a veces puede asociarse a artefactos que invalidan el análisis de deformación. La conformación del tórax canino permite la obtención de excelentes imágenes desde el acceso para-esternal derecho, pero el uso de la la proyección para-esternal derecha de cuatro cámaras (RP4Ch) para el análisis de deformación longitudinal no se ha investigado en perros.

Existen varios software para realizar el análisis de deformación mediante ecocardiografía 2-D ST. En medicina humana, se han demostrado diferencias en los resultados derivados de diferentes plataformas, y el post-procesado de los datos parece ser un factor determinante de esta variabilidad entre software. Debido a estas diferencias, los valores obtenidos con plataformas distintas en un mismo paciente podrían no ser comparables, ni algunos valores de referencia válidos. Estos hechos podrían ser relevante también en la práctica clínica veterinaria, pero la comparabilidad de los parámetros de deformación obtenidos utilizando distintos software no ha sido investigada en perros.

OBJETIVOS E HIPÓTESIS: Se ha realizado un primer estudio que evalúa los efectos de la sedación con acepromacina (ACP) y butorfanol (BUT) sobre valores ecocardiográficos

derivados de ecocardiografía 2-D ST en perros sanos, para establecer si la combinación utilizada puede o no considerarse adecuada para facilitar la realización de la prueba. De hecho, este protocolo de sedación se utiliza en perros para reducir el estado de ansiedad y podría permitir una mejor evaluación de la estructura y funcionalidad cardiacas. Según la hipótesis previa al estudio, los cambios en las variables ecocardiográficas examinadas iban a ser menores y sin importancia clínica, y el protocolo de sedación adecuado.

También se ha realizado un estudio sobre el uso novedoso de la vista RP4Ch para el análisis del strain y strain rate (SR) en perros sanos y con cardiopatías. Con este experimento se quiso determinar si el uso de la proyección no habitual es posible y los resultados fiables, dado que su obtención es más fácil en perros y podría facilitar la realización del análisis de deformación en la práctica clínica, y si las diferencias con la proyección estándar dan la posibilidad o no de utilizar sus valores de forma intercambiable. Según la hipótesis previa al estudio, la vista RP4Ch permitiría un análisis de deformación longitudinal fiable, y las dos proyecciones iban a proporcionar valores similares.

Finalmente, se ha realizado un tercer experimento para comprobar si hay diferencias entre las medidas de strain y SR longitudinales obtenidas en perros sanos y con cardiopatías a través de softwares de pos-procesado distintos. En medicina humana ya ha sido demostrado que los resultados del análisis de strain pueden variar dependiendo del algoritmo utilizado por cada distinto software, y según la hipótesis previa al estudio, se encontrarían valores no directamente comparables también en perros.

MATERIALES Y MÉTODOS: Para el estudio de sedación en perros sanos, se utilizaron 18 perros de más de 15 Kg de peso y más de 1 año de edad, de propiedad de voluntarios. Se realizaron: medida de presión arterial, analítica sanguínea, electrocardiografía y ecocardiografía. Confirmando con los exámenes realizados el estado de salud normal, se procedió a la sedación con una combinación de ACP (0.02 mg/Kg) y BUT (0.2 mg/Kg) intramuscular, y a los 30-40 minutos se repitieron la medida de presión arterial y la ecocardiografía. Se compararon los valores obtenidos, antes y después de la sedación, de presión arterial y frecuencia cardiaca. Además, se compararon índices de ecocardiografía convencional (incluyendo 44 parámetros, obtenidos a través de ecocardiografía bidimensional, Modo-M, Doppler espectral y Doppler tisular), y ecocardiografía 2-D ST (incluyendo strain longitudinal y circunferencial del VI, tanto globales como segmentarios). Las comparaciones se llevaron a cabo utilizando un test *t* para muestras pareadas ya que los valores demostraron una distribución normal según el test de Shapiro-Wilk, y se analizó la correlación de las variables con la frecuencia cardiaca. También se determinó la variabilidad inter-días por medio de los coeficientes de variación (CV).

Para el estudio sobre el uso novedoso de la vista RP4Ch para el análisis de deformación longitudinal del VI mediante ecocardiografía 2-D ST, se utilizaron pacientes del Hospital Clínico Veterinario de la Universidad de Murcia, y perros de propiedad de voluntarios. Se investigaron 26 perros sanos y 25 perros con enfermedad cardíaca, y se realizaron ecocardiografía y otros análisis complementarios cuando estimados necesarios. Se determinaron la fiabilidad y reproducibilidad de la proyección RP4Ch, y se compararon los valores de strain longitudinal, globales y segmentarios, y de SR longitudinal global obtenidos desde la vista RP4Ch y desde la vista estándar (vista apical izquierda de cuatro cámaras). Las comparaciones se llevaron a cabo utilizando un test *t* para muestras pareadas, ya que los valores demostraron una distribución normal según el test de Shapiro-Wilk. También se estudiaron la concordancia entre las dos proyecciones mediante los gráficos de Bland-Altman y los coeficientes de correlación intra-clases (ICC), y la variabilidad intra- e inter-observador en las medidas mediante CV e ICC.

Para el estudio sobre el efecto del software en medidas derivadas de la ecocardiografía 2-D ST, se utilizaron pacientes del Hospital Clínico Veterinario de la Universidad de Murcia y de la Universidad de Edimburgo. Dos cohortes de perros fueron examinadas: 44 perros (23 sanos, 21 con enfermedad cardíaca) cuyas imágenes ecocardiográficas se obtuvieron con un ecógrafo Philips en Murcia, y 40 perros (18 sanos, 22 con enfermedad cardíaca), cuyas imágenes se obtuvieron con un ecógrafo General Electric en Edimburgo. El análisis de deformación se realizó en cada cohorte con el software específico del vendedor y con el software independiente TomTec. Se compararon los valores de strain y SR longitudinal global obtenidos con los diferentes softwares utilizando un test *t* para muestras pareadas o una prueba de Wilcoxon, dependiendo de la normalidad en la distribución evidenciada por el test de Shapiro-Wilk. También se estudiaron la concordancia entre software mediante los gráficos de Bland-Altman, y la variabilidad intra- e inter-observador en las medidas mediante CV.

Para los dos primeros estudios, las ecocardiografías fueron realizadas por el doctorando o el tutor, y medidas siempre por uno o los dos investigadores. Para el tercer estudio, las ecocardiografías fueron realizadas por el doctorando o el tutor en Murcia, y por el doctorando u otro colaborador experto en Edimburgo, y todas fueron medidas por el doctorando.

RESULTADOS: Los resultados del estudio de sedación en perros indicaron que la combinación de ACP y BUT empleada, administrada por vía intramuscular de 30 a 40 minutos antes de la ecocardiografía, proporciona un grado de sedación adecuado para facilitar la prueba en perros sanos, ya que los animales toleraron el decúbito lateral durante

la prueba con mínima retención, y respiraron calmadamente, lo que es importante para reducir los artefactos generados por la respiración. Además, el protocolo empleado no alteró la mayoría de variables ecocardiográficas medidas. De hecho, los valores de strain global no se vieron afectados por la sedación, y solo un valor segmentario (apical lateral) disminuyó significativamente. Seis de 44 variables ecocardiográficas convencionales difirieron significativamente de los valores basales después de la sedación, incluyendo el volumen telediastólico del VI indexado a la superficie corporal (disminuido), la velocidad máxima del flujo transmitralico diastólico tardío (disminuida), las velocidades diastólicas tardías del anillo mitral, obtenidas a nivel septal, y del tricúspide, obtenidas a nivel lateral (disminuidas), el tiempo de eyección (aumentado) y el ratio entre las velocidades máximas diastólicas del flujo transmitrálico (aumentado). La presión arterial sistémica (media y diastólica) y la frecuencia cardíaca disminuyeron significativamente después de la sedación, y se observaron bradicardia (frecuencia cardiaca inferior a 60 lpm) en tres perros, e hipotensión (presión arterial sistólica inferior a 90 mmHg o media inferior a 70 mmHg) en dos perros, ambos fenómenos siendo transitorios. Se calcularon coeficientes de variación (CV) entre días inferiores al 10%.

Los resultados del estudio sobre el uso novedoso de la vista RP4Ch para el análisis de deformación longitudinal del VI mediante ecocardiografía 2-D ST indicaron que el análisis es fiable, aunque en algunos perros el movimiento fuera del sector de los segmentos apicales llegó a invalidar el análisis. Adicionalmente, los valores obtenidos desde la RP4Ch no son intercambiables con los medidos usando la proyección estándar. La reproducibilidad de los valores de deformación global obtenidos a partir de esta vista fue muy alta, como lo demuestran CV inferiores al 6%. Los CV para el SR también estuvieron dentro de límites clínicamente aceptables (<15%). Sin embargo, para los índices de strain segmentario, la reproducibilidad no siempre fue buena, con CV que alcanzaron el 21,3%.

Los resultados del estudio sobre el efecto del software en medidas derivadas de la ecocardiografía 2-D ST indicaron que la fiabilidad del análisis de deformación no es uniforme entre plataformas. De hecho, el análisis no se pudo realizar con el software independiente del proveedor para el 20% de las imágenes obtenidas con el sistema de ultrasonido Philips. Adicionalmente, en las dos cohortes se observaron diferencias significativas entre software, tanto para los valores de strain longitudinal global como para los valores de SR. Se demostraron variaciones de hasta 5.7 unidades en el strain global longitudinal en un mismo paciente, y los gráficos de Bland-Altman confirmaron la presencia de amplios límites de concordancia. Los coeficientes de variación intra-observador e inter-observador fueron inferiores al 10% para los valores de strain longitudinal global, mientras que las mediciones de SR mostraron una mayor varianza.

CONCLUSIONES Y RELEVANCIA CLÍNICA: La combinación de ACP y BUT empleada, administrada por vía intramuscular de 30 a 40 minutos antes de la ecocardiografía, es adecuada para facilitar la realización de esta prueba en perros sanos, y no altera la mayoría de variables ecocardiográficas medidas. Por lo tanto, este protocolo podría emplearse en perros sanos en la práctica clínica, aunque debido a la bajada de frecuencia cardiaca y presión arterial sistémica, su uso en perros con enfermedades cardiovasculares debe ser considerado, ya que podría ocasionar efectos indeseables.

La vista RP4Ch demostró ser fiable para la evaluación de strain y SR longitudinales mediante el uso de ecocardiografía 2-D ST en perros sanos y enfermos, aunque al ser los valores obtenidos de esta vista y de la vista estándar significativamente diferentes, no deberían ser utilizados indistintamente. El análisis desde la proyección RP4Ch podría revelarse útil cuando la vista estándar es difícil de obtener, o son presentes artefactos. Adicionalmente, el software empleado realizó un análisis de deformación global mejor que segmentario para ambas vistas, y esto podría sugerir que en perros la evaluación de la funcionalidad global del VI es mas recomendable.

La fiabilidad del análisis de deformación longitudinal no es uniforme entre software, a pesar del uso de imágenes de buena calidad obtenidas con velocidad de cuadro adecuada. Adicionalmente, hay diferencias significativas entre valores obtenidos con distintos software, que invitan al uso cuidadoso de valores de referencia en función del tipo de programa de post-procesado, y cautela en la comparación de mediciones seriadas en un mismo paciente, ya que diferencias de strain global longitudinal inferiores al 6% pueden ser atribuidas a la variabilidad entre software.

REFERENCE LIST

References

Abduch, M. C., Assad, R. S., Mathias, W. Jr., & Aiello, V. D. (2014). The echocardiography in the cardiovascular laboratory: a guide to research with animals. *Arquivos Brasileiros de Cardiologia*, 102(1), 97-103.

Alcidi, G. M., Esposito, R., Evola, V., Santoro, C., Lembo, M., Sorrentino, R., Lo Iudice, F., Borgia, F., Novo, G., Trimarco, B., Lancellotti, P., & Galderisi, M. (2017). Normal reference values of multilayer longitudinal strain according to age decades in a healthy population: a single-centre experience. *European Heart Journal - Cardiovascular Imaging,* 0, 1-7. doi:10.1093/ehjci/jex306

Amundsen, B.H., Crosby, J., Steen, P.A., Torp, H., Slørdahl, S.A., & Støylen, A. (2009). Regional myocardial long-axis strain and strain rate measured by different tissue Doppler and speckle tracking echocardiography methods: a comparison with tagged magnetic resonance imaging. *European Journal of Echocardiography,* 10(2), 229–237.

Amundsen, B. H., Helle-Valle, T., Edvardsen, T., Torp, H., Crosby, J., Lyseggen, E., Støylen, A., Ihlen, H., Lima, J. A. C., Smiseth, O. A., & Slørdahl, S. A. (2006). Noninvasive myocardial strain measurement by speckle tracking echocardiography: validation against sonomicrometry and tagged magnetic resonance imaging. *Journal of the American College of Cardiology*, 47(4), 789-793.

Armitage-Chan, E. (2008). Anesthesia and analgesia in dogs and cats. In R. E. Fish, M. J. Brown, P. J. Danneman, & A. Z. Karas (Eds.), *Anesthesia and analgesia in laboratory animals* (2nd ed., pp. 365-384). Amsterdam, The Netherlands: Academic Press.

Armstrong, W. F., & Ryan, T. (2010). *Feigenbaum's echocardiography* (7th ed.). Philadelphia, PA: Lippincott Williams & Wilkins.

Atkins, C., Bonagura, J., Ettinger, S., Fox, P., Gordon, S., Häggström, J., Hamlin, R., Keene, B., Luis-Fuentes, V., & Stepien, R. (2009). Guidelines for the diagnosis and treatment of canine chronic valvular heart disease. *Journal of Veterinary Internal Medicine,* 23(6), 1142-1150.

Baron Toaldo, M., Romito, G., Guglielmini, C., Diana, A., Pelle, N. G., Contiero, B., & Cipone, M. (2017). Assessment of left atrial deformation and function by 2-dimensional speckle tracking echocardiography in healthy dogs and dogs with myxomatous mitral valve disease. *Journal of Veterinary Internal Medicine,* 31(3), 641-649.

Baron Toaldo, M., Romito, G., Guglielmini, C., Diana, A., Pelle, N. G., Contiero, B., & Cipone, M. (2018). Prognostic value of echocardiographic indices of left atrial

morphology and function in dogs with myxomatous mitral valve disease. *Journal of Veterinary Internal Medicine*, 32(3), 914-921.

Becker, M., Kramann, R., Dohmen, G., Lückhoff, A., Autschbach, R., Kelm, M., & Hoffmann, R. (2007). Impact of left ventricular loading conditions on myocardial deformation parameters: analysis of early and late changes of myocardial deformation parameters after aortic valve replacement. *Journal of the American Society of Echocardiography,* 20(6), 681-689.

Bélanger, M. C. (2017). Echocardiography. In S. J. Ettinger, E. C. Feldman, & E. Côté (Eds.), *Textbook of veterinary internal medicine* (8th ed., pp. 393-410). Milton, ON, Canada: Elsevier.

Benjamini, Y., & Hochberg, Y. (1995). Controlling the false discovery rate: a practical and powerful approach to multiple testing. *Journal of the Royal Statistical Society Series B (Statistical Methodology),* 57(1), 289–300.

Berli, A.J., Jud Schefer, R., Steininger, K., & Schwarzwald, C. C. (2015). The use of strain, strain rate, and displacement by 2D speckle tracking for assessment of systolic left ventricular function in goats: applicability and influence of general anesthesia. *Cardiovascular Ultrasound*, 13, 11.

Biaggi, P., Carasso, S., Garceau, P., Greutmann, M., Gruner, C., Tsang, W., Rakowski, H., Agmon, Y., & Woo, A. (2011). Comparison of two different speckle tracking software systems: does the method matter? *Echocardiography*, 28(5): 539-547.

Blessberger, H., & Binder, T. (2010). Non-invasive imaging: two-dimensional speckle tracking echocardiography: basic principles. *Heart*, 96(9), 716-722.

Boon, J. (2011). *Veterinary echocardiography* (2nd ed.). Oxford, England: Blackwell Publishing.

Caivano, D., Rishniw, M., Birettoni, F., Patata, V., Giorgi, M. E., & Porciello, F. (2018). Left atrial deformation and phasic function determined by two-dimensional speckle-tracking echocardiography in dogs with myxomatous mitral valve disease. *Journal of Veterinary Cardiology,* 20(2), 102-114.

Caivano, D., Rishniw, M., Patata, V., Giorgi, M. E., Birettoni, F., & Porciello, F. (2016). Left atrial deformation and phasic function determined by 2-dimensional speckle tracking echocardiography in healthy dogs. *Journal of Veterinary Cardiology*, 18(2), 146-155.

Cameli, M., Caputo, M., Mondillo, S., Ballo, P., Palmerini, E., Lisi, M., Marino, E., & Galderisi, M. (2009). Feasibility and reference values of left atrial longitudinal strain imaging by two-dimensional speckle tracking. *Cardiovascular Ultrasound*, 7, 6.

Carluccio, E., Biagioli, P., Alunni, G., Murrone, A., Zuchi, C., Coiro, S., Riccini, C., Mengoni, A., D'Antonio, A., & Ambrosio, G. (2018). Prognostic value of right ventricular

dysfunction in heart failure with reduced ejection fraction: superiority of longitudinal strain over tricuspid annular plane systolic excursion. *Circulation: Cardiovascular Imaging,* 11(1), e006894. doi: 10.1161/CIRCIMAGING.117.006894.

Carnabuci, C., Hanås, S., Ljungvall, I., Tidholm, A., Bussadori, C, Häggström, J, & Höglund, K. (2013). Assessment of cardiac function using global and regional left ventricular endomyocardial and epimyocardial peak systolic strain and strain rate in healthy Labrador retriever dogs. *Research in Veterinary Science,* 95(1), 241-248.

Castel, A. L., Szymanski, C., Delelis, F., Levy, F., Menet, A., Mailliet, A., Marotte, N., Graux, P., Tribouilloy, C., & Maréchaux, S. (2014). Prospective comparison of speckle tracking longitudinal bidimensional strain between two vendors. *Archives of Cardiovascular Diseases*, 107(2), 96–104.

Cerqueira, M. D., Weissman, N. J., Dilsizian, V., Jacobs, A. K., Kaul, S., Laskey, W. K., Pennell, D. J., Rumberger, J. A., Ryan, T., & Verani, M. S. (2002). Standardized myocardial segmentation and nomenclature for tomographic imaging of the heart: a statement for healthcare professionals from the Cardiac Imaging Committee of the Council on Clinical Cardiology of the American Heart Association. *Circulation*, 105(4), 539-542.

Chapel, E. H., Scansen, B. A., Schober, K. E., & Bonagura, J. D. (2018). Echocardiographic estimates of right ventricular systolic function in dogs with myxomatous mitral valve disease. *Journal of Veterinary Internal Medicine*, 32(1), 64-71.

Chen, H. Y., Lien, Y. H., & Huang, H. P. (2014). Assessment of left ventricular function by two-dimensional speckle-tracking echocardiography in small breed dogs with hyperadrenocorticism. *Acta Veterinaria Scandinavica*, 56, 88.

Chetboul, V. (2010). Advanced techniques in echocardiography in small animals. *Veterinary Clinics of North America: Small Animal Practice*, 40(4), 529-543.

Chetboul, V., Damoiseaux, C., Lefebvre, H. P., Concordet, D., Desquilbet, L., Gouni, V., Poissonnier, C., Pouchelon, J. L., & Tissier, R. (2018). Quantitative assessment of both systolic and diastolic right ventricular morphology and function by conventional echocardiography and speckle tracking imaging in dogs: a prospective study in 104 healthy dogs. *Journal of Veterinary Science,* Jul 20. Retrieved from http://www.vetsci.org/journal/view.html?uid=1531&vmd=Full&.

Chetboul, V., Serres, F., Gouni, V., Tissier, R., & Pouchelon, J. L. (2007). Radial strain and strain rate by two-dimensional speckle tracking echocardiography and the tissue velocity based technique in the dog. *Journal of Veterinary Cardiology*, 9(2), 69-81.

Chetboul, V., Serres, F., Gouni, V., Tissier, R., & Pouchelon, J. L. (2008). Noninvasive assessment of systolic left ventricular torsion by 2-dimensional speckle tracking

imaging in the awake dog: repeatability, reproducibility, and comparison with tissue doppler imaging variables. *Journal of Veterinary Internal Medicine,* 22(2), 342-350.

Chetboul, V., & Tissier, R. (2012). Echocardiographic assessment of canine degenerative mitral valve disease. *Journal of Veterinary Cardiology*, 14(1), 127-148.

Cornell, C. C., Kittleson, M. D., Della Torre, P., Häggström, J., Lombard, C. W., Pedersen, H. D., Vollmar, A., & Wey, A. (2004). Allometric scaling of M-mode cardiac measurements in normal adult dogs. *Journal of Veterinary Internal Medicine*, 18(3), 311-321.

Cornick, J. L., & Hartsfield, S. M. (1992). Cardiopulmonary and behavioral effects of combinations of acepromazine/butorphanol and acepromazine/oxymorphone in dogs. *Journal of the American Veterinary Medical Association*, 200(12), 1952-1956.

Costa, S. P., Beaver, T. A., Rollor, J. L., Vanichakam, P., Magnus, P. C., & Palac, R. T. (2014). Quantification of the variability associated with repeat measurements of left ventricular two-dimensional global longitudinal strain in a real-world setting. *Journal of the American Society of Echocardiography*, 27(1), 50-54.

Culwell, N. M., Bonagura, J. D., & Schober, K. E. (2011). Comparison of echocardiographic indices of myocardial strain with invasive measurements of left ventricular systolic function in anesthetized healthy dogs. *American Journal of Veterinary Research*, 72(5), 650-660.

Cunningham, S. M., Roderick, K. V. (2016). Cardiovascular system introduction (p.67). In Aiello S. E. (Ed.), *The Merck Veterinary Manual* (p.67). Kenilworth, NJ: Merck & Co.

Dalen, H., Thorstensen, A., Aase, S. A., Ingul, C. B., Torp, H., Vatten, L. J., & Støylen A. (2010). Segmental and global longitudinal strain and strain rate based on echocardiography of 1266 healthy individuals: the HUNT study in Norway. *European Journal of Echocardiography*, 11(2), 176-183.

Decloedt, A., Borowicz, H., Slowikowska, M., Chiers, K., van Loon, G., & Niedzwiedz, A. (2017). Right ventricular function during acute exacerbation of severe equine asthma. *Equine Veterinary Journal*, 49(5), 603-608.

Decloedt, A., De Clercq, D., Ven Sofie, S., Van Der Vekens, N., Sys, S., Broux, B., & van Loon, G. (2017). Echocardiographic measurements of right heart size and function in healthy horses. *Equine Veterinary Journal,* 49(1), 58-64.

Decloedt, A., Verheyen, T., Sys, S., De Clercq, D., & van Loon, G. (2011). Quantification of left ventricular longitudinal strain, strain rate, and displacement in healthy horses by 2-dimensional speckle tracking. *Journal of Veterinary Internal Medicine*, 25(2), 330-338.

Decloedt, A., Verheyen, T., Sys, S., De Clercq, D., & van Loon, G. (2012). Tissue Doppler imaging and 2-dimensional speckle tracking of left ventricular function in horses exposed to lasalocid. *Journal of Veterinary Internal Medicine*, 26(5), 1209-1216.

Decloedt, A., Verheyen, T., Sys, S., De Clercq, D., & van Loon, G. (2013). Two-dimensional speckle tracking for quantification of left ventricular circumferential and radial wall motion in horses. *Equine Veterinary Journal*, 45(1), 47-55.

D'hooge, J., Barbosa, D., Gao, H., Claus, P., Prater, D., Hamilton, J., Lysyansky, P., Abe, Y., Ito, Y., Houle, H., Pedri, S., Baumann, R., Thomas, J., & Badano, L. P.; EACVI/ASE/Industry Task Force to Standardize Deformation Imaging. (2016). Two-dimensional speckle tracking echocardiography: standardization efforts based on synthetic ultrasound data. *European Heart Journal - Cardiovascular Imaging*, 17(6), 693-701.

Dickson, D., Shave, R., Rishniw, M., & Patteson, M. (2017). Echocardiographic assessments of longitudinal left ventricular function in healthy English Springer spaniels. *Journal of Veterinary Cardiology*, 19(4), 339-350.

Dukes-McEwan, J. (2002). Comparison between right and left cardiac windows to determine left ventricular volumes and ejection fraction in six dog breeds with differing somatotypes. *European Journal of Ultrasound*, 27, S4-S5.

Edvardsen, T., Helle-Valle, T., & Smiseth, O. A. (2006). Systolic dysfunction in heart failure with normal ejection fraction: speckle-tracking echocardiography. *Progress in Cardiovascular Diseases*, 49(3), 207–214.

Estrada, A., & Chetboul, V. (2006). Tissue Doppler evaluation of ventricular synchrony. *Journal of Veterinary Cardiology*, 8(2), 129-137.

van Everdingen, W. M., Maass, A. H, Vernooy, K., Meine, M., Allaart, C. P., De Lange, F. J., Teske A. J., Geelhoed, B., Rienstra, M., Van Gelder, I. C., Vos, M. A., & Cramer, M., J. (2017). Comparison of strain parameters in dyssynchronous heart failure between speckle tracking echocardiography vendor systems. *Cardiovascular Ultrasound,* 15(1), 25.

Farsalinos, K. E., Daraban, A. M., Ünlü, S., Thomas, J. D., Badano, L. P., & Voigt J. U. (2015). Head-to-head comparison of global longitudinal strain measurements among nine different vendors. The EACVI/ASE inter-vendor comparison study. *Journal of the American Society of Echocardiography*, 28(10), 1171-1181.

Flethøy, M., Schwarzwald, C. C., Haugaard, M. M., Carstensen, H., Kanters, J. K., Olsen, L. H., & Buhl, R. (2016). Left ventricular function after prolonged exercise in equine endurance athletes. *Journal of Veterinary Internal Medicine*, 30(4), 1260-1269.

Forsha, D., Risum, N., Rajagopal, S., Dolgner, S., Hornik, C., Barnhart, H., Kisslo, J., & Barker, P. (2015). The influence of angle of insonation and target depth on speckle-tracking strain. *Journal of the American Society of Echocardiography*, 28(5), 580–586.

Gehlen, H., & Bildheim, L. M. (2018). Speckle tracking analysis of myocardial deformation in correlation to age in healthy horses. *Journal of Veterinary Science,* Apr 26. Retrieved from http://www.vetsci.org/journal/view.html?uid=1481&vmd=Full&.

Gilbert, S. H., McConnell, F. J., Holden, A. V., Sivananthan, M. U., & Dukes-McEwan, J. (2010). The potential role of MRI in veterinary clinical cardiology. *The Veterinary Journal* 2010, 183(2), 124-134.

Glickman, M. E., Rao, S. R., & Schultz, M. R. (2014). False discovery rate control is a recommended alternative to Bonferroni-type adjustments in health studies. *Journal of Clinical Epidemiology*, 67(8), 850-857.

Gorcsan, J., 3rd, & Tanaka, H. (2011). Echocardiographic assessment of myocardial strain. *Journal of the American College of Cardiology*, 58(14), 1401-1413.

Greene, S. A., Hartsfield, S. M., & Tyner, C. L. (1990). Cardiovascular effects of butorphanol in halothane-anesthetized dogs. *American Journal of Veterinary Research*, 51(8), 1276-1279.

Griffiths, L. G., Fransioli, J. R., & Chigerwe, M. (2011). Echocardiographic assessment of interventricular and intraventricular mechanical synchrony in normal dogs. *Journal of Veterinary Cardiology*, 13(2), 115-126.

Hamabe, L., Kim, S., Yoshiyuki, R., Fukuyama, T., Nakata, T. M., Fukushima, R., & Tanaka, R. (2015). Echocardiographic evaluation of myocardial changes observed after closure of patent ductus arteriosus in dogs. *Journal of Veterinary Internal Medicine,* 29(1), 126-131.

Hansson, K., Häggström, J., Kvart, C., & Lord, P. (2002). Left atrial to aortic root indices using two-dimensional and M-mode echocardiography in cavalier King Charles spaniels with and without left atrial enlargement. *Veterinary Radiology & Ultrasound*, 43(6), 568-575.

Hein, S. J., Lehmann, L. H., Kossack, M., Juergensen, L., Fuchs, D., Katus, H. A., & Hassel, D. (2015). Advanced echocardiography in adult zebrafish reveals delayed recovery of heart function after myocardial cryoinjury. *PLOS ONE*, 10(4), e0122665. doi:10.1371/journal.pone.0122665.

Helle-Valle, T., Crosby, J., Edvardsen, T., Lyseggen, E., Amundsen, B. H., Smith, H. J., Rosen, B. D., Lima, J. A., Torp, H., Ihlen, H., & Smiseth, O. A. (2005). New

noninvasive method for assessment of left ventricular rotation: speckle tracking echocardiography. *Circulation,* 112(20), 3149-3156.

Ishikawa, K., Aguero, J., Gyun Oh, J., Hammoudi, N., Fish, L. A., Leonardson, L., Picatoste, B., Santos-Gallego, C. G., Fish, K. M., & Hajjar, R. J. (2015). Increased stiffness is the major early abnormality in a pig model of severe aortic stenosis and predisposes to congestive heart failure in the absence of systolic dysfunction. *Journal of the American Heart Association,* 4(5), e001925. doi:10.1161/JAHA.115.001925.

Kellihan, H. B., Stepien, R. L., Hassen, K. M., & Smith, L. J. (2015). Sedative and echocardiographic effects of dexmedetomidine combined with butorphanol in healthy dogs. *Journal of Veterinary Cardiology,* 17(4), 282-292.

Kojima, K., Nishimura, R., Mutoh, T., Takao, K., Matsunaga, S., Mochizuki, M., & Sasaki, N. (1999). Comparison of cardiopulmonary effects of medetomidine-midazolam, acepromazine-butorphanol and midazolam-butorphanol in dogs. *Zentralblatt für Veterinärmedizin. Reihe A,* 46(6), 353-359.

Kojima, K., Nishimura, R., Mutoh, T., Hong, S. H., Mochizuki, M., & Sasaki, N. (2002). Effects of medetomidine-midazolam, acepromazine-butorphanol, and midazolam-butorphanol on induction dose of thiopental and propofol and on cardiopulmonary changes in dogs. *American Journal of Veterinary Research*, 63(12), 1671-1679.

Kusunose, K., Penn, M. S., Zhang, Y., Cheng, Y., Thomas, J. D., Marwick, T. H., & Popović, Z. (2012). How similar are the mice to men? Between-species comparison of left ventricular mechanics using strain imaging. *PLOS ONE,* 7(6), e40061. doi:10.1371/journal.pone.0040061.

Lang, R. M., Badano, L. P., Mor-Avi, V., Afilalo, J., Armstrong, A., Ernande, L., Flachskampf, F. A., Foster, E., Goldstein, S, A., Kuznetsova, T., Lancellotti, P., Muraru, D., Picard, M. H., Rietzschel, E. R., Rudski, L., Spencer, K. T., Tsang, W., & Voigt, J. U. (2015). Recommendations for cardiac chamber quantification by echocardiography in adults: an update from the American Society of Echocardiography and European Association of Cardiovascular Imaging. *Journal of the American Society of Echocardiography*, 28(1), 1-39.

Lang, R. M., Bierig, M., Devereux, R. B., Flachskampf, F. A., Foster, E., Pellikka, P. A., Picard, M. H., Roman, M. J., Seward, J., Shanewise, J., Solomon, S. D., Spencer, K. T., Sutton M. S., & Stewart W. J; Chamber quantification Writing Group; American Society of Echocardiography's Guidelines and Standards Committee; European Association of Echocardiography. (2005). Recommendations for chamber quantification: a report from the American Society of Echocardiography's Guidelines and Standards Committee and the Chamber Quantification Writing Group,

developed in conjunction with the European Association of Echocardiography, a branch of the European Society of Cardiology. *Journal of the American Society of Echocardiography*, 18(12), 1440–1463.

Lecoq, L., Moula, N., Amory, H., Rollin, F., & Leroux, A. (2018). Two-dimensional speckle tracking echocardiography in calves: feasibility and repeatability study. *Journal of Veterinary Cardiology,* 20(1), 45-54.

Monteiro, E. R., Junior, A. R., Assis, H. M., Campagnol, D., & Quitzan, J. G. (2009). Comparative study on the sedative effects of morphine, methadone, butorphanol or tramadol, in combination with acepromazine, in dogs. *Veterinary Anaesthesia and Analgesia,* 36(1), 25-33.

Morita, T., Nakamura, K., Osuga, T., Yokoyama, N., Khoirun, N., Morishita, K., Sasaki, N., Ohta, H., & Takiguchi, M. (2017). The repeatability and characteristics of right ventricular longitudinal strain by speckle-tracking echocardiography in healthy dogs. *Journal of Veterinary Cardiology*, 19(4), 351-362.

Nagata, Y., Wu, V. C., Otsuji, Y., & Takeuchi, M. (2017). Normal range of myocardial layer-specific strain using two-dimensional speckle tracking echocardiography. *PLOS ONE*, 12(6), e0180584. doi: 10.1371/journal.pone.0180584.

Nagata, Y., Takeuchi, M., Mizukoshi, K., Wu, V. C., Lin, F. C., Negishi, K., Nakatani, S., & Otsuji, Y. (2015). Intervendor variability of two-dimensional strain using vendor-specific and vendor-independent software. *Journal of the American Society of Echocardiography,* 28(6), 630-641.

Nakamura, K., Kawamoto, S., Osuga, T., Morita, T., Sasaki, N., Morishita, K., Ohta, H., & Takiguchi, M. (2017). Left atrial strain at different stages of myxomatous mitral valve disease in dogs. *Journal of Veterinary Internal Medicine*, 31(2), 316-325.

Nakamura, Y., Wiegner, A. W., Gaasch, W. H., Bing, O. H. L. (1983). Systolic time intervals: assessment by isolated cardiac muscle studies. *Journal of the American College of Cardiology*, 2(5), 973-978.

Osuga, T., Nakamura, K., Lim, S.Y., Tamura, Y., Kumara, W. R., Murakami, M., Sasaki, N., Morishita, K., Ohta, H., Yamasaki, M., & Takiguchi, M. (2013). Repeatability and reproducibility of measurements obtained via two-dimensional speckle tracking echocardiography of the left atrium and time-left atrial curve analysis in healthy dogs. *American Journal of Veterinary Research*, 74(6), 864-869.

Osuga, T., Nakamura, K., Morita, T., Lim, S. Y., Yokoyama, N., Morishita, K., Ohta, H., & Takiguchi, M. (2015). Effects of various cardiovascular drugs on indices obtained with two-dimensional speckle tracking echocardiography of the left atrium and time-

left atrial curve analysis in healthy dogs. *American Journal of Veterinary Research*, 76(8), 702-709.

Page, A., Edmunds, G., & Atwell, R. B. (1993). Echocardiographic values in the Greyhound. *Australian Veterinary Journal*, 70(10), 361-364.

Pedro, B., Stephenson, H., Linney, C., Cripps, P., & Dukes-McEwan, J. (2017). Assessment of left ventricular function in healthy Great Danes and in Great Danes with dilated cardiomyopathy using speckle tracking echocardiography. *Journal of Veterinary Cardiology*, 19(4), 363-375.

Quiñones, M. A., Otto, C. M., Stoddard, M., Waggoner, A., Zoghbi, W. A; Doppler Quantification Task Force of the Nomenclature and Standards Committee of the American Society of Echocardiography. (2002). Recommendations for quantification of Doppler echocardiography: a report from the Doppler quantification task force of the nomenclature and standards committee of the American Society of Echocardiography. *Journal of the American Society of Echocardiography*, 15(2), 167-184.

R Core Team. (2014). *R: A language and environment for statistical computing*. Vienna, Austria: R Foundation for Statistical Computing.

Risum, N., Ali, S., Olsen, N. T., Jons, C., Khouri, M. G., Lauridsen, T. K., Samad, Z., Velazquez, E. J., Sogaard, P., & Kisslo, J. (2012). Variability of global left ventricular deformation analysis using vendor dependent and independent two-dimensional speckle-tracking software in adults. *Journal of the American Society of Echocardiography*, 25(11), 1195-1203.

Saponaro, V., Crovace, A., De Marzo, L., Centonze, P., & Staffieri, F. (2013). Echocardiographic evaluation of the cardiovascular effects of medetomidine, acepromazine and their combination in healthy dogs. *Research in Veterinary Science*, 95(2), 687-692.

Schefer, K. D., Bitschnau, C., Weishaupt, M. A., & Schwarzwald, C. C. (2010). Quantitative analysis of stress echocardiograms in healthy horses with 2-dimensional (2D) echocardiography, anatomical M-mode, tissue Doppler imaging, and 2D speckle tracking. *Journal of Veterinary Internal Medicine,* 24(4), 918-931.

Schwarzwald, C. C., Schober, K. E., Berli, A. S., & Bonagura, J. D. (2009). Left ventricular radial and circumferential wall motion analysis in horses using strain, strain rate, and displacement by 2D speckle tracking. *Journal of Veterinary Internal Medicine*, 23(4), 890-900.

Shiino, K., Yamada, A., Ischenko, M., Khandheria, B. K., hudaverdi, M., Speranza, V., Harten, M., Benajmin, A., Hamilton-Craig, C. R., Platts, D. G., Burstow., D. J., Scalia,

G. M., & Chan, J. (2017). Intervendor consistency and reproducibility of left ventricular 2D global and regional strain with two different high-end ultrasound systems. European Heart journal - Cardiovascular Imaging, 18(6), 707-716.

Silva, A. C., Muzzi, R. A., Oberlender, G., Nogueira, R. B., Muzzi, L. A., Reis, G. F., & Mantovani, M. M. (2013). Longitudinal strain and strain rate by two-dimensional speckle tracking in non-sedated healthy cats. *Research in Veterinary Science,* 95(3), 1175-80.

Smith, D. N., Bonagura, J. D., Culwell, N. M., & Schober, K. E. (2012). Left ventricular function quantified by myocardial strain imaging in small-breed dogs with chronic mitral regurgitation. *Journal of Veterinary Cardiology*, 14(1), 231-242.

Spalla, I., Locatelli, C., Zanaboni, A. M., Brambilla, P., & Bussadori, C. (2016a). Echocardiographic assessment of cardiac function by conventional and speckle-tracking echocardiography in dogs with patent ductus arteriosus. *Journal of Veterinary Internal Medicine*, 30(3), 706-713.

Spalla, I., Locatelli, C., Zanaboni, A. M., Brambilla, P., & Bussadori, C. (2016b). Speckle-tracking echocardiography in dogs with patent ductus arteriosus: effect of percutaneous closure on cardiac mechanics. *Journal of Veterinary Internal Medicine*, 30(3), 714-721.

Stepien, R. L. (1995). Sedation for cardiovascular procedures. In J. D. Bonagura (Ed.), *Kirk's Current Veterinary Therapy XII*. Philadelphia, PA: WB Saunders Co.

Støylen, A. (2015, September). Basic concepts. Motion and deformation. Retrieved from http://folk.ntnu.no/stoylen/strainrate/Basic_concepts.html

Suffoletto, M. S., Dohi, K., Cannesson, M., Saba, S., & Gorcsan, J., 3rd. (2006). Novel speckle-tracking radial strain from routine black-and-white echocardiographic images to quantify dyssynchrony and predict response to cardiac resynchronization therapy. *Circulation*, 113(7), 960–968.

Sugimoto, K., Fujii, Y., Sunahara, H., & Aoki, T. (2015). Assessment of left ventricular longitudinal function in cats with subclinical hypertrophic cardiomyopathy using tissue Doppler imaging and speckle tracking echocardiography. *The Journal of Veterinary Medical Science*, 77(9), 1101-1108.

Suzuki, R., Matsumoto, H., Teshima, T., & Koyama, H. (2013a). Clinical assessment of systolic myocardial deformations in dogs with chronic mitral valve insufficiency using two-dimensional speckle-tracking echocardiography. *Journal of Veterinary Cardiology,* 15(1), 41-49.

Suzuki, R., Matsumoto, H., Teshima, T., & Koyama, H. (2013b). Effect of age on myocardial function assessed by two-dimensional speckle-tracking echocardiography in healthy beagle dogs. *Journal of Veterinary Cardiology,* 15(4), 243-252.

Suzuki, R., Matsumoto, H., Teshima, T., & Koyama, H. (2013c). Influence of heart rate on myocardial function using two-dimensional speckle-tracking echocardiography in healthy dogs. *Journal of Veterinary Cardiology,* 15(2), 139-146.

Suzuki, R., Matsumoto, H., Teshima, T., & Koyama, H. (2013d). Noninvasive clinical assessment of systolic torsional motions by two-dimensional speckle tracking echocardiography in dogs with myxomatous mitral valve disease. *Journal of Veterinary Internal Medicine*, 27(1), 69-75.

Suzuki, R., Mochizuki, Y., Yoshimatsu, H., Ohkusa, T., Teshima, T., Matsumoto, H., & Koyama, H. (2016). Myocardial torsional deformations in cats with hypertrophic cardiomyopathy using two-dimensional speckle-tracking echocardiography. *Journal of Veterinary Cardiology,* 18(4), 350-357.

Suzuki, R., Mochizuki, Y., Yoshimatsu, H., Teshima, T., Matsumoto, H., Koyama, H. (2017). Determination of multidirectional myocardial deformations in cats with hypertrophic cardiomyopathy by using two-dimensional speckle-tracking echocardiography. *Journal of Feline Medicine and Surgery,* 19(12), 1283-1289.

Takano, H., Fujii, Y., Ishikawa, R., Aoki, T., & Wakao, Y. (2010). Comparison of left ventricular contraction profiles among small, medium, and large dogs by use of two-dimensional speckle tracking echocardiography. *American Journal of Veterinary Research*, 71 (4), 421-427.

Takano, H., Fujii, Y., Yugeta, N., Takeda, S., & Wakao, Y. (2011). Assessment of left ventricular function in affected and carrier dogs with duchenne muscular dystrophy using speckle tracking echocardiography. *BMC Cardiovascular disorders,* 11, 23.

Takano, H., Isogai, T., Aoki, T., Wakao, Y., & Fujii, Y. (2015). Feasibility of radial and circumferential strain analysis using 2D speckle tracking echocardiography in cats. *The Journal of Veterinary Medical Science*, 77(2), 193-201.

Thomas, W. P., Gaber, C. E., Jacobs, G. J., Kaplan, P. M., Lombard, C. W., Moïse, N. S., & Moses, B. L. (1993). Recommendations for standards in transthoracic two-dimensional echocardiography in the dog and cat. Echocardiography Committee of the Specialty of Cardiology, American College of Veterinary Internal Medicine. *Journal of Veterinary Internal Medicine*, 7, 247–252.

Trim, C. M. (1983). Cardiopulmonary effects of butorphanol tartrate in dogs. *American Journal of Veterinary Research,* 44(2), 329-331.

Visser, L. C. (2017). Right ventricular function: Imaging techniques. *Veterinary Clinics of North America: Small Animal Practice*, 47(5), 989-1003.

Visser, L. C., Scansen, B. A., Brown, N. V., Schober, K. E., & Bonagura, J. D. (2015). Echocardiographic assessment of right ventricular systolic function in conscious healthy dogs following a single dose of pimobendan versus atenolol. *Journal of Veterinary Cardiology,* 17(3), 161-172.

Visser, L. C., Scansen, B. A., Schober, K. E., & Bonagura, J. D. (2015). Echocardiographic assessment of right ventricular systolic function in conscious healthy dogs: repeatability and reference intervals. *Journal of Veterinary Cardiology,* 17(2), 83-96.

Voigt, J. U., Pedrizzetti, G., Lysyanski, P., Marwick, T. H., Houle, H., Baumann, R., Pedri, S., Ito, Y., Abe, Y., Metz, S., Song, J. H., Hamilton, J., Sengupta, P. P., Kolias, T. J., d´Hooge, J., Aurigemma, G. P., Thomas, J. D., & Badano, L. P. (2015). Definitions for a common standard for 2D speckle tracking echocardiography: consensus document of the EACVI/ASE/Industry Task Force to standardize deformation imaging. *European Heart Journal - Cardiovascular Imaging*, 16(1), 1-11.

Waldman, L. K., Fung, Y. C., & Covell, J. W. (1985). Transmural myocardial deformation in the canine left ventricle. Normal in vivo three-dimensional finite strains. *Circulation Research,* 57(1), 152–163.

Ward, J. L., Schober, K. E., Luis Fuentes, V., & Bonagura, J. D. (2012). Effects of sedation on echocardiographic variables of left atrial and left ventricular function in healthy cats. *Journal of Feline Medicine and Surgery,* 14(10), 678-685.

Wess, G., Keller, L. J. M., Klausnitzer, M., Killich, M., & Hartmann, K. (2011). Comparison of longitudinal myocardial tissue velocity, strain, and strain rate measured by two-dimensional speckle tracking and by color tissue Doppler imaging in healthy dogs. *Journal of Veterinary Cardiology,* 13(1), 31-43.

Wess, G., Mäurer, J., Simak, J., & Hartmann, K. (2010). Use of Simpson's method of disc to detect early echocardiographic changes in Doberman Pinschers with dilated cardiomyopathy. *Journal of Veterinary Internal Medicine*, 24(5), 1069-1076.

Wess, G., Sarkar, R., & Hartmann, K. (2010). Assessment of left ventricular systolic function by strain imaging echocardiography in various stages of feline hypertrophic cardiomyopathy *Journal of Veterinary Internal Medicine*, 24(6), 1375-1382.

Westrup, U., & McEvoy, F. J. (2013). Speckle tracking echocardiography in mature Irish Wolfhound dogs: technical feasibility, measurement error and reference intervals. *Acta Veterinaria Scandinavica*, 55, 41.

Zois, N. E., Olsen, N. T., Moesgaard, S. G., Rasmussen, C. E., Falk, T., Häggström, J., Pedersen, H. D., Møller, J. E., & Olsen, L. H. (2013). Left ventricular twist and

circumferential strain in dogs with myxomatous mitral valve disease. *Journal of Veterinary Internal Medicine*, 27(4), 875-883.

Zois, N. E., Tidholm, A., Nägga, K. M., Moesgaard, S. G., Rasmussen, C. E., Falk, T., Häggström, J., Pedersen, H. D., Åblad, B., Nilsen, H. Y., & Olsen, L. H. (2012). Radial and longitudinal strain and strain rate assessed by speckle-tracking echocardiography in dogs with myxomatous mitral valve disease. *Journal of Veterinary Internal Medicine*, 26(6), 1309-1319.

APPENDIX

Paper published on the American Journal of Veterinary Research (Volume 78, No. 2, pp. 158-167, February 2017)

doi: 10.2460/ajvr.78.2.158.

Effects of a combination of acepromazine maleate and butorphanol tartrate on conventional and two-dimensional speckle tracking echocardiography in healthy dogs

Giorgia Santarelli DVM, MSc

Jesús Talavera López DVM, PhD

Josefa Fernández del Palacio DVM, PhD

Received January 20, 2016.
Accepted May 17, 2016.

From the Division of Veterinary Cardiology-Pulmonology, Veterinary Teaching Hospital, and the Department of Veterinary Medicine and Surgery, Faculty of Veterinary Medicine, University of Murcia, Campus Espinardo, 30100, Murcia, Spain.

Address correspondence to Dr. Santarelli (giorgia.santarelli1@um.es).

OBJECTIVE
To determine effects of a combination of acepromazine maleate and butorphanol tartrate on conventional echocardiographic variables and on strain values obtained by use of 2-D speckle tracking echocardiography (STE) in healthy dogs.

ANIMALS
18 healthy medium- and large-size adult dogs.

PROCEDURES
Transthoracic echocardiographic examination (2-D, M-mode, color flow, spectral Doppler, and tissue Doppler ultrasonography) and high-definition oscillometric blood pressure measurement were performed before and after dogs were sedated by IM administration of a combination of acepromazine (0.02 mg/kg) and butorphanol (0.2 mg/kg). Adequacy of sedation for echocardiographic examination was evaluated. Circumferential and longitudinal global and segmental strains of the left ventricle (LV) were obtained with 2-D STE by use of right parasternal short-axis and left parasternal apical views. Values before and after sedation were compared.

RESULTS
The sedation combination provided adequate immobilization to facilitate echocardiographic examination. Heart rate and mean and diastolic blood pressures decreased significantly after dogs were sedated. A few conventional echocardiographic variables differed significantly from baseline values after sedation, including decreased end-diastolic LV volume index, peak velocity of late diastolic transmitral flow, and late diastolic septal mitral and tricuspid annulus velocities, increased ejection time, and increased mitral ratio of peak early to late diastolic filling velocity; global strain values were not affected, but 1 segmental (apical lateral) strain value decreased significantly.

CONCLUSIONS AND CLINICAL RELEVANCE
Results indicated that acepromazine and butorphanol at the doses used in this study provided sedation adequate to facilitate echocardiography, with only mild influences on conventional and 2-D STE variables. (*Am J Vet Res* 2017;78:158–167)

Paper accepted by the journal Research in Veterinary Science (on the 30th of August 2018)

Accepted manuscript (unformatted and unedited PDF) available online at:

https://doi.org/10.1016/j.rvsc.2018.08.008

Copy of the acceptance email:

Ref: RVSC_2017_963_R2
Title: Evaluation of the right parasternal four-chamber view for the assessment of left ventricular longitudinal strain and strain rate by two-dimensional speckle tracking echocardiography in dogs
Journal: Research in Veterinary Science

Dear Ms. Santarelli,

I am pleased to inform you that your paper has been accepted for publication. My own comments as well as any reviewer comments are appended to the end of this letter. Now that your manuscript has been accepted for publication it will proceed to copy-editing and production.

Thank you for submitting your work to Research in Veterinary Science. We hope you consider us again for future submissions.

Kind regards,

Paolo Pasquali
Editor-in-Chief
Research in Veterinary Science

Paper accepted by the American Journal of Veterinary Reasearch (on the 21th of August 2018)

Copy of the acceptance email:

RE: AJVR-18-02-0038.R3, "Intersoftware variability of strain parameters derived from two-dimensional speckle tracking echocardiography in dogs"

Dear Ms. Santarelli:

I am pleased to inform you that your manuscript is accepted for publication in the American Journal of Veterinary Research, provided that you respond meaningfully to suggestions and questions raised by the editor at the time of editing. The manuscript is now in line for editing; nothing further is required of you at this time. Manuscripts are edited according to the date of this editorial decision. As a reminder, please be aware that a manuscript processing fee of $110 for each printed page or fraction thereof will be billed at the time the manuscript is published. Final Reviewer comments are copied below for your information.

Sincerely,

Helen L. Simons, PhD, DVM
Associate Editor
American Veterinary Medical Association